Secondary Electron Emission from Solids

O. HACHENBERG AND W. BRAUER

Heinrich-Hertz-Institute, German Academy of Sciences, Berlin, and Institute for Solid State Research, Theoretical Department, German Academy of Sciences, Berlin

I. Introduction

The phenomenon of secondary emission (SE) from solids was discovered by Austin and Starke in 1902 and has since been the subject of numerous experimental and theoretical investigations. It consists in the following process: If primary electrons (P) impinge on a solid, secondary electrons (S) are observed leaving the surface into free space.

The maximal experimental information about these S can be obtained (neglecting spin) by measuring of the number of S emitted per second from 1 cm^2 of the surface with energy E in the direction $\mathbf{\Omega}(\vartheta,\varphi)$. This function is the detailed current density of observed S, denoted by $j_s(E,\mathbf{\Omega})$.

$j_s(E,\mathbf{\Omega})$ can depend only on the states of the interacting systems, that is to say, on the properties of the primary beam and on the physical and chemical properties of the emitter, such as chemical composition, crystal structure, surface conditions, temperature, etc.

Thus, it is clear that it must be the aim of experimental investigations of SE to measure the function $j_s(E,\mathbf{\Omega})$ in its dependence on the parameters mentioned. The theory of SE, on the other hand, has to derive these results from first principles by means of appropriate approximations.

Since McKay (*1*) published his review on SE in this journal in 1948, a considerable number of recent experimental and theoretical studies on this subject have appeared (summaries are given in refs. *2–5a*); although they have contributed a great deal to clarify the problems, our experimental as well as theoretical knowledge of the function $j_s(E,\Omega)$ is still unsatisfactory.

As to the experimental side, the reason for this fact lies in the difficulties connected with the measurement of slow electrons ($E < 20$ ev) emitted from carefully cleaned surfaces. Theoretical difficulties are caused by the complexity of the SE phenomenon, the complete treatment of which necessitates a detailed study of a series of single problems. This has been only partly achieved.

In the following pages we shall first give a qualitative description of how the different elementary processes of SE are connected with one another and finally lead to the distribution function $j_s(E,\Omega)$. Then we shall comment on the essential experimental investigations, particularly those published in recent years. No attempt is made to give a complete list. The following theoretical considerations are intended (within the limits of this paper) to indicate how the observed results can be derived from fundamentals and at the same time to give hints for further interesting experimental studies of SE.

Experimental arrangements as well as the technical application of the phenomenon will not be included in this article. Moreover, phenomena effected by SE only (such as fatigue phenomena, Malter effect) will not be discussed in detail.

II. Qualitative Connection of the Different Elementary Processes

In order to clarify the meaning of the single processes effective in SE, we shall examine how a calculation of the function $j_s(E,\Omega)$ has to proceed in principle.

The first interaction occurring in this regard is that of the P with the potential barrier on the surface of the solid. If this is taken into account, the impinging primary beam will be divided into two parts, the reflected part and the part of P penetrating into the solid. The latter part will interact with the nuclei and electrons of the solid.

Thereby the P will suffer both elastic collisions with atomic nuclei, whereby their direction of motion is more or less changed, and loss of energy through interaction with electrons. The first process results in splitting the primary beam and thus partly in a reversed motion toward the surface. The P thus moving against the incident primary beam will also produce excited S and will partly escape from the surface into free space. The cal-

culation of these processes will result in the distribution of the states of P in the solid and the part of slowed-down reemitted P.

It is necessary to know the spatial distribution of the states of P if one wishes to study the spatial dependence of excitation of crystal electrons caused by P. This excitation process, which is also important for the energy loss of P, is obviously due to the Coulomb interaction between P and crystal electrons. A calculation of this process results in the number of crystal electrons per second and cubic centimeter, $S(x,E,\Omega)$, going over into a state (E,Ω) at a point x.

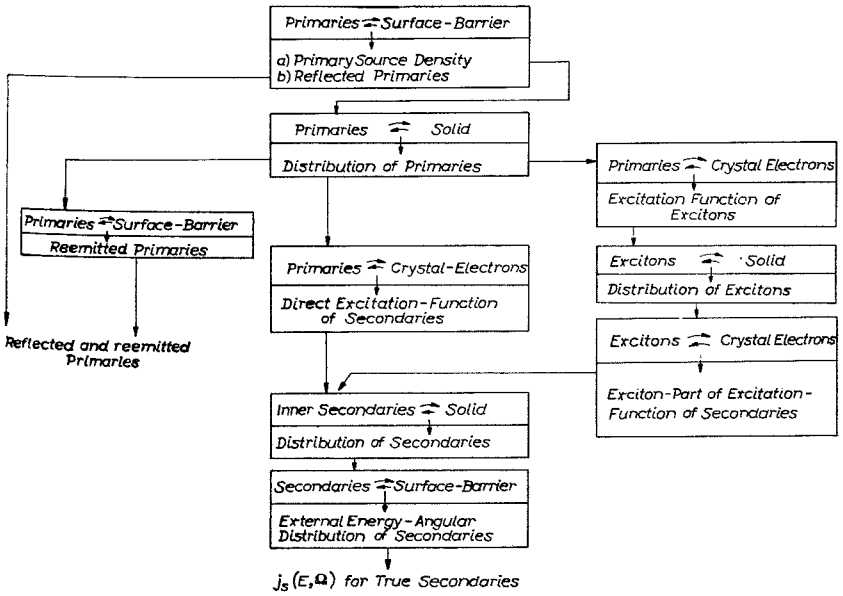

FIG. 1. Scheme of the secondary-emission process.

The inner S thus generated will interact with the different components of the solid, such as electrons and phonons. During their motion they will spread over the solid in a similar manner as the P mentioned above and will partly reach the surface where they will be reflected or emitted according to their energy and direction of incidence.

If certain presuppositions are made with respect to the surface, the distribution function $N(0,E,\Omega)$, i.e., the number of inner S per cubic centimeter in (E,Ω) at $x = 0$, will result in the required function $j_s(E,\Omega)$, which will have to be compared with the corresponding results of measurements.

It must be pointed out that the above consideration is only concerned

with direct excitation of S by P (which will mostly be the case, however). But, in fact, it may happen, that, for instance, the P will first produce excitons. The excitons will then move through the solid and may eventually lend their energy for the excitation of S. This will result in a part of indirectly excited S, whose actual existence, however, could not yet be proved for certain.

The different elementary processes, the interaction of which will finally lead to the current density distribution of outer S which is principally capable of measurement, are shown in their interrelation in the scheme (Fig. 1).

III. Experimental Results

Our knowledge of the mechanism of SE has considerably advanced in the last years. Theoretical studies have largely contributed to this. On the other hand, a major number of experimental results must be mentioned. In order to discuss SE, a good deal of use must be made of single experimental results. The following chapters will preferably deal with those results of measurements which are important for enlarging our knowledge of the SE mechanism and thus cannot be denied a certain significance for theoretical investigations.

A. Distribution Functions

A complete description of SE consists—as we mentioned above—in stating the function $j_s(E,\Omega)$. This function of two variables can be represented by a group of curves, one of the two variables occurring as a curve parameter. Thus, we obtain either the energy distribution of directed secondaries $j_s(E,\Omega_0)$ or the angular distribution of monoenergetic secondaries $j_s(E_0,\Omega)$. Of course, each of the two groups of curves can be derived from the other. The latter function seems to be measurable with less difficulty. This function we shall call the energy angular distribution. Usually the emission current is related to the unit of the primary current. But because of the proportionality of these two currents, this specification is often omitted.

Now integration of $j_s(E,\Omega)$ over all angles of a hemisphere leads to the pure energy distribution of secondaries $j_s(E)$, the integration over energy to the pure angular distribution $j_s(\Omega)$, and the integral over energy and angles to the yield δ of SE, if j_s is related to the unit of primary current. Since the energy distribution enables us to subdivide the S in a suitable manner, we shall first discuss this distribution function.

1. Energy Distribution. a. General considerations. If the number of electrons emitted by the target in the energy interval $(E, E + \Delta E)$ is plotted against the energy E, the result will be a distribution curve whose typical

shape is shown in Fig. 2. Three groups of electrons may be distinguished in this distribution curve.

One group of electrons has the energy E_p° of the primary beam. It is evident that this group must be considered to be elastically reflected P.

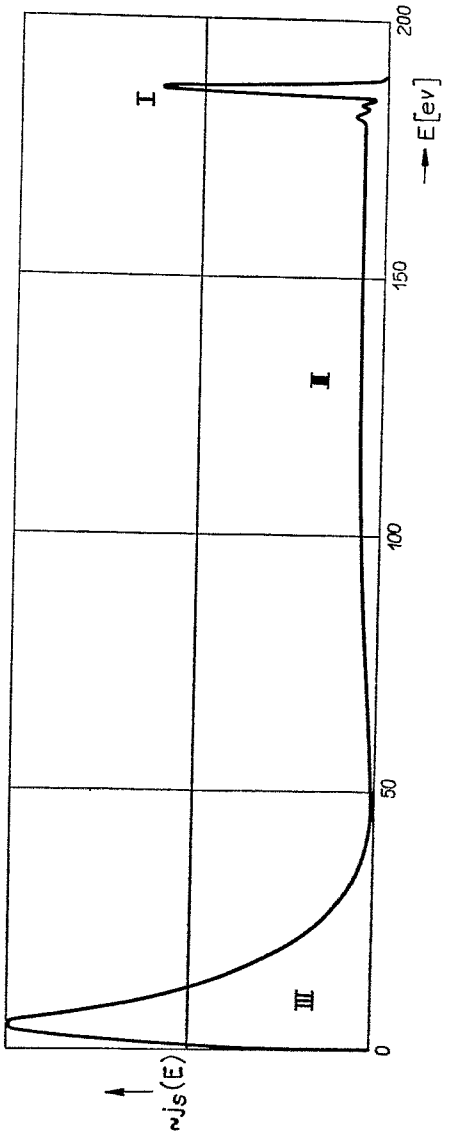

FIG. 2. The general shape of the energy distribution of secondary electrons.

A second group distributed in the spectrum between $E_p°$ and *ca.* 50 ev has a shape that may be compared with the spectrum of an electron beam having passed through a thin film. By analogy with those electrons, we assume that the electrons of this group are reflected to the surface only after having passed through a more or less thick layer of the target material. The electrons of this group are called rediffused P.

A third group is indicated below 50 ev by a sharp maximum of the distribution curve at a few electron volts. According to the relative frequency of this group— the number of these electrons is sometimes greater than that of the P—we must suppose that in this case we are *not* faced with P, but have to do with true S of the solid. It is mainly in this group that we shall be interested in the following.

Although the different groups are distinctly marked in the distribution curve, it is not possible to separate them exactly. In particular, there is no borderline distinction between rediffused P and true S. For practical purposes, the latter two groups are separated at $E \approx 50$ ev. It is natural that in such a way some true S with high energies should be included in the number of rediffused P, while on the other hand there must be rediffused electrons with $E < 50$ ev.

b. Methods of measurement. Measuring the energy distribution of true S is basically a problem of electron optics. The electrons escaping from a point of the target are distributed over all directions of a hemisphere. For the usual methods of measurement—except the retarding field method—it is necessary to cut out a beam with a narrow aperture angle by means of diaphragms. The electrons of this beam are separated according to their energies by a dispersing field and then focused on a point. As in spectroscopy, the quality of the arrangement is described in terms of its resolution and depends on the dispersion of the field and the quality of the image.

Apart from the retarding field method, all arrangements that have as yet been used are based on the above points of view.

Let us first consider the retarding field method. The electrons emitted radially from the target move against a spherically symmetric field, and only those reach the spheric collector which have sufficient energy to over come the potential difference. The retarding field curve, from which the energy distribution is obtained by differentiation, is measured at the cage. This method is relatively simple as to the arrangement, and for this reason it is particularly convenient for use in heatable tubes. Provided that the spherical cage is sufficiently great relative to the target and that no tertiary electrons are generated at the inner surface of the cage, an accuracy of 6% of the applied retarding voltage can be reached.[1] It is true, however, that because of subsequent differentiation small accidental errors of measurement will be likely to overshadow the fine structures of the curve.

[1] By private communication from G. Appelt, who undertook an electron-optical examination of this method.

The transverse magnetic field method was first worked out by Ramsauer (*6*) for slow electrons and has since repeatedly been used for determining the energy distribution of S. The method is based on the focusing properties of semispherical electron paths in a homogeneous magnetic field. Because of the aperture error of the mapping, the resolution of this method is linked with the aperture angle of the electron beam. The resolution is dependent on E and can be increased at *ca.* 5 ev up to 0.2 ev. In order to avoid undesired deflection of the primary beam in the magnetic field, the beam must be arranged parallel to the magnetic field. From this follows that the primary beam must be orthogonal to the secondary beam.

The longitudinal magnetic field method makes use of the focusing properties of the long magnetic coil. By a fixed system of diaphragms, only electrons of a definite energy are united in the focal plane, in which the diaphragm of the cage is arranged. If the strength of the magnetic field is varied, electrons of different energy are successively obtained in the collector cage. The method was thoroughly investigated by Kollath (*7*) and used for a series of measurements. Kollath stated a resolution better than 0.5 ev.

The transverse electric field has recently been used by Harrower (*8*) for measuring the energy distribution of S. For the purpose of energy analysis and focusing, he used a cylindrical condenser with 127.2° deflection. The electron beam entering the analyzer is focused on the slit after deflection. The energy distribution is obtained from the current at the cage divided by E. The resolution varies in proportion to $1/E$ accordingly.

Regarding resolution, the three latter procedures are entirely sufficient even for precision measurements. But working with slow electrons gives rise to a number of additional difficulties which may exert a strong influence on the measured results. The most important points to be observed in measurements are the following: The space in front of the emitter must be free of any fields; low space charge must be avoided and the influence of external fields, particularly perturbing magnetic fields, must be excluded as well.

The contact potentials of the electrodes should be known. Lastly, the surface conditions of the target material are of prime importance. Thin adsorbed surface layers—even in monomolecular form—may falsify the result through variation of the work function and may influence the position of the frequency maximum. Particular attention should therefore be paid to highest vacua and clean surfaces.

It must be attributed to the influence of the various sources of error that measurements taken from the same materials by different authors agree only in outline. The data concerning the position of the frequency maximum often differ by several volts.

c. Metals. Observing the necessary precautions, several authors carried out measurements for different metals. Let us take as an example the measurements made by Kollath (*9*), who studied a series of metals by the same

method of measurements. For all metals examined, the distribution curve of true S has a marked maximum between 1.3 and 2.5 ev. At greater energies, the curve drops monotonically to very small values already beyond

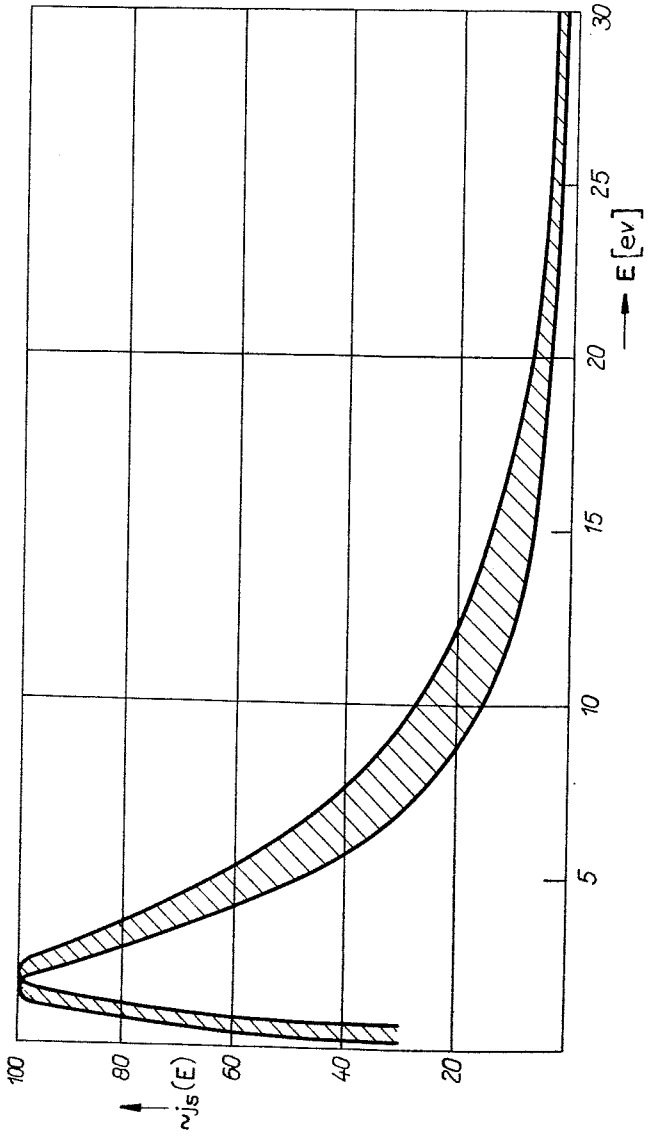

FIG. 3. Range of energy spectra measured for 10 different metals according to R. Kollath [*Ann. Physik* [6] **1**, 357 (1947)].

20 ev. If Kollath's distribution curves for various metals are compared with one another, it is obvious that they are very similar. All distribution curves lie in a narrow range. The spreading is marked in Fig. 3 by the section lined.

The energy distribution for $E_p°$ in 20 ev $< E_p° <$ 1,000 ev is observed as independent of $E_p°$. Changes in the distribution function appear only below $E_p° = 20$ ev (Fig. 4). The distribution curves then get more shallow, the maximum shifts upward, and the half-width increases in the case of Mo as was found by Harrower (*10*).

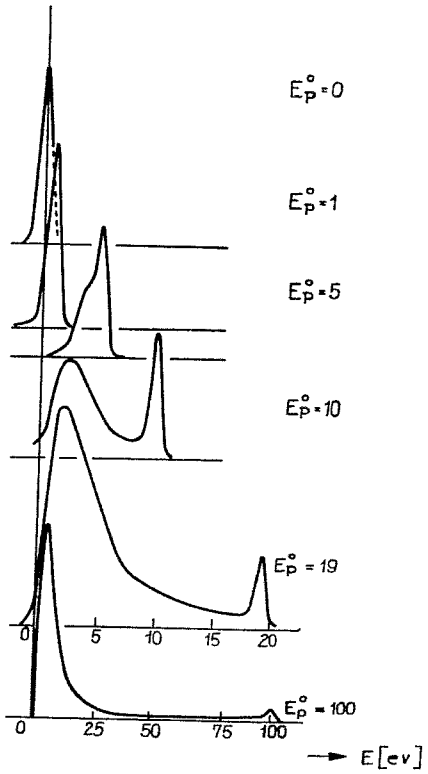

FIG. 4. Energy distribution of secondary and reflected primary electrons from a Mo target for five different values of $E_p°$ between 0 and 20 ev according to G. A. Harrower [*Phys. Rev.* **104**, 52 (1956)].

An investigation of angular dependence of the energy distribution was carried out for Mo and Ag by Kuschnir and Frumin (*11*), who found a shifting of the maximum from 2.5 ev at $\vartheta = 40°$ to 25 ev at $\vartheta = 80°$ (ϑ exit angle). Recently, R. Winkler [*Ann. Physik*, to be published] was able to

show that this surprisingly great shift was caused by uncorrected fields in front of the emitter. Regarding the necessary corrections Winkler obtains for Ni a very small shift of the maximum in the cited direction.

d. Subsidiary maxima. Though normally the energy distribution curves of metals are fairly smooth, they show slight subsidiary maxima if the target is extensively heated before measurement. They were first discovered by Haworth for Mo and later on for Cb (*12*). Similar subsidiary maxima have

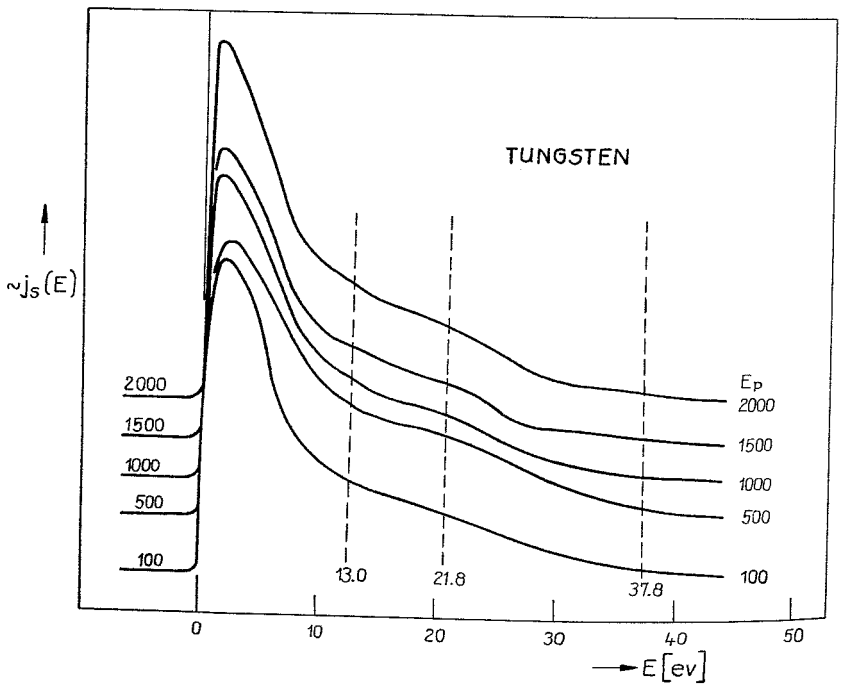

FIG. 5. Energy distribution of secondary electrons from a W target with subsidiary maxima at 13.0, 21.8, and 37.8 ev (the normally larger low-energy maximum has been attenuated) according to G. A. Harrower [*Phys. Rev.* **102,** 340 (1956)].

been found for Be layers and Mo sheets by Kollath (*9*). Recently, Harrower (*8*) has carried out exact measurements for W and Mo. He was able to confirm the SE maxima (Fig. 5) and in addition found a whole series of subsidiary maxima above 50 ev up to 300 ev—i.e., in the range of rediffused *P*. At last O. H. Zinke (*Phys. Rev.* **106,** 1163 (1957)] has found a series of subsidiary maxima of Mg.

We consider the existence of the subsidiary maxima in the energy distribution curves as proved, although the conditions under which they were

obtained seem somewhat unusual, in particular with respect to the extensive heat treatment of the targets.

Harrower (following an idea of Lander, (*13*)) tried to interpret the subsidiary maxima by means of Auger processes. Such a process would be as follows (cf. Fig. 6): An electron is excited from a deep level D by a primary collision. The created empty level is filled with an electron of the next higher band C. The energy $E_D - E_C$ released by this process does not appear as a radiation quantum outside the solid; it is at once used for exciting an electron from the band C or even from the upper band A. The electron then appears outside the solid with an energy $(E_D - E_C) - E_A$. If the S comes

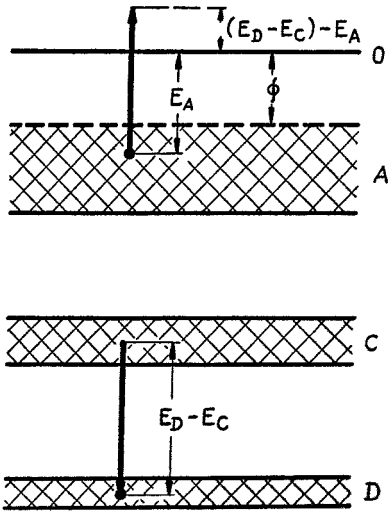

FIG. 6. Schematic representation of the energy band structure of a metal target material with Auger process.

from band C, its energy would be $E_D - 2E_C$. Now for W as well as for Mo, the position of the energy levels is known from X-ray spectra. Calculating the possible Auger processes by means of these levels, Harrower was able to interpret the maxima he had found. The result for W is shown in Table I. The calculated energies agree reasonably well with the measured subsidiary maxima. It must not be overlooked, however, that Table I contains only part of the possible processes. For the time being, it cannot be explained why the other transitions were not found as well.

For theoretical considerations it is necessary to judge how frequent these Auger processes are. Electrons in deep levels are important for energy loss of P as well as for the excitation process of S. It seems to follow from the only

TABLE I. COMPARISON OF CALCULATED AUGER ENERGIES WITH OBSERVED SUBSIDIARY MAXIMA OF W ACCORDING TO HARROWER[a]

Auger transition	Calculated value	Observed value
	Both electrons originally in same band	
$5d - 6sp$	$51 - 2 \times 19 = 13$	13
$5p - 6sp$	$63 - 2 \times 19 = 25$	25
$4d - 6sp$	$245 - 2 \times 19 = 207$	212
$4p - 5d$	$450 - 2 \times 51 = 348$	340
$4p - 5s$	$450 - 2 \times 93 = 264$	264
	Electrons originally in different bands	
$(4s - 4p) - 5s$	$(590 - 450) - 93 = 47$	46
$(4p - 4d) - 5d$	$(450 - 245) - 51 = 154$	160
$(4p - 4d) - 4f$	$(450 - 245) - 31 = 174$	173
$(4d - 4f) - 5d$	$(245 - 31) - 51 = 163$	164
$(4d - 4f) - 6sp$	$(245 - 31) - 19 = 195$	199
$(5s - 4f) - 6sp$	$(93 - 31) - 19 = 43$	38

[a] G. A. Harrower, *Phys. Rev.* **102,** 340 (1956).

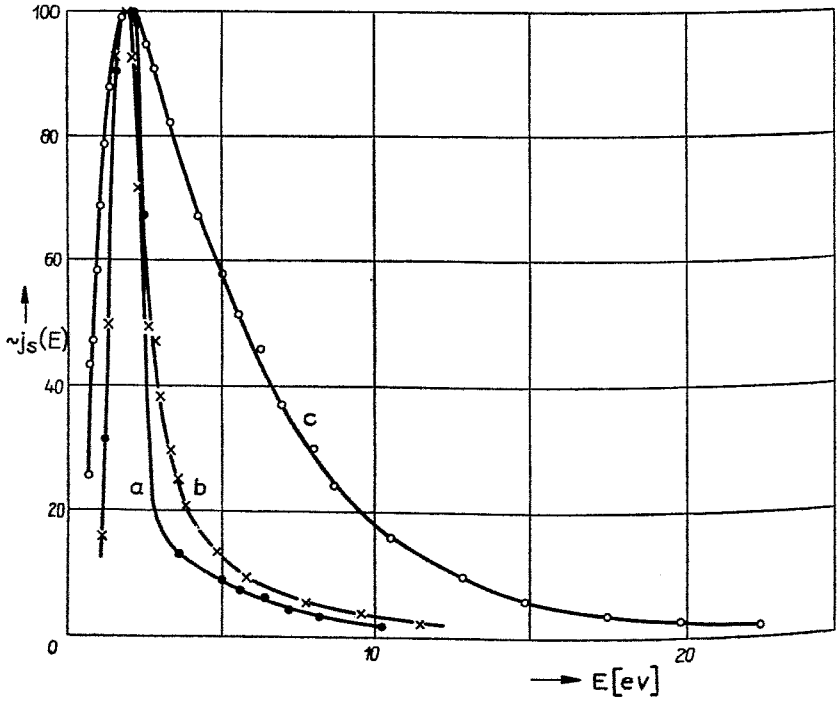

FIG. 7. Energy distribution of secondary electrons emitted by $SbCs_3$ layers and Cs. (a) $SbCs_3$ according to R. Kollath [*Ann. Physik.* [6] **1,** 357 (1947)]. (b) $SbCs_3$ according to G. Appelt and O. Hachenberg [*Ann. Physik.* to be published]. (c) Cs according to R Kollath [*loc. cit.*].

slightly indicated subsidiary maxima that such processes are less frequent, but it cannot be overlooked that the subsidiary maxima may be smeared out by the transport process of the S toward the surface. Evidently, a valid conclusion cannot be drawn without an exact investigation of the transport process.

e. Semiconductors and insulators. Though charge phenomena at the surface and in the layer make it extremely difficult to measure the energy distribution of S emitted by insulators, there are recent measurements from which reliable conclusions can be drawn, for it seems possible to overcome the technical difficulties of measurement by means of the single-pulse method.

Typical semiconductors like Ge, Se, or PbS behave in their energy distribution of S like metals. This does no longer hold for substances with a high SE yield. Compared with metals, Kollath (*9*) found for Cs_3Sb an increased emission of slow electrons in the range 0–4 ev, while the maximum of the distribution remained at the same position (Fig. 7). Measurements carried out by Appelt and Hachenberg (*14*) for Cs_3Sb and Cs_3Bi confirmed this result.

Emission of a relatively greater number of slow electrons is not confined to intermetallic compounds. Also alkali halides as well as alkali earth oxides behave similarly, though perhaps less markedly. After Vudinsky had found enhanced emission of slow S in heated layers, also Shulman and Dementyev (*15*), who used the pulse method, found an increased emission of slow electrons for NaCl and KBr, and more recently Whetten and Laponsky (*16*) for MgO single crystals. So it seems obvious that intensified emission of slow electrons as well as low position of the frequency maxima may be regarded as a phenomenon common to insulators with high SE yields.

The shapes of distribution curves of alkali halides and alkali earth oxides depend on primary energy. Shulman and Dementyev (*15*) pointed out that in the case of NaCl the relative number of slow electrons increases with increasing primary energy for $E_p^\circ < E_{pm}^\circ$.[2] Whetten and Laponsky (*16*) confirmed the same behavior for MgO (Fig. 8).

The existence of subsidiary maxima in the case of insulators has not yet been proved with certainty. Their presence was indicated earlier by Geyer (*17*), yet a confirmation obtained with modern apparatus is still lacking. According to the interpretation of subsidiary maxima by Auger processes in the case of metals, it would be natural to expect similar maxima for the result of later measurements.

f. Qualitative interpretation. The general trend of the energy distribution curves is very similar to a Maxwell distribution (Fig. 3), but there is no physical connection at all between them. Occasional considerations made in this regard are unfounded.

All distributions measured for metals have their maxima near 2 ev,

[2] E_{pm}° defines the primary energy corresponding to the yield maximum (B, 3).

that is to say, at a fairly equal distance above vacuum level. It seems that the existence of this maximum may rather be connected with the escape mechanism than with the inner properties of the solid.

The transport of S towards the surface will contribute to a certain extent to smooth discrete peaks in the distribution function because of inelastic collisions and will lead to an increase of the density of electrons in the vicinity of the Fermi level.

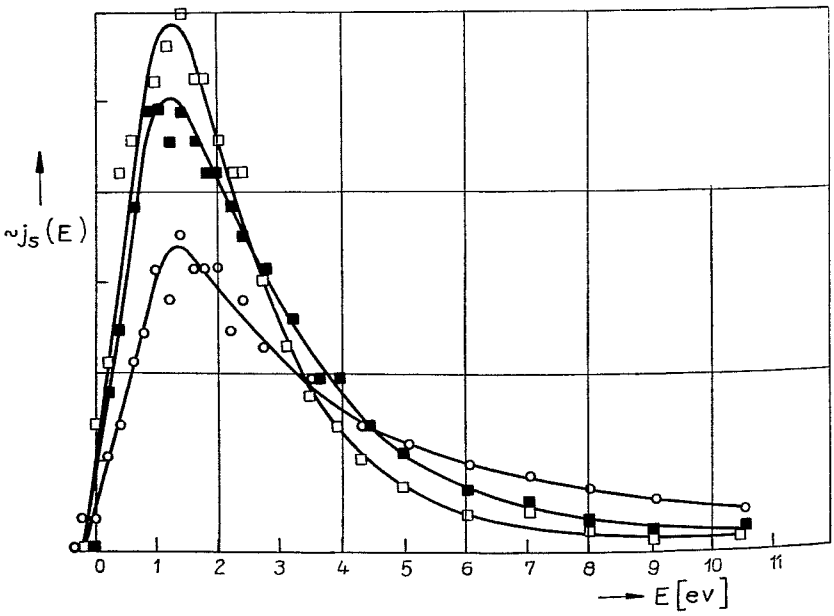

FIG. 8. Energy distribution of secondary electrons from a MgO single crystal target according to N. R. Whetten and A. B. Laponsky [*Phys. Rev.* **107**, 1521 (1957)] at different values of $E_p°$. ○, $E_p° = 100$ ev; ■, $E_p° = 800$ ev; □, $E_p° = 2400$ ev.

The slope of the distribution is strongly influenced by the surface barrier, in particular the maximum of the distribution curve is produced by the latter. Despite the fact that the density of occupied levels in metals increases towards low energies, the strong influence of the surface barrier on slow electrons—closely above vacuum level—results in such a decrease in the number of emitted electrons that a maximum is produced at a nearly constant distance above vacuum level.

The position of the maximum is dependent on the energy angular distribution of the internal excited electrons and on the potential barrier. If there is a low potential barrier, the maximum is generally to be expected

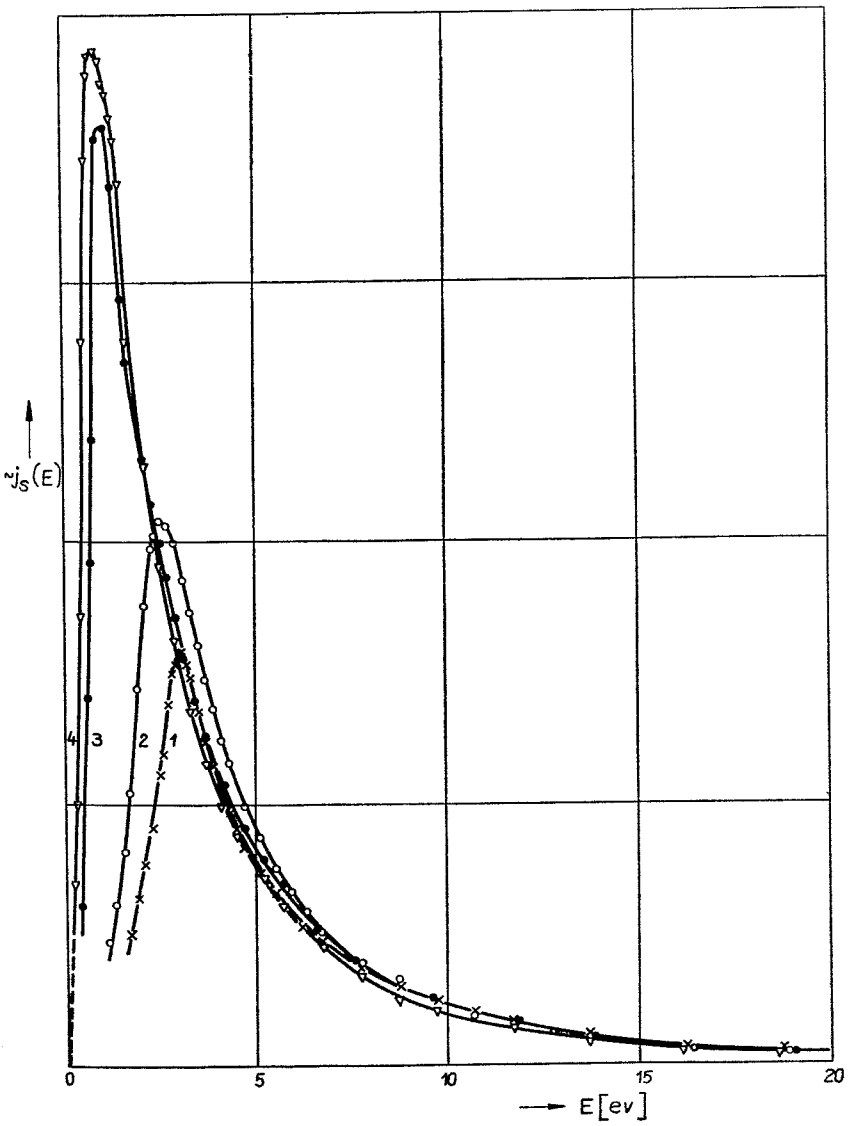

FIG. 9. Energy distribution of secondary electrons emitted by a CsGe target at different forming conditions according to G. Appelt [Thesis, Dresden (1958)]. Curves 1 to 4 correspond to subsequent formation states with decreasing work-function.

at low energies. The energy ($E \approx 1$ ev) at which the maximum occurs in the case of alkali halides points to this direction.

A series of measurements by Appelt (*18*) for GeCs layers represents a striking indication of the influence of the potential barrier on energy distribution. During the formation process, the work function of GeCs layers decreases, as can be inferred from the increase of the photo yield. Distribution curves 1 to 4 shown in Fig. 9 correspond to subsequent formation states with decreasing work function causing a shift of the maximum to lower energies. The yield rises at the same time.

Only above the maximum (at $E > 10$ ev) will the influence of the potential barrier diminish, and here we can relate the particularities of the distribution curve—i.e., especially the subsidiary maxima—with the occupation density of the excited states in the solid itself.

2. Energy Angular Distribution. As stated above, the energy angular distribution is the function which completely describes SE, but measurements of this kind have only[3] been carried out by Jonker (*19, 20*). The main reason for this may be seen in the difficulties regarding the technical apparatus required for these measurements. On the one hand, the cage must be moved around the target in high vacuum; on the other hand, the apparatus must admit a separation of S by their different energies. Jonker solved this difficult problem by using for energy analysis an electric retarding field between two spherically concentric shells. The cage, which is rigidly fixed to the outer shell, can be turned along a slit in the inner shell in opposite direction to the inner shell and to the target connected with it.

a. True secondary electrons. Measurements were carried out for a Ni target at 500-ev primary energy within the range of true S. The author separated the S with $E = 1.5$ ev, 10 ev and 20 ev from the emitted electrons and studied their angular distribution. The result is shown in Fig. 10. It can be seen that the true S leave the surface distributed in first approximation to a cosine law. For the 20-ev electrons, the cosine law is satisfied in an almost ideal manner, as illustrated by the circle inscribed for comparison into Fig. 10. Slower electrons show certain deviations. The distribution is somewhat flattened in the polar diagram. If these deviations are regarded to be valid for the general behavior, and if one takes into consideration that for electron optical reasons the distributions of the electrons with $E \approx 0$ ev must again be a cosine distribution, then the following picture will result: For $E \approx 0$ ev, a pure cosine law is to be expected; with rising secondary electron energy E in Jonker's normalization of the curves, a certain broadening

[3] As was stated above, R. Winkler recently measured angular energy distribution from Ni at $E_p^\circ = 2.10^3$ ev. He found by recalculation that his results are in full agreement with those of Jonker.

of the cosine distribution will be observed, which, however, will have disappeared again at $E = 20$ ev.

The distribution curves are independent of the crystal structure of the target, and no fine structure was to be found in the distribution. The distribution is practically independent of the angle of incidence of the P.

From the cosine distribution of the "true" S follows that the internal S hit the inner surface with a cosine distribution of current density. The distribution of the directions of S within the solid must therefore be isotropic. Thus, we have obtained an important statement which will be used later in the theoretical part. Lastly, the group of curves measured by Jonker

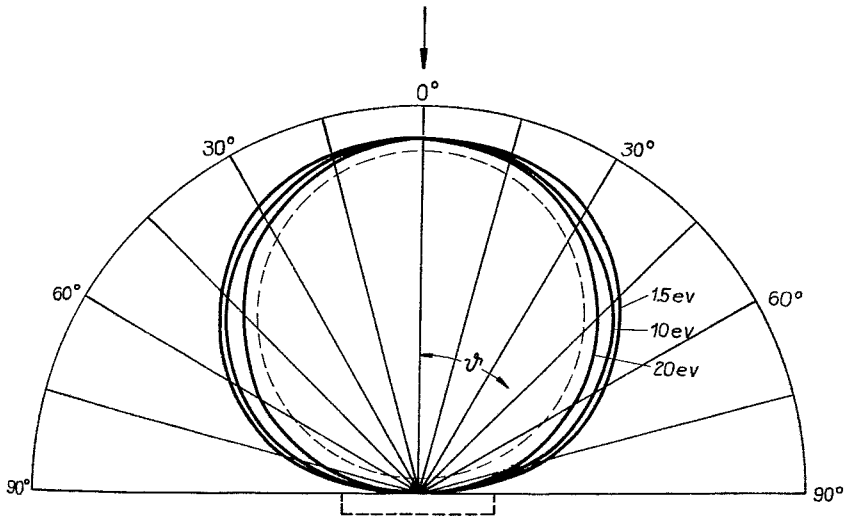

FIG. 10. The energy angular distribution of secondary electrons, with normal incidence of the primary beam according to J. L. H. Jonker [*Philips Research Rept.* **12**, 249 (1957)].

shows that, strictly speaking, the energy distribution of S depends on the angle of escape.[3] For this reason, the method of measuring the energy distribution of a directed beam of S gives only an approximate result for the correct pure energy distribution.

b. Rediffused primaries. An angular distribution which is approximately a cosine distribution was also found for the rediffused primaries ($E > 50$ ev) by Jonker, who examined a Ni target. The angular distribution remains unchanged for all energies within the range 50 ev $< E <$ 450 ev. With oblique incidence of the primary beam, the distribution curves also change very little; the curves are only slightly dented in the direction of the inci-

dent beam. This result is important for the interpretation of the transport process of P in the solid. Hence, the part of primaries appearing in the rediffusion current is distributed isotropically over all directions.

The elastically reflected P behave in a different way. They have a distinct maximum in the direction of the incident beam. Moreover, with oblique incidence of P there will occur distinct peaks in the direction of the "optically" reflected primary beam. A detailed discussion of this seems unnecessary within the scope of this article.

3. Angular Distribution. The pure angular distribution is to be derived from energy angular distribution by integration over the whole energy range of S. For the range of true S of $0 < E < 50$ ev, the pure angular distribution is very closely a cosine distribution, as can immediately be seen from the above discussion on energy angular distribution.

Measurements by Jonker (*19*) for Ni targets confirm the result to be expected. The small deviations in the energy range 1 ev $< E <$ 10 ev that may have appeared in the preceding discussion on energy angular distribution will nearly disappear in measurements of the total emission of electrons.

There is a similar result for rediffused P of the range 50 ev $< E < E_p°$. Their angular distribution is practically a cosine distribution. In the case of rediffused electrons, distribution depends slightly on the angle of incidence of P, but this fact is only of minor importance, considering the present state of the discussion on that process.

It must be stated that the cosine distribution is nearly independent of the primary energy in the range 100 ev $< E_p° <$ 450 ev and has been measured for single crystals as well as polycrystals.

B. Secondary Electron Yield

1. Definition. The number of external S produced by one P in the target is called the "yield". It is an important quantity of SE and has accordingly been measured for numerous substances and under various experimental conditions. Because of the proportionality of primary and secondary currents, the yield is usually defined as the quotient of the electron current i_t emitted by the target divided by the impinging primary electron current i_p:

$$\delta = \frac{i_t}{i_p} \tag{1}$$

On the other hand, δ is dependent on the primary electron energy $E_p°$. The dependence on $E_p°$ supplies the yield curve $\delta(E_p°)$ representing a characteristic curve for each sample. Its general trend has been similar for all substances examined. Beginning at low energies, the yield will increase with

increasing primary energy, pass through a flat maximum δ_m, and then fall off monotonically. Figure 11 shows the typical shape of a yield curve, recording in addition a few characteristic quantities that will be used in a later chapter. On principle it would be possible, as we pointed out above, to calculate the yield δ defined in (1) in a complete theory of SE. Current theories, however, always calculate a "yield" by considering the quotient of the current i_s of true S and the current of penetrating P. If one wishes to compare this theoretical yield with yield measurements, the latter have to be "corrected". As is shown by the energy distribution of the S emitted by the target, three groups of S are to be distinguished: true S, rediffused P, and elastically reflected P. That is to say, $i_t = i_s + \eta i_p + r i_p$, if rediffused ($\eta$) and reflected ($r$) P are indicated as fractions of i_p. When neglecting the excitation of S by rediffused P, we shall obtain the following definition for yield

$$\delta_{\text{corr}} = \frac{\delta - (\eta + r)}{1 - r} \tag{2}$$

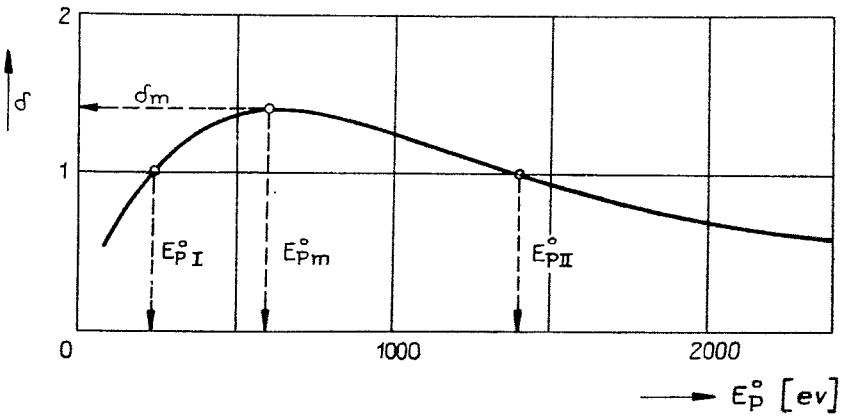

FIG. 11. The general shape of the yield curve δ ($E_p°$).

2. Method of Measurement. In general, the measurement of the yield is simple, particularly for metals. The P coming from one of the usual electron guns hit a plate surrounded as completely as possible by a spherical collector (Fig. 12). For positive voltage at the collector, i_t can be measured directly on the latter. With a second instrument applied to target and collector combined, we can at the same time obtain i_p, that is, the total amount of electrons entering into the collector sphere through the diaphragm. Thus, we have determined the yield δ. Notwithstanding a properly chosen geometry of the electrodes, a source of error in measurement caused

by the occurrence of tertiary electrons has to be taken into account. These electrons are generated by reflected and rediffused P at the inner surface of the collector and can partly return to the target. Tertiary electrons can effectively be suppressed by arranging a grid with a slightly negative potential (≈ -10 ev) before the inner surface of the collector. Besides that, such an arrangement enables us, by properly choosing the potentials at the electrodes, to separate the true S from the rediffused and reflected P, and thus to determine the "true yield" by (2).

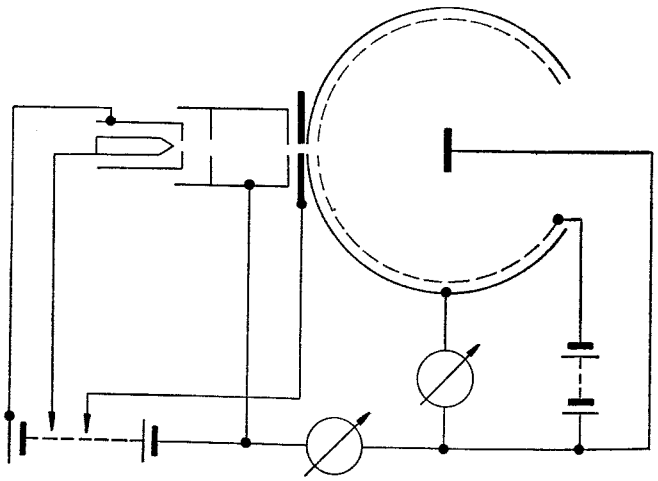

FIG. 12. Device to determine the yield and rediffusion coefficient of metals and semiconductors.

In yield measurements, the targets must be prepared most carefully. Adsorbed layers can have a strong influence on the measurements even if they are only monomolecular layers because they alter the work function. In order to obtain accurate yield values, one should preferably evaporate polycrystalline layers in highest vacuum ($< 10^{-10}$ Torr) and use them for measurements without delay. This procedure must certainly be given preference to the practice of the extremely prolonged heating of the samples that has hitherto been in use.

In the case of semiconductors and insulators, yield measurements are made much more difficult by the existence of surface and inner charges of the solid. These difficulties are overcome by the dynamic methods with periodic pulses introduced by Salow (*21*). This procedure certainly avoids surface charges, but it does not guarantee that inner charges are fully compensated. A solution of the latter problem was attained by Johnson (*22*)

by means of pulsing methods with single pulses of low current intensity. After each measuring pulse, full compensation of the charges is effected through a heat treatment of the sample. The technical details of the different procedures have been described in the preceding surveys (*1*, *2*, *5*), so that we need not discuss them here any further.

3. Metals. a. Maximum yields. During the last few years yield measurements of metals have not given remarkable new results. The yield data for metals compiled by Kollath (*5*) are shown in Table II.

TABLE II. MAXIMUM YIELDS FROM DIFFERENT METALS

Atomic number	Element symbol	δ_m	$E_{pm}°$	$E_{pI}°$	$E_{pII}°$	References
3	Li	0.5	85	—	—	Kollath[a]
4	Be	0.5	200	—	—	Kollath[a]
11	Na	0.82	300	—	—	Woods[b]
12	Mg	0.95	300	—	—	Kollath[a]
13	Al	0.95	300	—	—	Kollath[a]
19	K	0.7	200	—	—	Kollath[a]
22	Ti	0.9	280	—	—	Kollath[a]
26	Fe	1.3	(400)	120	1,400	Kollath[a]
27	Co	1.2	(500)	200	—	Kollath[a]
28	Ni	1.35	550	150	1,750	Kollath[a]
29	Cu	1.3	600	200	1,500	Kollath[a]
37	Rb	0.9	350	—	—	Kollath[a]
40	Zr	1.1	350	175	(600)	Kollath[a]
41	Cb	1.2	375	175	1,100	Kollath[a]
42	Mo	1.25	375	150	1,300	Kollath[a]
46	Pd	>1.3	>250	120	—	Kollath[a]
47	Ag	1.47	800	150	>2,000	Kollath[a]
48	Cd	1.14	450	300	700	Kollath[a]
50	Sn	1.35	500	—	—	Kollath,[a] Woods[b]
51	Sb	1.3	600	250	2,000	Kollath,[a] Appelt[c]
55	Cs	0.72	400	—	—	Kollath,[a]
56	Ba	0.82	400	—	—	Kollath,[a]
73	Ta	1.3	600	250	>2,000	Kollath,[a]
74	W	1.35	650	250	1,500	Kollath[a]
78	Pt	1.5	750	350	3,000	Kollath,[a] Appelt[d]
79	Au	1.45	800	150	>2,000	Kollath,[a]
80	Hg	1.3	600	350	>1,200	Kollath,[a]
81	Tl	1.7	650	70	>1,500	Kollath,[a]
82	Pb	1.1	500	250	1,000	Kollath,[a]
83	Bi	1.5	900	80	>2,000	Kollath,[a] Appelt[c]
90	Ta	1.1	800	—	—	Kollath[a]

[a] R. Kollath, *Handbuch d. Physik* **21**, 232 (1956).
[b] J. Woods, *Proc. Phys. Soc.* (*London*) **B67**, 843 (1954).
[c] G. Appelt and O. Hachenberg, *Ann. Physik*, to be published.
[d] G. Appelt, unpublished (1955).

The differences between the data given by different authors for the respective metals (±7%) are relatively large, considering that measurements can be obtained by means of comparatively simple methods of measurement. In the first line, the differences will be due to different surface structure of the samples examined and to adsorbed surface layers. In comparing the yields with other properties of metals, one has to take into account the disagreement between the measured data.

Maximum yields from metals are between 0.6 and 1.7. The differences as from metal to metal are remarkably small compared with other characteristic data of metals, such as density, conductivity, or the number of electrons per cubic centimeter, which vary over a much wider range.

Nevertheless, Table II enables us to ascertain two different groups of metals. One group is formed by the alkalis and earth alkalis along with a few other light elements, whose maximum yields range between 0.6 and 1. The metals of that group are characterized at the same time by a relatively low work function. A second group is formed by the heavy metals, whose yields range between 1.1 and 1.7. This group includes the bulk of the other metals.

Numerous attempts were made in the past to correlate the variation of yield as from metal to metal with other characteristic data of the metals in order to obtain a clue as to which properties of metals have the predominant influence on the yield. Thus, McKay (*1*) tried to correlate the maximum yield with the work function of metals. He found that high yields are connected with high work functions and vice versa. This qualitative relation between work function and yield seems somewhat surprising. Obviously, one has to suppose that a complicated relation is hidden behind this connection.

Bruining (*2*) compared the maximum yields with the density of metals and found a loose connection such that the yield will increase with density. Finally, Sternglass (*23*) correlated the maximum yield with the position of the metals within the periodic system of elements. The yield rises in each horizontal line from the alkalis to the multivalent metals. Certainly a greater importance must be attributed to this remarkable relation.

b. Shape of yield curves. The dependence of the yield on primary energy is similar for all metals. Baroody (*24*) made this similarity particularly conspicuous by normalizing the curves for different metals in such a way that he plotted δ/δ_m against E_p°/E_{pm}° as abscissa. Presented in this form, the curves for the different metals lie in a narrow range, so that the presentation might be called a universal yield curve for metals (Fig. 13). Together with Table II, it permits a sufficient characterization of the yield curve of metals.

A few remarks have still to be made concerning the shape of the curve for low and very high primary energy. With respect to low primary energy, investigations made by Shulman and Myakinin (*25*) and those by Harrower

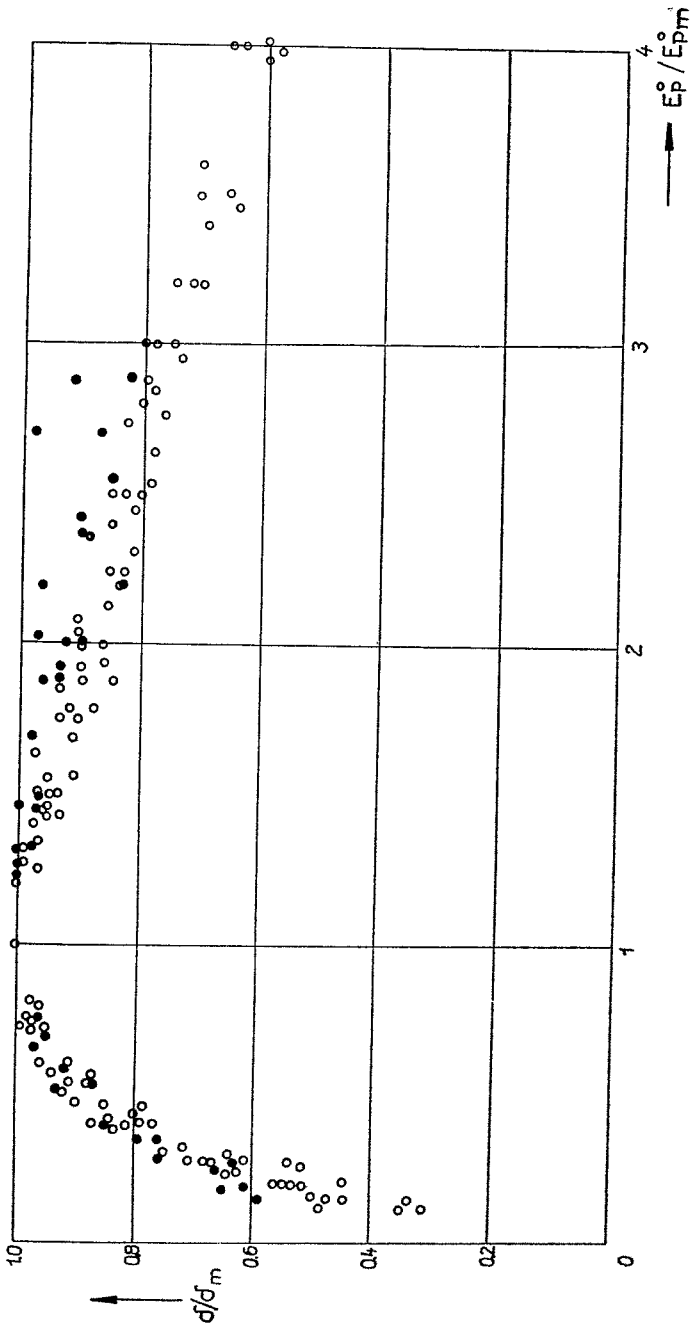

FIG. 13. Normalized yield for different metals according to R. Kollath [*Handbuch d. Physik* **21**, 232 (1956)]. Open circles mean corrected yields with respect to rediffused P.

(*10*) must be mentioned. In both studies true S are separated from reflected P by means of the energy distribution curve. True S are shown to occur only above $E_p^\circ \approx 4$–7 ev. From then on their number rises monotonically with E_p°. Above $E_p^\circ = 20$ ev, the form of the spectrum of true S remains invariant.

For high primary energies ($E_p^\circ \geqslant 10{,}000$ ev) the electrons released from the sample increasingly contain rediffused P. The share of true S is rather small. According to Trump and van de Graaff (*26*), it decreases to 0.12 for W and to 0.025 for C at 300 kev. As was shown by Palluel (*27*) and Holliday and Sternglass (*28*) the number of rediffused P depends on the atomic number of the sample. As rediffused P passing through the surface layer will also excite S, the true S, at high primary energy, δ will contain a part which is equally dependent on the atomic number.

4. Semiconductors and Insulators. a. Maximum yields. If we exclude the extremely high yields occasionally found which are possibly caused by field-enchanced emission, we can define the range of maximum yields as approximately

$$1 < \delta_m < 20$$

At the lower limit of this range we have the well-known semiconductive elements Ge, Si, Se, and also the typical semiconductors Cu_2O and PbS; quartz, mica, or CdS have a somewhat higher yield, and the same can be said of glasses. Substances with high yields include intermetallic compounds of the types A_IB_V and A_IB_{IV}. The highest yields are found for alkali halides, alkali oxides, and alkali earth oxides. Because of their high yield and their resistivity against electron bombardment, the latter have become especially important for technical purposes. In the forming process, various alloys such as AlMg, AgMg, CuBe, NiBe, and others apparently produce MgO or BeO spots or layers at the surface, which are responsible for the high yields (*5*). A survey of the values δ_m and E_{pm}° measured for the most important substances is given in Table III.

The differences between the data shown in Table III for the same substances are extraordinarily great. On the one hand, you can find divergences caused by the use of different methods of measurement. So measurements made on insulators can be strongly influenced by fields existing within the substances (*29*), and the data obtained with the new method of single pulses of low current intensity doubtlessly must be preferred to those obtained with earlier methods. On the other hand, the yield of substances with a high yield depends in a remarkable degree on the individual properties of the sample examined, such as crystal state, lattice imperfections, or surface structure. According to Bruining and de Boer (*30*) and to Knoll, Hachenberg, and Randmer (*31*), slight electron bombardment during the

measurements is sufficient to decrease the yield of KCl permanently. Studying NaCl crystals, Shulman (*32*) found that a crystal polished with water has a maximum yield of $\delta_m = 8$, while immediately after splitting the yield is 13 — 16. From previous experience with crystalline insulators one is tempted to regard the higher values as representative for pure crystals.

b. Shape of yield curves. The shape of $\delta(E_p^\circ)$ from semiconductors and insulators is roughly similar to that of metals. The yield first increases with increasing primary energy, then passes through a flat maximum, and decreases again with high primary energy. Generally, it can be stated that E_{pm}° is high for substances with high maximum yields. The maximum can move up to 1,500 ev. If one tries, however, to represent all the curves that have been obtained from insulators by a universal curve, one finds for $E_p^\circ > E_{pm}^\circ$ a stronger divergence for the curves of different substances than it was the case with metals. (*14*).

c. Qualitative interpretation. Measurements by the pulse method with a very low current intensity generally show the *same* high yields as earlier measurements with static methods. The results can be regarded as a further confirmation that high yields must be attributed to the substances themselves and that they are not caused by field-enhanced emission within the layer.

Which of the fundamental properties of semiconductors and insulators are responsible for the greater variation range of the yield cannot be made out with certainty for all cases. At least we have certain ideas based on the energy band model of the solids, and they proved to be useful.

The basic feature characterizing a semiconductor is the position of optical lattice absorption within the spectrum. From it we find the amount of energy necessary to raise an electron from the highest occupied level into the next higher excited state. Since, with rare exceptions, the first excited level lies in the conduction band, we are used to identify this energy with the distance of the conduction band from the valence band in the band model of semiconductors.

This energy plus the energy difference between vacuum level and the bottom of the conduction band is therefore necessary to produce one S in the solid. Now the observed high yields of substances with great energy gap are probably not caused by an increased source density of the S produced, since it may be assumed that because of the increased energy gap the excitation rate of S will decrease.

The high yields therefore must be due to an increase of the depth of escape. The following mechanism for energy loss of S may play a role in insulators: (1) electron-phonon interaction, (2) interaction with valence electrons, if the excitation energy of S in the upper band is greater than the

TABLE III. MAXIMUM YIELDS FROM SEMICONDUCTORS AND INSULATORS

Group	Substance	δ_m	E_{pm}°	References
Semiconductive elements	Ge (single crystal)	1.2–1.4	400	*a,b,c,d*
	Si (single crystal)	1.1	250	*a*
	Se (amorphous)	1.3	400	*c,e*
	Se (crystal)	1.35–1.40	400	*c,e*
	C (diamond)	2.8	750	*f*
	C (graphite)	1	250	*g,h*
	B	1.2	150	*a*
Semiconductive compounds	Cu_2O	1.19–1.25	400	*i,j*
	PbS	1.2	500	*k*
	MoS_2	1.10		*i*
	MoO_2	1.09–1.33		*l*
	WS_2	0.96–1.04		*i*
	Ag_2O	0.98–1.18		*l*
	ZnS	1.8	350	*m*
Intermetallic compounds	$SbCs_3$	5–6.4	700	*n,o,p*
	SbCs	1.9	550	*n*
	$BiCs_3$	6–7	1,000	*n*
	Bi_2Cs	1.9	1,000	*n*
	GeCs	7	700	*d*
	Rb_3Sb	7.1	450	*q*
Insulators	LiF (evaporated layer)	5.6		*i*
	NaF (layer)	5.7		*i*
	NaCl (layer)	6–6.8	600	*i,r,s*
	NaCl (single crystal)	14	1,200	*t,u,v,w,x*
	NaBr (layer)	6.2–6.5		*i*
	NaBr (single crystal)	24	1,800	*x,y*
	NaJ (layer)	5.5		*i*
	KCl (layer)	7.5	1,200	*i,z*
	KCl (single crystal)	12		*v,a'*
	KJ (layer)	5.5		*i*
	KJ (single crystal)	10.5	1,600	*w*
	RbCl (layer)	5.8		*i*
	KBr (single crystal)	12–14.7	1,800	*w,a'*
	BeO	3.4	2,000	*b'*
	MgO (layer)	4	400	*i,c'*
	MgO (single crystal)	23	1,200	*d',e'*
	BaO (layer)	4.8	400	*f'*
	BaO—SrO (layer)	5–12	1,400	*g'*
	Al_2O_3 (layer)	1.5–9	350–1,300	*s,b',f',t*
	SiO_2 (quartz)	2.4	400	*h',s*
	Mica	2.4	300–384	*s*

Glasses	Technical glasses	2–3	300–420	*s*
	Pyrex	2.3	340–400	*s,i'*
	Quartz-glass	2.9	420	*s,h'*

[a] L. R. Koller and J. S. Burgess, *Phys. Rev.* **70,** 571 (1946).
[b] J. B. Johnson and K. G. McKay, *Phys. Rev.* **93,** 668 (1953).
[c] H. Gobrecht and F. Speer, *Z. Physik* **135,** 602 (1953).
[d] G. Appelt, Thesis, Dresden (1958).
[e] G. Oertel, *Ann. Physik* [7] **1,** 305 (1958).
[f] J. B. Johnson, *Phys. Rev.* **92,** 843 (1953).
[g] H. Bruining, Thesis, Leiden (1938).
[h] E. J. Sternglass, *Phys. Rev.* **80,** 925 (1950).
[i] H. Bruining and J. H. de Boer, *Physica* **6,** 823 (1939).
[j] N. B. Gornij, *J. Exptl. Theoret. Phys.* (*U.S.S.R.*) **26,** 79 (1954).
[k] O. Hachenberg, unpublished (1944).
[l] A. Afanasjewa, P. W. Timofejew, and A. Ignaton, *Physik. Z. Sowjetunion* **10,** 831 (1936).
[m] N. B. Gornij, *J. Exptl. Theoret. Phys.* (*U.S.S.R.*) **26,** 88 (1954).
[n] G. Appelt and O. Hachenberg, *Ann. Physik,* to be published.
[o] N. D. Morgulis and B. I. Djatlowitskaja, *J. Tech. Phys.* (*U.S.S.R.*) **10,** 657 (1940).
[p] P. V. Timofejew and J. Lemkowa, *J. Tech. Phys.* (*U.S.S.R.*) **10,** 20 (1940).
[q] W. Kanef, *Ann. Physik,* to be published.
[r] M. M. Vudinsky, *J. Tech. Phys.* (*U.S.S.R.*) **9,** 271 (1939).
[s] H. Salow, *Z. tech. Physik* **21,** 8 (1940); *Physik. Z.* **41,** 434 (1940).
[t] A. R. Shulman, W. L. Makedonsky, and J. D. Yaroshetsky, *J. Tech. Phys.* (*U.S.S.R.*) **23,** 1152 (1953).
[u] A. R. Shulman, *J. Tech. Phys.* (*U.S.S.R.*) **25,** 2150 (1955).
[v] A. R. Shulman and B. P. Dementyev, *J. Tech. Phys.* (*U.S.S.R.*) **25,** 2256 (1955).
[w] D. N. Dobrezow and A. S. Titkow, *Doklady Acad. Nauk U.S.S.R.* **100,** 33 (1955).
[x] D. N. Dobrezow and T. L. Matskevich, *J. Tech. Phys.* (*U.S.S.R.*) **27,** 736 (1957).
[y] T. L. Matskevich, *J. Tech. Phys.* (*U.S.S.R.*) **26,** 2399 (1956).
[z] M. Knoll, O. Hachenberg, and J. Randmer, *Z. Physik* **122,** 137 (1944).
[a'] B. Petzel, Thesis, Dresden (1958).
[b'] K. H. Geyer, *Ann. Physik* [5] **42,** 241 (1942).
[c'] G. Blankenfeld, *Ann. Physik* [6] **9,** 48 (1950).
[d'] N. R. Whetten and A. B. Laponsky, *J. Appl. Phys.* **28,** 515 (1957).
[e'] J. B. Johnson and K. G. McKay, *Phys. Rev.* **91,** 582 (1953).
[f'] H. Bruining and J. H. de Boer, *Physica* **5,** 17 (1938).
[g'] J. B. Johnson, *Phys. Rev.* **73,** 1058 (1948).
[h'] H. Krüger, Thesis, Berlin (1957).
[i'] C. W. Mueller, *J. Appl. Phys.* **16,** 453 (1945).

energy gap, and finally (3) interaction with lattice defects. In the case of insulators with great energy gap, mechanism (2) is of no importance. In the case of metals, mechanisms (1) and (3) are less effective than the interaction with free electrons, which is responsible for the relatively low yields of metals.

5. Temperature Dependence. a. General considerations. The above con-

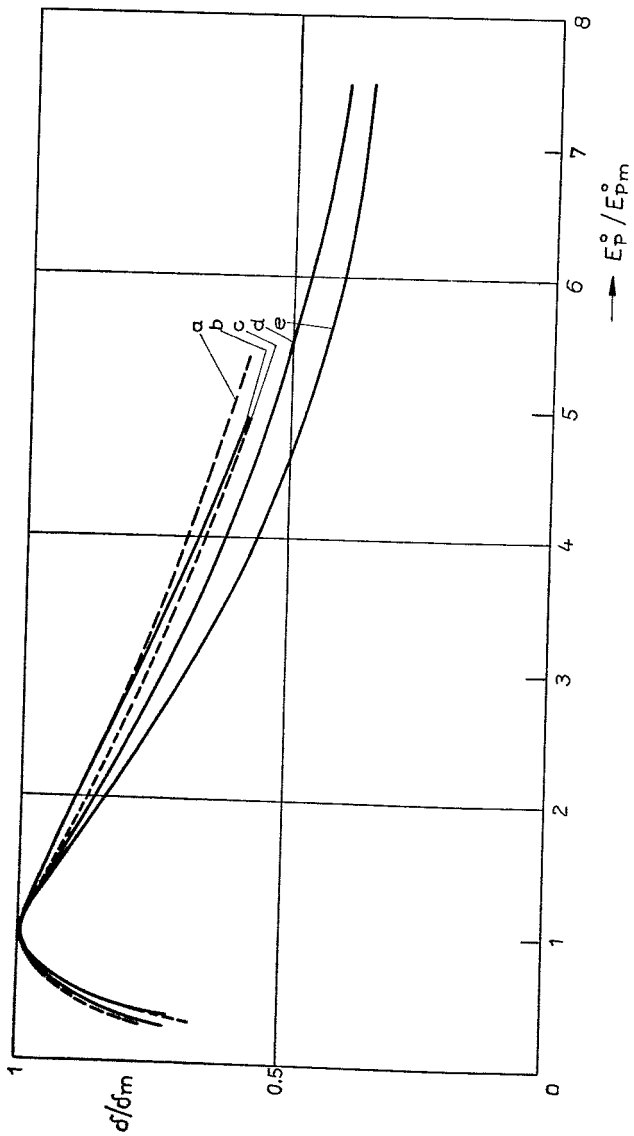

FIG. 14. Normalized yield curves for different materials. (a) $SbCs_3$. (b) Mean yield curve of the metals. (c) KBr according to B. Petzel [Thesis, Dresden (1958)]. (d) Quartz. (e) Glass according to H. Salow [*Z. tech. Physik* **21**, 8 (1940); *Physik. Z.* **41**, 434 (1940)].

clusions can be proved by the examination of the temperature-dependence of the yield. Of course, we must confine ourselves to phenomena connected with reversible variations of the yield. Those variations which evidently originate from variations of adsorbed surface layers or are connected with permanent changes of the crystal are not taken into consideration. Since interaction processes between excited S and the various components of the solid have a direct effect on the range of S and hence on the yield, a certain classification of the phenomena in the case of semiconductors and insulators could be made (cf. Hachenberg, *33*). Obviously, solids can be classified by the following groups:

1. In crystalline solids with great energy gap and relatively few lattice defects, interaction of S with lattice vibrations is predominant. The range of S, and hence the yield, becomes temperature-dependent. They must decrease with rising temperature.

2. If in solids the number of free electrons in the conduction band is sufficiently high, the interaction of S with lattice vibrations is overshadowed by interaction with free electrons.

3. In the case of a small energy gap, interactions of S with electrons of the valence band become most important; semiconductors of this group will behave in a similar manner as metals.

4. Finally, in a solid with considerable disorder, in extreme cases in an amorphous solid, the range of S will no longer depend on interaction with lattice vibrations; solids of this kind should not show any dependence of the yield on temperature.

b. Experimental results. For metals, where measurements can be carried out with some ease, the result of recent investigations is rather unequivocal. The yield is constant in the whole temperature range measured. Morotsov (*34*) and Wooldridge (*35*, *36*) found that the temperature coefficient of the yield is smaller than the temperature coefficient of linear extension. Blankenfeld (*37*) too, found no variations $> 1\%$ for Ni in the temperature range from 20° to 400° C. Only Sternglass (*38*) found a temperature dependence, which, however, may be due to adsorption layers at the surface in particular, since he did not use a tube that could be subjected to heat treatment.

Of greater interest for our discussion are the results obtained from semiconductors and insulators. For Ge, Johnson and McKay (*39*) found a continuous decrease by 5% in a temperature range of 20° to 600° C. In spite of different donations with activators, the decrease remained the same for all samples.

Ge has diamond structure; the energy gap between valence band and conduction band is 0.78 ev, the electron affinity is nearly 4.4 ev. A rise in temperature mentioned above is combined with an increase in the number of conduction electrons for pure Ge samples, e.g., from 6×10^{14} per cm^3

to 7×10^{16} electrons per cm^3; since, on the other hand, for samples doped with Ga and Sb the density of conduction electrons rises from 3.4×10^{18} to 3.5×10^{18} electrons per cm^3, the very different changes in the density of conduction electrons could not have effected the observed change in the yield that is the same in all cases. It is to be supposed, therefore, that the yield is largely independent of the density of conduction electrons in the conduction band for electron densities $< 10^{18}$ per cm^3. The diffusion of S is mainly determined by interaction with valence electrons and partly by interaction with lattice vibrations, as is proved by the small temperature effect. Thus Ge belongs to those solids which are characterized by group 3.

Arranging intermetallic compounds of types A_IB_V and A_IB_{IV} into the above groups presents more difficulties. Cs_3Sb layers were examined by Appelt and Hachenberg (*14*) and CsGe layers by Appelt (*18*) as to the dependence of the yield on temperature. As both types of layers are very unstable compounds that are subject to changes under the influence of temperature, measurements can be made only under great precautions. Nevertheless, it was possible also in these cases to prove a real dependence of the yield on temperature in a range of $-30°$ to $+70°$ C. The energy gap in the case of Cs_3Sb amounts to 1.2 ev. The layers apparently take up a surplus of Cs atoms into the lattice. Thus, the diffusion of S will largely depend on interaction with valence electrons and lattice imperfections and only to a lesser degree on interaction with lattice vibrations.

Glasslike insulators must be regarded as solids with a high degree of disorder. As these absorb only in the far ultraviolet, interaction with valence electrons is rather improbable. Thus, the mobility of S is predominantly determined by the degree of disorder. Measurements on Pyrex glass by Mueller (*40*), on technical glasses by Blankenfeld (*37*) and by Shulman, Makedonsky, and Yaroshetsky (*41*), and on quartz glass by Krüger (*42*) agree in showing no dependence of the yield on temperature, so that this group of substances has obviously to be arranged under group 4.

A marked dependence of the yield on temperature is to be expected for alkali halide single crystals as well as alkaline earth oxide crystals. Resulting from the great energy gap (≈ 10 ev) and the relatively small amount of lattice imperfections in such crystals, excited electrons can spread in the conduction band over relatively wide ranges; the latter are predominantly limited by interaction with lattice vibrations. With rising temperature, the number of lattice vibrations increases nearly proportional to T, and the range decreases correspondingly. Now if the range of P is smaller than or similar to that of S, variation of the depth of escape has no remarkable influence on the yield. On the other hand, the yield must decrease in proportion with the depth of escape for primary energies $E_p° > E_{pm}°$.

A first estimation of the range of the S was attempted by Hachenberg

(*33*); he found a dependence of the depth of escape as proportional to $1/T$. An improved investigation of the diffusion process was carried out by Dekker (*43*, *44*) who found a dependence of the depth of escape d_s that can be approximately described by

$$d_s \sim T^{-\frac{1}{2}}$$

Thus, it has become highly important in yield measurements to determine exactly the dependence of the yield on temperature in the range $E_p^\circ > E_{pm}^\circ$.

Knoll, Hachenberg, and Randmer (*31*) determined the temperature-dependence of the yield by a static method for evaporated layers of KCl and found $\delta \sim T^{-1}$. Today it is clear that such measurements should be carried out only with good single crystals having a perfect surface and only by means of a pulse method with the lowest possible current intensity. A surface altered by polishing or corrosion is capable to blot out the whole temperature effect of the yield, as was shown by Shulman (*32*). Measurements satisfying the above demands were carried out by Johnson and McKay (*45*) for MgO crystals. For $E_p^\circ = 2000$ ev, they found $\delta_1/\delta_2 = 0.78$ for $T_1 = 1013°$ K and $T_2 = 298°$ K, which approaches the law $\delta \sim T^{-\frac{1}{2}}$. For KCl, KI, and KBr, Shulman and Dementyev (*15*) found a temperature dependence of the yield between 0° and 300° C, which can also be described by the relation proposed by Dekker. Strikingly high yields and also marked temperature dependence was found by Matskevich (*46*) for a special NaBr sample. For $T_2 = 300°$ K and $T_1 = 600°$ K, he obtained $\delta_1/\delta_2 = 0.4$, while 0.72 would have to be expected according to the relation proposed by Dekker. The observed variation approximately corresponds with a law $\delta \sim T^{-1,2}$. Finally, Petzel (*47*) made a series of measurements on KCl and KBr; Fig. 15 gives the yield curves for KBr and Fig. 16 shows ln δ for six different values of E_p° plotted against ln T in the case of KCl. For $E_p^\circ > 4$ kev, the measurements satisfy the $T^{-\frac{1}{2}}$ law. While the stronger dependence on temperature found by some authors may be attributed to a secondary effect—possibly to field-enhanced emission, which decreases when temperature rises—there are, on the other hand, samples with surface imperfections showing too little influence of temperature. Nevertheless, the experimental results obtained up to date may be regarded as a confirmation of the ideas developed.

To conclude with, let us point out that the shape of yield curves also shows a dependence on temperature. Particularly the position of the maximum shifts to lower values with rising temperature. As shown in Fig. 15 for KBr, the maximum shifts from 1,600 to 1,300 ev at a temperature variation from 35° to 300° C, which indicates a decrease of depth of escape of S.

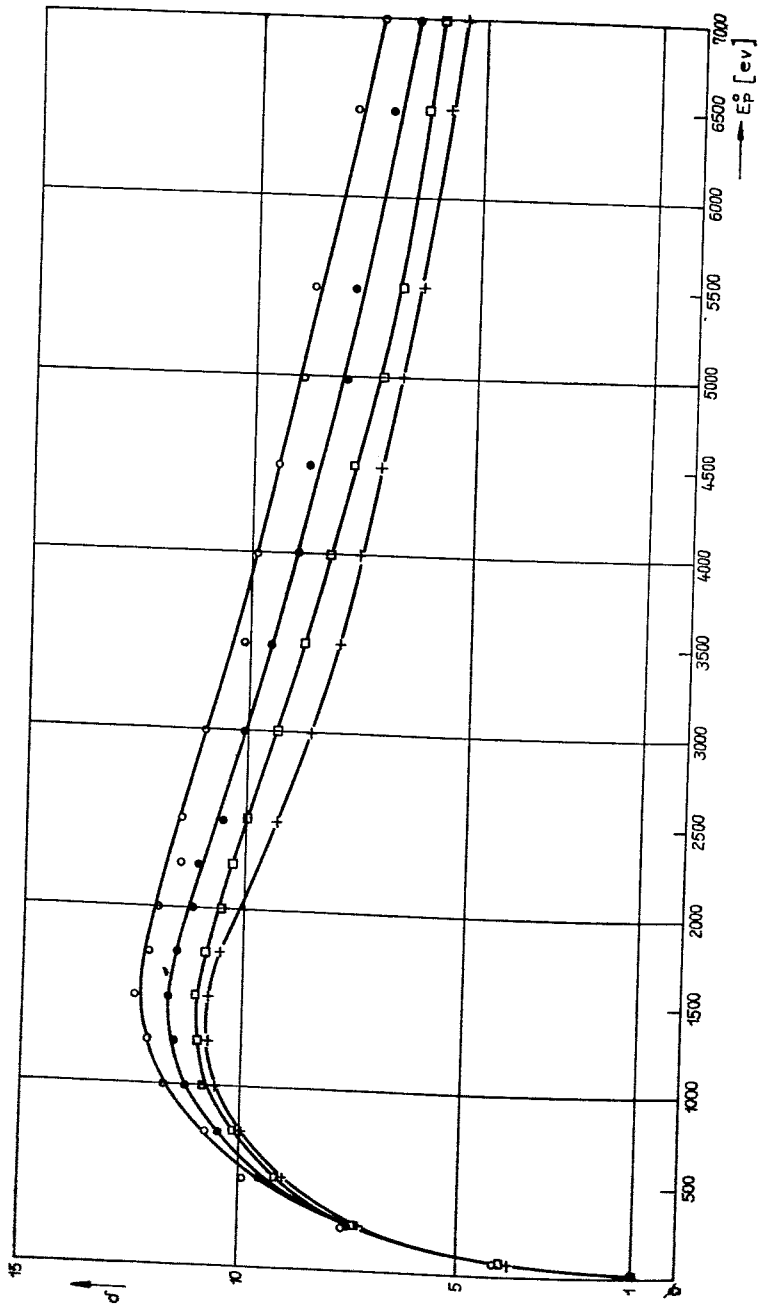

FIG. 15. Yield curves of a KBr single crystal at different values of temperature. ○T = 35° C. ●T = 100° C. □T = 200° C. +T = 300° C. [B. Petzel, Thesis, Dresden (1958)].

6. Influence of Work Function on Yield. The influence of the potential barrier at the surface on yield is fully ascertainable. From measurements by Jonker we know that the angular distribution of internal S in a solid is isotropic; the electron current density impinging on the surface from the inside, therefore, has a cosine distribution. If, in addition, the energy distribution of the internal electrons is known the influence of the potential barrier can be stated explicitly (cf. Sec. IV,E).

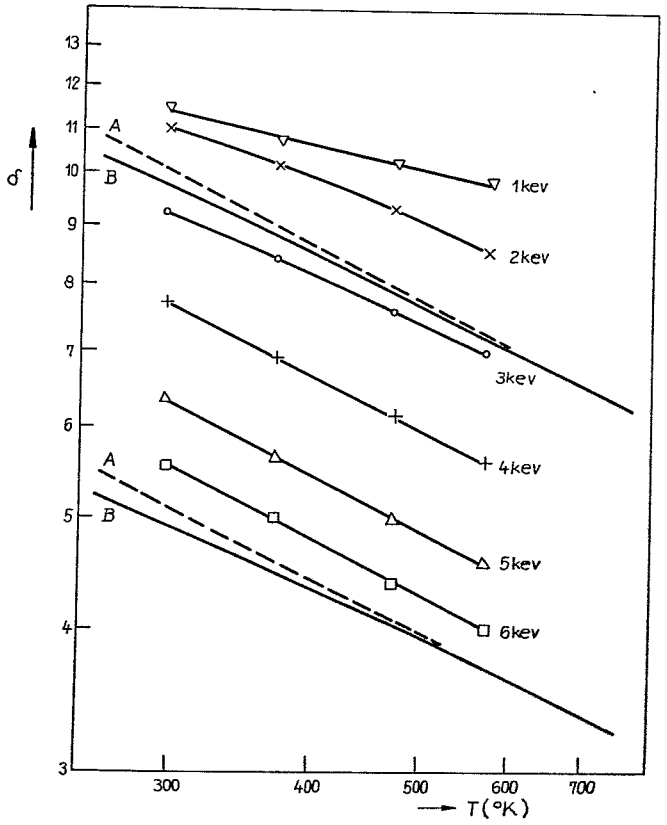

FIG. 16. Variation of yield of a KCl single crystal target with temperature at different values of $E_p°$. Curve A $\sim T^{-1/2}$. Curve B: $\sim\{2[\exp.(h\nu/kT) - 1]^{-1} + 1\}^{-1/2}$ ($\nu = 6.3 \times 10^{12}$ cps). [B. Petzel, Thesis, Dresden (1958)].

For an experimental examination of the influence of work function, a metallic target whose work function is known is covered with a very thin—say, monomolecular—layer of another metal. This layer is supposed to have a negligibly small part in the production of S, but it will alter the work

function of the target to a measurable extent. An alteration of SE yield will then have to be attributed to the alteration of work function.

Sixtus (*48*) was the first to carry out such yield measurements for a W target covered with Th layers of different thickness. The Th layers reduced work-function from 4.52 to 3.3 ev and 2.6 ev; at the same time, maximum yield increased from 1.8 to 2.0 and 2.2. Thus, lower work function results in higher yield.

A number of other authors studied the dependence of yield on work-function in a similar manner. We confine ourselves to mentioning the measurements of Treloar (*49*), who found a decrease in yield for an oxidized W layer as against the pure W target from $\delta_1 = 1.31$ to $\delta_2 = 1.06$ while the work function increased from 4.52 ev to 6.3 ev.

The influence of the work function on secondary emission is obviously very small if compared with its extraordinary effect on thermal and photoelectric emission.

With use of the yield formula (67) (Sec. IV,E2), we can calculate the influence of variation of work function on the yield. As result, one obtains ($E_F = 5$ ev) for δ_2/δ_1 the value 0.72, whereas we find from Treloar's experimental values $\delta_2/\delta_1 = 0.81$. This result is nearly the same as that obtained by Baroody (*24*).

The influence of work function on the yield measurements is certainly manifold, though it has not always been possible to distinguish it clearly from other factors.

It is known that yields from different crystal faces of a solid are marked by small differences. Knoll and Theile (*50*) succeeded in making these differences visible by depicting crystalline layers by means of *S*. The differences in work function of different crystal planes are sufficient to account for the observed differences in yield.

In the majority of yield measurements, the surface of the targets to be measured is affected with adsorbed layers that are more or less unknown. These exert a certain influence on the measurements by altering the work function. Part of the disagreement between the yield values stated by different authors has certainly been caused in this way.

7. Miscellaneous Problems. a. Oblique incidence of primaries. So far perpendicular incidence has been considered exclusively. Oblique incidence of the primary beam results in an increase of the yield with increasing angle of incidence. This dependence on the angle of incidence, however, becomes noticeable for primary energies $E_p^\circ > E_{pm}^\circ$ only. Bruining (cf. ref. *2*) was able to represent the dependence of the yield on the angle of incidence by the relation

$$\ln\left(\frac{\delta_\Theta}{\delta_0}\right) = \text{const}\ (1 - \cos\Theta)$$

In order to understand this effect, it must be taken into account, that according to Jonker (*20*) the distribution of S is nearly isotropic and independent of the angle of incidence of the primary beam. It therefore seems improbable that an anisotropy of excitation, which might exist, should be responsible for the increase of the yield.

It is a change in the spatial distribution of P in the solid resulting in an increased source density of S which is effected by oblique incidence.

Since the spatial distribution of P is strongly dependent on the diffusion process of the primary beam, there must be different effects of its straggling. For weak diffusion, that is in the case of the primary beam taking a nearly linear path, the range perpendicular to the surface of the target decreases with $\cos \Theta$; the source density of S in the layer near the surface increases accordingly. For strong diffusion, the influence of the direction of incidence on the distribution of P decreases. A corresponding decrease of the dependence of the yield on the angle of incidence from the light elements to the heavy elements can be observed in the measurements that have as yet been made.

b. Depth of origin of secondaries. Because of their interactions with the electrons and phonons in the solid, the S released within the target have only a limited range d_s. Only those electrons can contribute to the yield which on arrival at the surface still have sufficient energy to overcome the surface barrier. Only the electrons excited in a certain surface layer of thickness d_s are able to escape.

Experiments on the dependence of the yield on the thickness of layers resulted in distinct saturation values above a certain thickness. These values of the thickness of the layers are to be regarded as the maximum depths of origin of S. The depth of origin obtained in this way is independent of the primary energy—as was first proved by Djatlowitskaja (*51*)—and depends only on the respective material of the target.

Values of about 100 A were found for metals, KCl rendered a value of about 500 A (*52*), in qualitative accordance with the above ideas on the transport process in SE.

c. Time constant. So far we have exclusively considered the stationary process of SE. If a target is exposed to a rectangular pulse of P, the yield of SE reaches its full value only after a certain length of time from the beginning of the pulse. This building-up process can be described by the time constant of SE.

The time constant is extraordinarily small. Therefore, it has not yet been possible to determine it by way of experimental measurements. The experiments that have so far been made result only in an upper limit for its value.

On the one hand, various indirect methods have been used to determine

the time constant. Attempts have been made to conclude its value from measurements with dynatrons, or to determine its value by means of the upper limit of the working range of clystrons the reflector of which had been replaced by an SE electrode. Also high-frequency multiplyers have been used for this purpose. The obtained result is that the time constant must have a value smaller than 1×10^{-11} sec.

The only direct method to determine its value was used by Greenblatt (*53*). By deflecting back and forth an electron beam across a narrow slit with a frequency of 400 mc, he produced primary pulses of a duration of 6×10^{-11} sec. The S pulses released by these pulses he analyzed as to their deformation. The measured broadening of the S pulse of 7×10^{-11} sec has to be attributed to the time the electrons pass through the deflecting mechanism, so that the time constant of SE itself must certainly be smaller than 7×10^{-11} sec.

For the time being, an evaluation of this quantity must be left to theoretical discussion (cf. IV,G2).

C. The Interaction of Primary Electrons with Solids

Though P are more or less only carriers of the energy needed for the excitation of S, their behavior within the solid is nevertheless of fundamental importance for the whole process, even decisive with regard to some particular problems; therefore, the behavior of P in solids will be discussed in more detail than is usual in most special studies on SE.

1. The Paths of Primaries. We can get a first idea about the paths of P from the investigation of electrons passing through thin films. When a parallel electron beam strikes a thin layer perpendicularly, it is both stopped and scattered. First let us consider the scattering process. Except the few cases when electron waves are refracted at the lattice of the layer, the directions of motion of the electrons after passing through appear in a continuous distribution around the direction of incidence. This distribution depends on the thickness, the substance of the layer, and the velocity of the electrons.

We obtain a good insight into the scattering process by comparison with observations made on the paths of electrons in the Wilson chamber. On entrance into the layer, the electron beam is dispersed in the same or even a higher degree than on entrance into the gas of the Wilson chamber (Fig. 17). The electron beam transmits its energy into an almost semispherical range around the point of incidence. Part of the P runs counter to the original beam. This is due to scattering events with scattering angles $> 90°$ and coupling of several moderate angle scatterings adding up to deflections of the electron beam paths $> 90°$.

The excitation in every layer consists of two components, one being

effected by the direct beam, the other by the rediffused beam. It is necessary to know both components if one wishes to obtain accurate information on the source function of S.

2. Rediffusion. The current of rediffused P cannot be measured in the solid itself. As we stated above, it is possible outside the solid to separate true S with sufficient accuracy from reflected and rediffused P by means of a retarding potential of about 50 ev.

For thin layers, the part of rediffused electrons was determined by its dependence on the thickness of the layer. This part increases with the thickness of the layer and arrives at a maximum. The thickness at which the maximum is reached is called "rediffusion range."

FIG. 17. Path of 40-kev electrons in the Wilson chamber at normal pressure.

Rediffusion range and rediffusion coefficient η still depend on the angle of incidence of the P, and, of course, on their energy.

For the energy range of P with normal incidence that we are only concerned with here, η has recently been measured by Palluel (*27*) and by Holliday and Sternglass (*28*). Figure 18 indicates η plotted against primary energy for a number of metals. η approaches an upper limit between 0.05 and 0.5 with increasing primary energy. For all metals, the curves rise starting from low energies up to about 15 kev.

For a number of insulators, Matskevich (*54*) carried out measurements by a pulse method and found similar results.

The relation between the upper limit of η, say at a primary energy of 20 kev, and the atomic number of metals becomes apparent from Fig. 19.

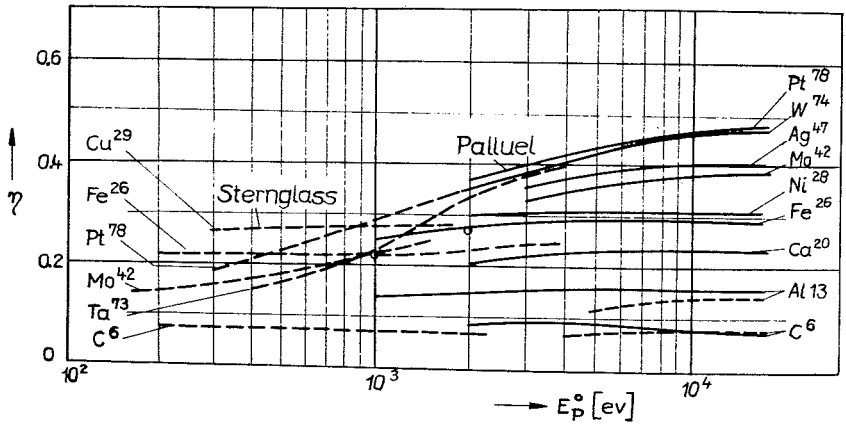

FIG. 18. Rediffusion coefficient η of different metals.

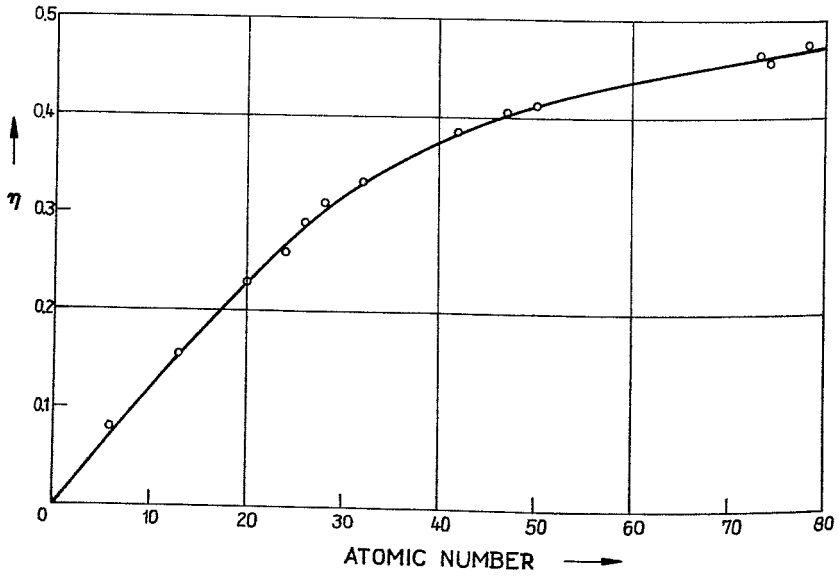

FIG. 19. Upper limit of rediffusion coefficient η of different metals plotted against the atomic number.

First the rediffusion coefficient rises linearly with Z; for $Z > 30$, however, one finds a minor increase of the coefficient. In the case of the heaviest metals, it approaches the limit 0.5. The deviation of the single dots from the curve is remarkably small, so that rediffusion is mainly dependent on

the atomic number, while the other characteristic quantities of atoms are of minor importance for rediffusion. The value of $\eta = 0.5$ for the heaviest metals indicates that in this case the electrons of the beam are distributed isotropically before they are absorbed to any relevant degree. If a normally incident electron beam is totally diffused without considerable absorption, half the incident electrons should eventually be re-emitted.

For light elements, on the other hand, diffusion of the beam seems to play a minor role in comparison with absorption. The beam is weakened, and the P have lost a great amount of their energy before any diffusion worth mentioning takes place. The energy distribution curve of rediffused electrons runs nearly horizontal. Just below primary energy, the continuum is superposed by single sharp peaks indicating that a P on penetration into the solid undergoes single discrete losses of energy. In these cases, electrons have either raised crystal electrons from deeper levels into the conduction band or have eventually excited plasma oscillations.

Moreover, Harrower (*8*) found slight maxima in the range 50 ev $<$ E $<$ 250 ev; they could be interpreted as Auger electrons.

3. Energy Loss of Primaries. a. Elementary processes. It is obvious that it must be of great use for a theoretical treatment of the subject to know the elementary processes effecting the loss of energy of P. We found evidence of the elementary processes in the energy distribution of a primary beam after passing through a thin film.

The energy distribution of the P on the exit side indicates three different processes:

1. An electron beam after passing through a thin film has mainly a continuous energy distribution, which practically begins shortly below the primary energy. It originates apparently from the excitation of electrons of the outer shells of the atoms, which in the case of metals are raised to the unoccupied levels closely above the Fermi surface. As the excited electrons are probably distributed in an energy range of $\approx$ 15 ev above the Fermi level, the spectrum is smeared out, so that it is not possible to distinguish single transitions between energy bands with an energy difference $<$ 10 ev. In particular, we cannot distinguish the transitions occurring within the conduction band from transitions from the next occupied band. However, the energy distribution is continuous in a much wider range, so that it must be concluded that the excitation of outer electrons must overshadow the excitations from deeper levels.

Excitations from deeper atomic shells are slightly indicated in the spectrum by Auger electrons. Obviously we may suppose that the number of these transitions is small.

2. A further mechanism of energy loss is to be attributed to the excitation of plasma oscillations. These transitions are observed as a series of

sharp maxima shortly below the primary energy with the same energetic distance (*55*).

The corresponding loss of energy per centimeter, too, seems obviously small in most cases as compared with the excitation of single electrons.

b. The stopping-power law. The excitation processes by the P taken together determine the average loss of energy $-dE_p/dx$ per unit path length and define the range R of the electrons in the solid.

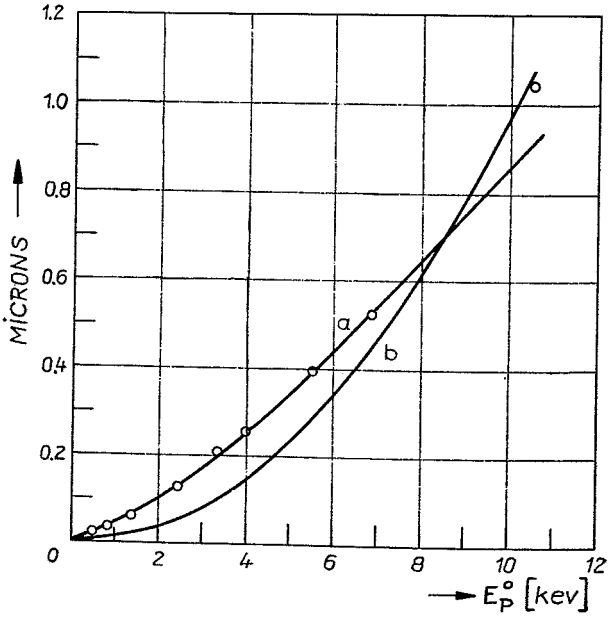

FIG. 20. Practical range R for electrons in aluminum [J. R. Young, *J. Appl. Phys.* **27**, 1 (1956)]. (a) $R = 0.042E_p^{\circ 1.3}$. (b) $R = 0.0093E_p^{\circ 2}$.

In earlier studies, the range R was preferably measured by means of fast electrons, and a quadratic dependence on E_p°—the Whiddington law—was found. This was occasionally adopted also for electrons with 100 ev $< E_p^\circ <$ 10,000 ev and was introduced into semiempirical theories of SE.

In more recent experimental investigations, the stopping-power law was measured for the range of primary energy mentioned above. Young (*56*) studied the penetration of P in Al for 0.5 kev $< E_p^\circ <$ 11 kev. His results are represented in Fig. 20. For $E_p^\circ > 8.5$ kev, he confirmed the Whiddington law; for $E_p^\circ < 8.5$ kev, he found

$$R \sim E_p^{\circ 1.3}$$

and thus clearly proved that the Whiddington law is not valid in the range we are primarily concerned with.

Analogous measurements on Al_2O_3 films carried out by Young (*57*) brought very similar results. The law of the rate of energy loss was here for 0.3 kev $< E_p^\circ <$ 7.25 kev

$$R = 0.0115 E_p^{\circ 1.35} \qquad (R \text{ in mg/cm}^2,\ E_p^\circ \text{ in kev})$$

Lane and Zaffarano (*58*) also investigating Al_2O_3 found an exponent 1.66.

Therefore, the Whiddington law must be replaced by another law with a smaller exponent of about 1.5 for the range that we are interested in.

c. The energy loss of the primary electron beam. As a result of the diffusion of the electron beam, the differential energy loss to be derived from the stopping power law is not identical with the energy $\left(\frac{dW}{dx}\right) dx$ dissipated in the layer of thickness dx. This quantity is important for the derivation of the source function of S in the solid. In order to obtain knowledge of this quantity, we need the energy distribution and the number of electrons that have passed through thin films of different thickness. Young (*59*) carried out such measurements on Al_2O_3 films and determined the respective energy losses of the electron beam dependent on the thickness of the layers. The average energy loss dW/dx remains practically constant over the entire penetration depth.

4. Spatial Source Distribution of Secondary Electrons. The spatial distribution of the sources of S in a solid during continuous bombardment with P has not yet been paid special attention, as far as we know, though it is of utmost importance for the problem of SE.

An experimental determination of the source function cannot, however, be achieved directly, for it is impossible to measure directly the electrons excited per second in a volume element of the solid. It is only possible to determine the loss of energy of the primary beam in a layer at the depth x and then to assume that a constant fraction of this amount of energy is employed for the production of S.

Perhaps one can proceed in the following way: We imagine the solid as cut at a plane denoted by the coordinate x_0. First one has to measure the primary beam flowing at the separation surface towards points $x > x_0$, then the current of rediffused electrons coming from the range $x > x_0$ has to be defined. Both currents combined make up the flow of energy at the point x_0. Then the same procedure has to be repeated for a point x_1; the difference of both numbers denotes the amount of energy absorbed in the layer $x_1 - x_0$.

Exact measurements of both fractions (fraction of incident P and

rediffused fraction) at separation surfaces of the sample have not yet been made. On the other hand, the electron beam as well as the energy loss of electrons has often been measured for beams passing through thin films. More recent measurements with electrons of $E_p^\circ = 2.5 - 10$ kev, carried out by Young (*59*) for Al_2O_3 films, determine the fraction of energy of the primary beam absorbed in films of different thickness. Now Al_2O_3 has a relatively small fraction of re-diffused electrons, the rediffusion coefficient being $\eta \approx 0.12$, so that the fraction of rediffused electrons can be regarded as a correction. If one differentiates the curve measured by Young and adds the fraction resulting from rediffusion, we obtain the energy absorbed in a layer of definite thickness which may be regarded as a measure for the source density of the S.

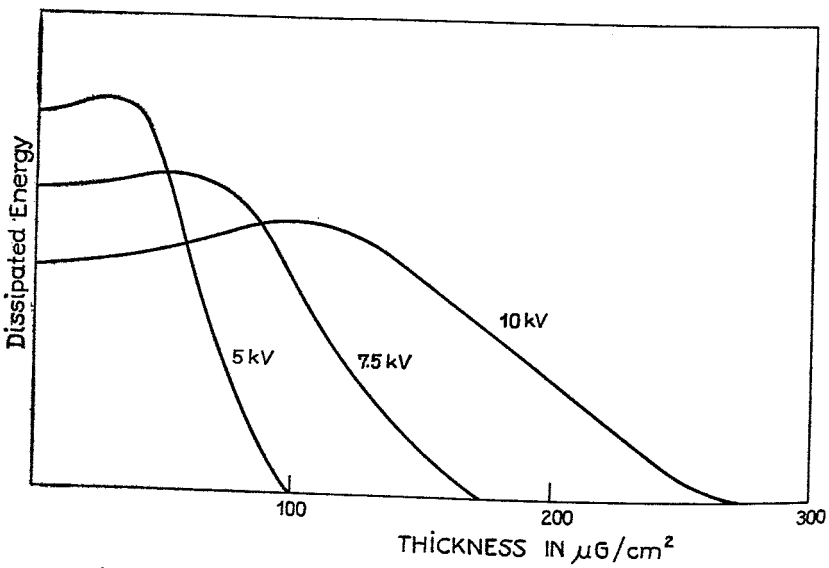

FIG. 21. Dissipated energy in dependence of the space coordinate.

The source functions for three different primary energies are plotted in Fig. 21. At about one-third of the maximum range of the electron beam, the curves have a flat maximum, which moves toward the surface if rediffusion becomes more important. The curves end at the limit range of the electron beam; the surface enclosed is proportional to the energy of the primary beam.

A similar result had been obtained earlier by Hachenberg (*60*) from KCl single crystals. If one supposes that the production of color centers in crystals under electron bombardment takes place proportional to the

energy dissipated per volume element by the electron beam, one can obtain the source function directly by photometrization. KCl single crystals were bombarded with 60 and 90 kev electrons; then the crystals were sliced perpendicularly to the bombarded surface and photometrized photographically. The resulting coloration curves (Fig. 22) were much the same as those shown in Fig. 21. In this way it was possible to obtain the approximate dependence of the source function on the depth in the solid; yet a question that is important for the theory, namely how much of the energy absorbed is used for the excitation of S, has still to be answered.

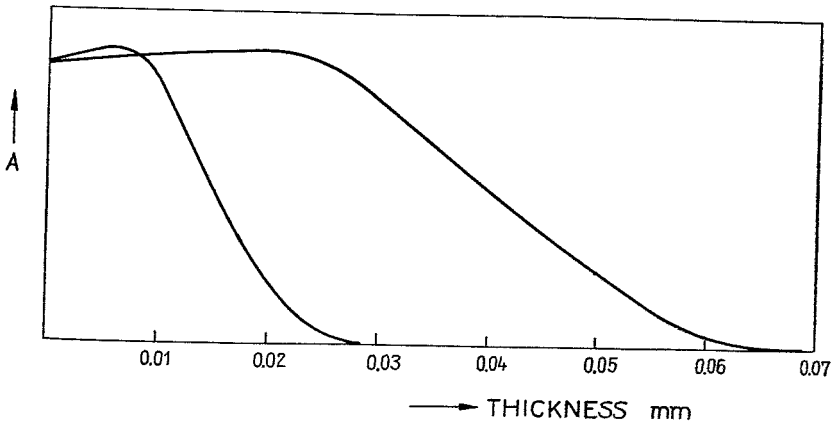

FIG. 22. Coloration of KCl single crystals after bombarding with 60-kev and 90-kev electrons [O. Hachenberg, unpublished].

IV. THEORY OF SECONDARY EMISSION

A. *Interaction between a Free Electron and a Bloch Electron*

1. General Formulas. All calculations on the phenomena resulting from interaction between a relatively fast electron and an electron of the solid (energy loss of P, excitation of S) start from the quantum-mechanical formula for the transition probability per second into the interval $d\alpha$:

$$P_{\alpha_0,\ \ldots\ (\alpha,\ \ldots)d\alpha\ \ldots} = \frac{2\pi}{\hbar}|(\alpha,\ \ldots|H_w|\alpha_0,\ \ldots)|^2\delta(E_\alpha,\ \ldots - E_{\alpha_0,\ \ldots})d\alpha\ \ldots \quad (3)$$

where the quantum numbers $\alpha_0\ \ldots$, respectively, $\alpha\ \ldots$ denote the stationary initial and final states of the unperturbed system, which is characterized by a Hamiltonian H_0. H_w denotes the perturbation operator inducing the transitions. Let us orthonormalize all occurring wave functions to a periodicity volume V. Then

$$\frac{1}{\sqrt{V}} e^{i(\mathbf{K},\mathbf{R})}$$

are the wave functions of the free particle with energy

$$E_p = \frac{\hbar^2}{2m} \mathbf{K}^2$$

For the corresponding functions of the Bloch electron we have

$$\psi_{\mathbf{k}}(\mathbf{r}) = \frac{1}{\sqrt{V}} u_{\mathbf{k}}(\mathbf{r}) e^{i(\mathbf{k},\mathbf{r})},\ E = E(\mathbf{k}) \tag{4}$$

with

$$\int_{1\text{cm}^3} |u_{\mathbf{k}}|^2 d^3\mathbf{r} = 1,\ u_{\mathbf{k}}(\mathbf{r} + \mathbf{G}) = u_{\mathbf{k}}(\mathbf{r})$$

where $\mathbf{G}$ is an arbitrary lattice vector. The vector $\mathbf{k}$ is regarded as a wave vector in the extended zone scheme. Thus, we can write for the matrix element in (3):

$$(\mathbf{k}',\mathbf{K}'|H_w|\mathbf{k},\mathbf{K}) = \frac{1}{V^2} \int_V \psi_{\mathbf{k}'}{}^* \psi_{\mathbf{k}} \frac{{e_0}^2}{|\mathbf{R} - \mathbf{r}|} e^{-\lambda|\mathbf{R}-\mathbf{r}|} e^{i(\mathbf{K}-\mathbf{K}',\mathbf{R})} d^3\mathbf{r} d^3\mathbf{R}$$

where the screened Coulomb potential is taken for the interaction operator H_w. If necessary, we may use the pure Coulomb potential with $\lambda = 0$.

Integration over $\mathbf{R}$ can be carried out without difficulty, so that

$$(\mathbf{k}',\mathbf{K}'|H_w|\mathbf{k},\mathbf{K}) = \frac{4\pi {e_0}^2}{(q^2 + \lambda^2)^2 V^2} \int_V \psi_{\mathbf{k}'}{}^* \psi_{\mathbf{k}} e^{i(\mathbf{q},\mathbf{r})} d^3\mathbf{r}, \mathbf{q} = \mathbf{K} - \mathbf{K}'$$

If we further define *(61)*

$$I = \int_V \psi_{\mathbf{k}'}{}^* \psi_{\mathbf{k}} e^{i(\mathbf{q},\mathbf{r})} d^3\mathbf{r}$$

then the transition probability per second becomes

$$P_{\mathbf{kK}}(\mathbf{k}',\mathbf{K}') = \frac{32\pi^3 {e_0}^4}{\hbar V^2 (q^2 + \lambda^2)^2} |I|^2 \delta(E_{\mathbf{kK}} - E_{\mathbf{k}'\mathbf{K}'}) \tag{5}$$

Because of the boundary conditions used, all occurring wave vectors range over discrete values. From (4) it may be seen *(62)* that the integral I can be written as

$$I = \sum_{\mathbf{G}(V)} e^{i(\mathbf{k}-\mathbf{k}'+\mathbf{q},\mathbf{G})} \cdot I_0, I_0 = \int_{\text{unit cell}} \psi_{\mathbf{k}'}{}^* \psi_{\mathbf{k}} e^{i(\mathbf{q},\mathbf{r})} d^3\mathbf{r}$$

If N is the number of atoms in V, then it follows from the periodic boundary condition that

$$\sum_{\mathbf{G}(V)} e^{i(\mathbf{k}-\mathbf{k}'+\mathbf{q},\mathbf{G})} = N \sum_{\mathbf{H}} \delta_{\mathbf{k}',\mathbf{k}+\mathbf{q}+2\pi\mathbf{H}}$$

$\mathbf{H}$ denotes the vectors in the reciprocal lattice derived from the crystal lattice vectors $\mathbf{G}$ by the relation

$$(\mathbf{G},\mathbf{H}) = \text{integer}.$$

So we see (*63*) that a finite transition probability for the process $\mathbf{kK} \rightarrow \mathbf{k}'\mathbf{K}'$ exists only in the case of conservation of quasi momentum, i.e., if

$$\mathbf{k}' = \mathbf{k} + \mathbf{q} + 2\pi\mathbf{H} \tag{6}$$

Then the integral I can be written:

$$I = N \sum_{\mathbf{H}} \delta_{\mathbf{k}',\mathbf{k}+\mathbf{q}+2\pi\mathbf{H}} I_0$$

If we define the "form factor" F as

$$F = \int_{\text{unit cell}} u_{\mathbf{k}'}^* u_{\mathbf{k}} e^{i(\mathbf{k}-\mathbf{k}'+\mathbf{q},\mathbf{r})} d^3\mathbf{r} \tag{7}$$

then

$$I = n \sum_{\mathbf{H}} \delta_{\mathbf{k}',\mathbf{k}+\mathbf{q}+2\pi\mathbf{H}} F \text{ with } n = \frac{N}{V} \tag{8}$$

An evaluation of F requires the explicit form of the Bloch wave functions $\psi_{\mathbf{k}}(\mathbf{r})$, which is not known in general. Generally, however, we can state that in any case $|F| \leqslant \int |u_{\mathbf{k}}|^2 d^3\mathbf{r} = 1/n$, that is to say, $1/n$ represents an upper limit for F.

2. $\mathbf{H} = 0$ *processes.* If we first consider the transitions corresponding $\mathbf{H} = 0$ according to (6), we see that for $\mathbf{q} \rightarrow 0$ the form factor F tends toward

$$\int_{\text{unit cell}} |u_{\mathbf{k}}|^2 d^3\mathbf{r} = \frac{1}{n} \tag{9}$$

i.e., toward its upper limit. Because of the q^{-4} in (5), the processes with small $\mathbf{q}$ play a particularly important role. By (7) F possesses the same value (9) in $\mathbf{H} = 0$ processes for all $\mathbf{q}$, if we make the additional assumption that the crystal electron is entirely free, i.e., that $u_{\mathbf{k}}(\mathbf{r}) \equiv 1$. The reader will observe that $\mathbf{H} = 0$ follows necessarily from this assumption, but not vice versa. Of course, $\mathbf{H} = 0$ processes do not necessarily correspond to an interaction with free crystal electrons. In $\mathbf{H} = 0$ processes we shall later replace F by the approximation (9).

3. $\mathbf{H} \neq 0$ *processes.* A corresponding discussion of the form factor for

$\mathbf{H} \neq 0$ processes is far more difficult. As we mentioned above, the function $u_{\mathbf{k}}(\mathbf{r})$ is by no means a constant. Moreover, for $\mathbf{H} \neq 0$ processes, F differs essentially at the limit of very small $\mathbf{q}$ from its corresponding behavior for $\mathbf{H} = 0$ processes. In that case, the integral (7) tends to

$$\int_{\text{unit cell}} u_{\mathbf{k}'}^* u_{\mathbf{k}} e^{i(\mathbf{k}-\mathbf{k}',\mathbf{r})} d^3\mathbf{r}, \mathbf{k}' = \mathbf{k} + 2\pi\mathbf{H}$$

Because of the orthogonality of eigenfunctions belonging to different eigenvalues, this becomes equal to zero (*64*).

In order to examine the behavior of F in the neighborhood of $\mathbf{q} = 0$, it is convenient to expand it into a Taylor series about this point:

$$\begin{aligned} F(\mathbf{q}) &= F(0) + \sum_l \left.\frac{\partial F}{\partial q_l}\right|_0 q_l + \frac{1}{2}\sum_{l,j} \left.\frac{\partial^2 F}{\partial q_l \partial q_j}\right|_0 q_l q_j + \cdots \\ &= F^{(0)} + F^{(1)} + F^{(2)} + \cdots = F^{(1)} + F^{(2)} + \cdots \end{aligned} \tag{10}$$

In order to obtain $F^{(1)}$, F can exactly be transformed into the following expression (*65*):

$$F = \frac{\hbar^2}{mi} \frac{(\mathbf{q},\mathbf{A}(\mathbf{H};\mathbf{k}',\mathbf{k}))}{\Delta E_{\mathbf{k}'\mathbf{k}} - (\hbar^2/2m)(\mathbf{q},\mathbf{q}+2\mathbf{k})} \tag{11}$$

where (*62*)

$$\mathbf{A}(\mathbf{H};\mathbf{k}',\mathbf{k}) = \int_{\text{unit cell}} u_{\mathbf{k}'}^* \operatorname{grad} u_{\mathbf{k}} e^{-2\pi i(\mathbf{H},\mathbf{r})} d^3\mathbf{r} \tag{12}$$

and

$$\Delta E_{\mathbf{k}'\mathbf{k}} = E(\mathbf{k}') - E(\mathbf{k})$$

Taking

$$\epsilon(\mathbf{k},\mathbf{H}) = \Delta E_{\mathbf{k}+2\pi\mathbf{H},\mathbf{k}}$$

we obtain from (11) without difficulty (*62*)

$$F^{(1)} = \frac{\hbar^2}{im\epsilon} (\mathbf{q},\mathbf{A}(\mathbf{k}+2\pi\mathbf{H},\mathbf{k})) \tag{13}$$

Since $\epsilon(\mathbf{k},0) = 0$, it is evident that an expansion of F by (11) is essentially based on the assumption $\mathbf{H} \neq 0$. Of course, the "linear approximation" $F \approx F^{(1)}$ for the form factor F is only valid for sufficiently small $\mathbf{q}$, i.e., only as long as, say, $|F^{(2)}| \ll |F^{(1)}|$. In order to realize the meaning of this relation, we must express $\mathbf{A}(\mathbf{H};\mathbf{k}',\mathbf{k})$ in terms of certain explicit functions. If, for instance, we choose the "nearly free approximation"

$$\psi_{\mathbf{k}}(\mathbf{r}) = \frac{1}{\sqrt{V}} e^{i(\mathbf{k},\mathbf{r})} \left\{1 - \frac{m}{2\pi\hbar^2} \sum_{\mathbf{H}' \neq 0} \frac{v_{\mathbf{H}'}}{(\mathbf{k},\mathbf{H}') + \pi\mathbf{H}'^2} e^{2\pi i(\mathbf{H}',\mathbf{r})}\right\}$$

with the energy

$$E(\mathbf{k}) = \frac{\hbar^2}{2m} k^2$$

we find by an easy calculation (*65*):

$$F = -\frac{v_{\mathbf{H}}}{(\mathbf{k},\mathbf{H}) + \pi\mathbf{H}^2} \sum_{n=1}^{\infty} \left(-\frac{2\pi\hbar^2}{m}\right)^{n-1} \frac{1}{\epsilon^n} (\mathbf{q},\mathbf{H})^n = \sum_{n=1}^{\infty} F^{(n)} \tag{14}$$

For estimating in what cases $F^{(2)}$ may be neglected with respect to $F^{(1)}$, we must remember that (5) depends quadratically on F. It can be seen to be necessary for this purpose that

$$2|F^{(2)}| \ll |F^{(1)}|$$

or using (14)

$$4\frac{\hbar^2}{m} |(\pi\mathbf{H},\mathbf{q})| \ll \epsilon \tag{15}$$

This inequality for the loss of momentum $\mathbf{q}$ suffered by the P (*66*) can be transformed by means of the specialization $\mathbf{q}||\mathbf{H}$, $\mathbf{q} = \mathbf{q}_{\min}$ into a condition necessary for (15):

$$4\frac{\hbar^2}{m} \pi H q_{\min} \ll \epsilon \tag{16}$$

where $\mathbf{q}_{\min}$ is the minimum $\mathbf{q}$ vector for a given initial state $(\mathbf{k},\mathbf{K})$ and fixed $\mathbf{H} \neq 0$ .It is easy to prove (Fig. 23) that

$$q_{\min} = \frac{2\pi}{K} [(\mathbf{k},\mathbf{H}) + \pi\mathbf{H}^2] \left[1 - \frac{(\mathbf{K},\mathbf{k} + 2\pi\mathbf{H})}{K^2}\right] \tag{17}$$

neglecting terms of higher order in $1/K$. As long as

$$|(\mathbf{K},\mathbf{k} + 2\pi\mathbf{H})| \ll \mathbf{K}^2 \tag{18}$$

the last factor in (17) may be neglected; thus (using the approximation $E(\mathbf{k}) = (\hbar^2/2m)k^2$), we obtain

$$q_{\min} = \frac{2\pi}{K} [(\mathbf{k},\mathbf{H}) + \pi\mathbf{H}^2] = \left(\frac{m}{\hbar^2}\right)^{1/2} \frac{\epsilon}{(2E_p)^{1/2}} \tag{19}$$

It is easy to see that (18) is satisfied if

$$E_p \gtrsim 10^2 \frac{\hbar^2}{2m} (k_F + 2\pi H)^2 \approx 3 \times 10^3 \text{ ev}$$

In the same way we obtain from (16) and (19)

$$E_p \gtrsim 10^2 \cdot 8 \frac{\hbar^2}{m} (\pi H)^2 \tag{20}$$

For the smallest $H \neq 0$, we can take $\pi H = 1\text{A}^{-1}$ approximately. Then it follows from (20)

$$E_p \gtrsim 5 \times 10^3 \text{ ev}$$

as a necessary condition for the linear approximation (13) to hold in the case of nearly free electrons. According to Butcher (*67*), this approximation holds fairly well for the alkali metals Na, K, Rb.

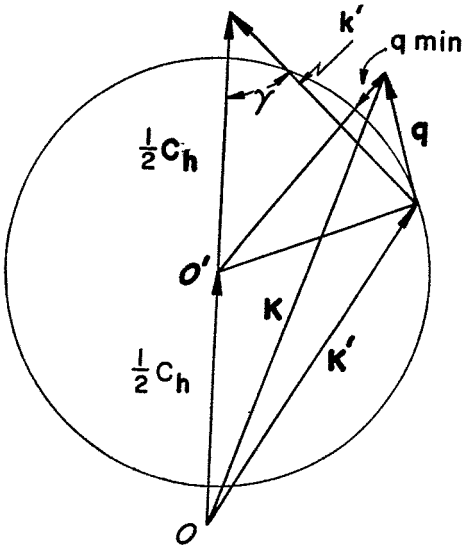

FIG. 23. Energy momentum sphere.

Another way to obtain an approximation of F consists in regarding the excited electrons as free, such that $u_{\mathbf{k}}(\mathbf{r}) \equiv 1$. Then

$$F = \int u_{\mathbf{k}} e^{i(\mathbf{k}-\mathbf{k}'+\mathbf{q},\mathbf{r})} d^3\mathbf{r} = \int u_{\mathbf{k}} e^{-2\pi i(\mathbf{H},\mathbf{r})} d^3\mathbf{r} \tag{21}$$

i.e., independent of the final state. Since the plane wave is not an eigenfunction of the Hamiltonian with periodic potential, it is natural that $F(0) \neq 0$ holds for this approximation. Apparently the form factor for small $\mathbf{q}$—in classical language, for great impact parameters—becomes too great. But the overestimation of these collisions is not so serious if one chooses $\lambda \neq 0$ limiting the interaction to distances $< \lambda^{-1}$. Finally the linear and the free approximation for F can be combined, and we obtain at once

$$F = -\frac{v_{\mathbf{H}}(\mathbf{q},\mathbf{H})}{\epsilon[(\mathbf{k},\mathbf{H}) + \pi\mathbf{H}^2]} \tag{22}$$

The meaning of this expression differs from the $F^{(1)}$ resulting from (14) in so far as it may be used even at the Brillouin zone boundaries because of the assumption $\psi_{\mathbf{k}'}(\mathbf{r}) = (1/\sqrt{V})e^{i(\mathbf{k}',\mathbf{r})}$. We may therefore integrate over the final states in (22).

B. Energy Loss of Primary Electrons

1. General Formulas. For the energy loss of a P per unit path length we obtain at once, regarding (5) and (8):

$$-\frac{dE_p}{dx} = -\frac{m}{\hbar K}\sum_{\mathbf{k}\mathbf{k}'\mathbf{K}'} \Delta E_{\mathbf{K}'\mathbf{K}} P_{\mathbf{k}\mathbf{K}}(\mathbf{k}',\mathbf{K}')$$

$$= \frac{32\pi^3 m e_0^4 n^2}{\hbar^2 K V^2}\sum_{\mathbf{k}\mathbf{k}'\mathbf{K}'} \Delta E_{\mathbf{K}'\mathbf{K}} \frac{|F|^2}{(q^2+\lambda^2)^2}\,\delta_{\mathbf{k}',\mathbf{k}+\mathbf{q}+2\pi\mathbf{H}}\,\delta(E_{\mathbf{k}\mathbf{K}} - E_{\mathbf{k}'\mathbf{K}'})$$

$$= \frac{32\pi^3 m e_0^4 n^2}{\hbar^2 K V^2}\sum_{\mathbf{H}\mathbf{k}\mathbf{K}'} \Delta E_{\mathbf{K}'\mathbf{K}} \frac{|F|^2}{(q^2+\lambda^2)^2}\,\delta(E_{\mathbf{k}\mathbf{K}} - E_{\mathbf{k}'\mathbf{K}'})$$

$\mathbf{k}$ running over all occupied initial states of the crystal electrons in V. Converting to integrals by

$$\sum_{\mathbf{k}} \to \frac{2V}{(2\pi)^3}\int \ldots d^3\mathbf{k}, \quad \sum_{\mathbf{K}'} \to \frac{V}{(2\pi)^3}\int \ldots d^3\mathbf{K}'$$

we obtain

$$-\frac{dE_p}{dx} = \frac{m e_0^4 n^2}{\pi^3\hbar^2 K}\sum_{\mathbf{H}}\int\int \Delta E_{\mathbf{K}'\mathbf{K}} \frac{|F|^2}{(q^2+\lambda^2)^2}\,\delta(E_{\mathbf{k}\mathbf{K}} - E_{\mathbf{k}'\mathbf{K}'})\,d^3\mathbf{k}\,d^3\mathbf{K}'$$

Integrating over $\mathbf{K}'$, one uses the δ-function. The remaining two integrations over the final states turn out to run over the so-called "energy momentum sphere" because of the equation (Fig. 23):

$$\delta(E_{\mathbf{k}\mathbf{K}} - E_{\mathbf{k}'\mathbf{K}'}) = \frac{m}{\hbar^2}\frac{1}{2R_0}\,\delta(R - R_0)$$

The energy momentum sphere has its center at O', where

$$00' = \frac{1}{2}\mathbf{C}_{\mathbf{H}} = \frac{1}{2}(\mathbf{K} + \mathbf{k} + 2\pi\mathbf{H})$$

its radius R_0 being given by

$$R_0^2 = \frac{1}{2}\left[K^2 + \frac{2m}{\hbar^2}E(\mathbf{k}) - \frac{1}{2}\mathbf{C}^2_{\mathbf{H}}\right]$$

where for the excited electrons, the assumption

$$E(\mathbf{k}') = \frac{\hbar^2}{2m} k'^2$$

is used. Further we have $\mathbf{R} = \mathbf{K}' - \frac{1}{2}\mathbf{C}_{\mathbf{H}}$. If $d\Omega$ means the element of solid angle on the sphere, we finally obtain

$$-\frac{dE_p}{dx} = \frac{m^2 e_0^4 n^2}{2\pi\hbar^4 K} \sum_{\mathbf{H}} \int d^3\mathbf{k} R_0 \int d\Omega \Delta E_{\mathbf{K}'\mathbf{K}} \frac{|F|^2}{(q^2 + \lambda^2)^2} \tag{23}$$

2. $\mathbf{H} = 0$ *Processes.* Let us first examine the term $\mathbf{H} = 0$ in (23). According to our earlier consideration we can write $F = 1/n$. If we further observe that

$$\Delta E_{\mathbf{K}'\mathbf{K}} = \frac{\hbar^2}{2m}(K^2 - K'^2) = \frac{\hbar^2}{2m}[2(\mathbf{K},\mathbf{q}) - \mathbf{q}^2]$$

we obtain the loss of energy caused by $\mathbf{H} = 0$ processes by the following formula:[4]

$$-\frac{dE_p}{dx}\bigg|_{\mathbf{H}=0} = \frac{m e_0^4}{4\pi^3\hbar^2 K} \int d^3\mathbf{k} R_0 \int d\Omega \frac{2(\mathbf{K},\mathbf{q}) - \mathbf{q}^2}{(q^2 + \lambda^2)^2}$$

While the integration over the sphere (neglecting the Pauli principle for the final states) can be carried out exactly (*68*), the integration over the initial states of the Fermi sphere can be carried out expanding the integrand with respect to $1/K$. After a few somewhat complicated integrations, we find for $E_p \gtrsim 100$ ev

$$-\frac{dE_p}{dx} = \frac{\mathbf{k}_F^3 e_0^4}{3\pi E_p} \ln\left(\frac{E_p}{E_\lambda} + 1\right), \quad E_\lambda = \frac{\hbar^2}{2m}\lambda^2 \tag{24}$$

Formula (24) was derived earlier by van der Ziel (*69*), who proceeded in another manner supposing $k \ll k'$.

3. $\mathbf{H} \neq 0$ *Processes.* In order to calculate the loss of energy resulting from the terms with $\mathbf{H} \neq 0$ in (23), we may proceed as follows(*68*): We choose the approximation (22) for F and compensate the overestimated contributions of great $\mathbf{q}$ by replacing

$$\Delta E_{\mathbf{K}'\mathbf{K}} = \Delta E_{\mathbf{k}'\mathbf{k}} \text{ in (23) by } \epsilon(\mathbf{k},\mathbf{H}).[5]$$

Now we choose $\lambda = 0$ and, integrating over final and initial states, we obtain a stopping-power law of the following form:

[4] Here we must choose $\lambda \neq 0$ because of $\mathbf{q}_{\min} = 0$ for $\mathbf{H} = 0$ processes, in order to avoid divergences.

[5] Using instead the true loss of energy $\Delta E_{\mathbf{k}'\mathbf{k}}$, we obtain $-dE_p/dx = A'$, with a constant A', which, at about 5,000 ev, leads to a loss of energy greater than that measured. The integration over ranges with large values of q violates the condition $F^{(1)} \gg F^{(2)}$.

$$-\left.\frac{dE_p}{dx}\right|_{\mathbf{H}\neq 0} = \frac{A}{E_p}\ln\frac{E_p}{C} \qquad \text{for } E_p > 5\times 10^3 \text{ ev} \tag{25}$$

where $A \sim |v_{\mathbf{H}}|^2$ and C is an energy of the order of a few electron volts.

Though the approximations leading to (25) are very likely to change the quantitative character of this formula, it is possible, for information, only to estimate the ratio of energy loss in $\mathbf{H} = 0$ and $\mathbf{H} \neq 0$ processes, e.g., in the case of Na. Taking $|v_{\mathbf{H}}|^2 = 1/10$ for the minimal vectors $\mathbf{H} \neq 0$, all others can be neglected in the used approximation (*67*), and we find a preponderance in stopping power of $\mathbf{H} = 0$ processes with respect to $\mathbf{H} \neq 0$ processes by about a factor 10. If we further calculate the theoretical range for $\mathbf{H} = 0$ processes in the case of Na and $E_p^\circ = 5 \times 10^3$ ev according to (24), we find $R_{\text{theor.}}^{(H=0)} \approx 20\, R_{\text{exp.}}$, that is to say, $\mathbf{H} = 0$ processes alone do not seem to play the principal role for energy loss of P.

Let us point out once more, however, that these considerations are by no means to be regarded as exact, and that they are restricted to alkali metals.

4. Loss of Energy in Bethe Processes. After all that has been said, it may be taken for granted that even for metals the energy loss by interaction with weakly bound electrons is not sufficient to describe the experimental facts.

Thus it seems desirable to consider the loss of energy caused by the relatively tightly bound crystal electrons. Since it is possible to describe the eigenfunctions of these electrons in deeper levels fairly well by appropriately combined atomic wave functions, we may suppose that the loss of energy $-dE_p/dx = f(E_p,a)$ (a symbolizing atomic parameters) can be represented by a relation as already given by Bethe (*70*) in 1930:

$$-\frac{dE_p}{dx} = \frac{2\pi N e_0^4}{E_p}\ln\frac{E_p}{E_j} \tag{26}$$

N denotes the number of electrons per cubic centimeter, E_j a suitably averaged ionization energy. It can be seen that the three stopping power laws (24), (25), (26) have the same functional dependence on E_p but differ as to the meaning of the constants. While the influence of N is limited to the absolute value of the loss of energy, the average ionization energy E_j determines, in a not too large range of E_p, the exponent n of that power law which approximately describes the true stopping-power law within this range.

For if we calculate from

$$-\frac{dE_p}{dx} = f(E_p,a) = \frac{A}{E_p}\ln\frac{E_p}{E_j}$$

the range $R(E_p^\circ)$ by

$$R(E_p^\circ) = \int_0^{E_p^\circ} \frac{dE_p}{f(E_p,a)} = \frac{E_j^2}{A} \int_0^{(E_p^\circ/E_j)^2} \frac{dy}{y} = \frac{E_j^2}{A} \operatorname{li}\left(\frac{E_p^\circ}{E_j}\right)^2 \tag{27}$$

it can be seen from the slope of the function li (x), by which power law $R \sim E_p^{\circ n}$ as an approximation of (27) can be attained.

So we find, e.g., that in the range between $y = 3$ and 30

$$\operatorname{li}(y^2) \sim y^{1,39}$$

This means, if applied to an ionization energy of the order of 100 ev: For E_p° values between 300 and 3000 ev the energy loss takes place in accordance with a law of approximate validity

$$R \sim E_p^{\circ 1,39}$$

This, however, confirms almost exactly the energy-range relation found by Young in experiments with Al_2O_3. Making the further assumption that all 50 electrons of Al_2O_3 take part in the stopping process ($E_j = 100$ ev being their mean ionization energy), we obtain the quantitative loss of energy measured. Therefore, Young as well as Lane and Zaffarano found a remarkable accordance between the results of their measurements and Bethe's formula in the case of Al_2O_3.[6] The results on the energy loss of P in the energy range about 1 kev can be summarized as follows: In addition to a certain qualitative accordance between theory and experiments, even a quantitative accordance has been found in some cases. The decision, however, as to which special mechanism is the most efficient one (it is also necessary to take into account the loss of energy caused by excitation of plasma oscillations) will be different with different substances.

For the purpose of a better survey, a number of different substances should be examined in a wide energy range as to their energy-range relations. Until this will be done, we shall have to content ourselves with using the above-mentioned semiquantitative considerations combined with phenomenological theories (G. 3) and empirical data for the formulation of a theory of SE.

C. Excitation of Secondary Electrons

1. General Formulas. The number of S excited into the state $\mathbf{k}'$ in the volume V per second by one P is given by (5) and (8) as

$$\sum_{\mathbf{k}\mathbf{K}'} P_{\mathbf{k}\mathbf{K}}(\mathbf{k}',\mathbf{K}') = \frac{8e_0^4 n^2}{\hbar V} \sum_{\mathbf{H}} \int d^3\mathbf{k} \frac{|F|^2}{(q^2+\lambda^2)^2} \delta(E_{\mathbf{k}\mathbf{K}} - E_{\mathbf{k}'\mathbf{K}'})$$

[6] The special calculation of the average ionization energy E_j seems somewhat arbitrary, however. Hardly anything else than an approximate accordance between range measurements in Al_2O_3 and formula (26) has been found as yet.

This rate of excitation is related to the primary current density $\hbar K/mV$. If instead we choose the primary current density unity and calculate the excitation function per cubic centimeter, we obtain

$$\frac{8e_0^4mn^2}{\hbar^2KV}\sum_{\mathbf{H}}\int d^3\mathbf{k}\,\frac{|F|^2}{(q^2+\lambda^2)^2}\,\delta(E_{\mathbf{k}\mathbf{K}}-E_{\mathbf{k}'\mathbf{K}'}) \tag{28}$$

Now if we ask for the number of excitations per second and cubic centimeters into the interval $d^3\mathbf{k}'$ related to the primary current density unity, it follows from (28)

$$S(\mathbf{k}')d^3\mathbf{k}' = \frac{me_0^4n^2}{\pi^3\hbar^2K}\,d^3\mathbf{k}'\sum_{\mathbf{H}}\int d^3\mathbf{k}\,\frac{|F|^2}{(q^2+\lambda^2)^2}\,\delta(E_{\mathbf{k}\mathbf{K}}-E_{\mathbf{k}'\mathbf{K}'}) \tag{29}$$

In order to obtain the mere energy dependence of the excitation function, i.e., $S(E')$, we take into account the expression for $\delta(E_{\mathbf{k}\mathbf{K}}-E_{\mathbf{k}'\mathbf{K}'})$ already used in the theory of energy loss. Hence, $(d^3\mathbf{k}'=k'^2dk'd\Omega_{\mathbf{k}'})$:

$$S(E')dE' = \frac{m^3e_0^4n^2}{2\pi^3\hbar^6K}\,k'dE'\sum_{\mathbf{H}}\int d^3\mathbf{k}\,\frac{1}{R_0}\int d\Omega_{\mathbf{k}'}\delta(R-R_0)\,\frac{|F|^2}{(q^2+\lambda^2)^2} \tag{30}$$

From Fig. 23 it can be seen that

$$R^2 = k'^2+\frac{1}{4}\mathbf{C}_{\mathbf{H}}^2-k'|\mathbf{C}_{\mathbf{H}}|\cos\gamma$$

and therefore

$$2RdR = -k'|\mathbf{C}_{\mathbf{H}}|d\cos\gamma$$

Hence

$$d\Omega_{\mathbf{k}'} = \frac{2R}{k'|\mathbf{C}_{\mathbf{H}}|}\,dRd\varphi \qquad (\varphi \text{ azimuth resp. to } \mathbf{C}_{\mathbf{H}})$$

If this is introduced into (30), the required function becomes

$$S(E')dE' = \frac{m^3e_0^4n^2}{\pi^3\hbar^6K}\,dE'\sum_{\mathbf{H}}\int d^3\mathbf{k}\,\frac{1}{|\mathbf{C}_{\mathbf{H}}|}\int_0^{2\pi}d\varphi\,\frac{|F|^2}{(q^2+\lambda^2)^2} \tag{31}$$

2. $\mathbf{H}=0$ *Processes. a. Energy angular dependence.* If in (28) we take $\lambda=0$ and use $1/n$ for F, the calculation of the function $S(\mathbf{k}')$ will amount to the following integration over the Fermi sphere:

$$\int d^3\mathbf{k}\,\frac{\delta(E_{\mathbf{k}\mathbf{K}}-E_{\mathbf{k}'\mathbf{K}'})}{q^4}$$

From this integration follows without neglect

$$S_{\mathbf{H}=0}(\mathbf{k}') = \frac{m^2 e_0^4}{\pi^2 \hbar^4 K} \frac{K^2 k'^2 - (k',\mathbf{K})^2 - (k'^2 - k_F^2)(\mathbf{K} - \mathbf{k}')^2}{|\mathbf{K} - k'|^3 (k'^2 - k_F^2)^2} \tag{32}$$

if the following condition is fulfilled:

$$|(\mathbf{k}',\mathbf{K} - \mathbf{k}')| \leqslant k_F |\mathbf{K} - \mathbf{k}'| \tag{33}$$

in all other cases $S_{\mathbf{H}=0}(\mathbf{k}')$ becomes zero. This condition yields a nonzero transition probability for excitation only into the states of the shadowed area in Fig. 24. Further it can be seen from (32) that excitations become the more probable, the more E' approaches E_F; in classical analogy this means an increase in the number of collisions with increasing collision parameter.

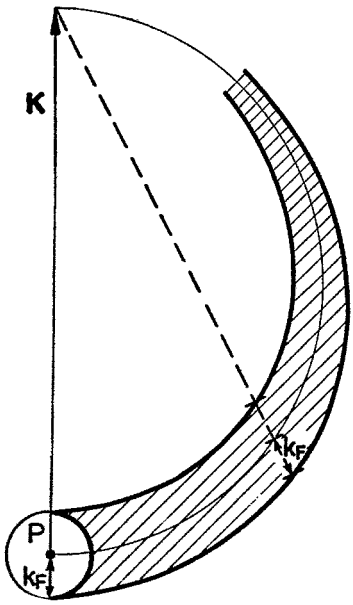

FIG. 24. Shadowed area gives the range for excitation function $S_{\mathbf{H}=0}(\mathbf{k}') \neq 0$ [H. W. Streitwolf, *Ann. Physik*, [7] **3**, 183 (1959)].

For fixed E' Fig. 25 shows graphically the variation of excitation probability with the angle for two values of E'. As we might expect we can see that the most frequent excitations with small loss of energy produce S moving practically perpendicularly to $\mathbf{K}$, that is, parallel to the surface if the incidence is normal.

b. Energy dependence. (*i*) *Metals.* In order to calculate the function $S_{\mathbf{H}=0}(E')$ we have to proceed from (31). With $\lambda = 0$ and $F = 1/n$, we have first to calculate the integral over φ. This results in

$$S(E') = \frac{2m^3e_0^4}{\pi^2\hbar^6K}\int d^3\mathbf{k}\,\frac{K^2(k'^2+k^2)-2(\mathbf{K},\mathbf{k})^2-k^2(k'^2-k^2)}{(k'^2-k^2)^3|\mathbf{K}-\mathbf{k}|^3}$$

The remaining integration over the Fermi sphere can also be carried out exactly and gives (*68*):

$$S(E') = \frac{e_0^4k_F^3}{3\pi E_p(E'-E_F)^2} \tag{34}$$

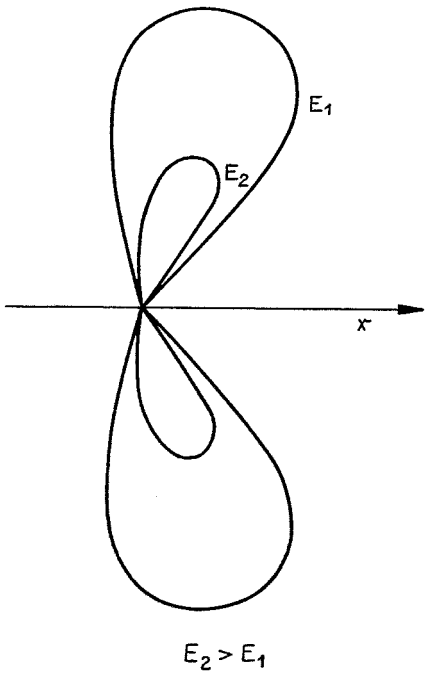

FIG. 25. Angular dependence of the excitation function $S_{\mathbf{H}=0}(\mathbf{k}')$ for two energies [H. W. Streitwolf, *Ann. Physik*, (7) **3**, 183 (1959)].

Formula (34) as shown in Fig. 26 was earlier derived by Baroody (*24*), who proceeded from classical considerations based on the Sommerfeld model of a free electron gas. The singularity at $E' = E_F$ in (34) is irrelevant for the outer S, because of the finite work function of all metals, the secondaries with $E' \approx E_F$ cannot appear outside the solid.

(*ii*) *Insulators.* We shall calculate the excitation function for the following simplified insulator model: The width of the valence band be negligibly small, so that all its electrons can be described by a wave function $\psi_0(\mathbf{r}) = (1/\sqrt{V})u_0(\mathbf{r})$ with the wave vector $\mathbf{k} = 0$, and $-\Delta E$ is the energy

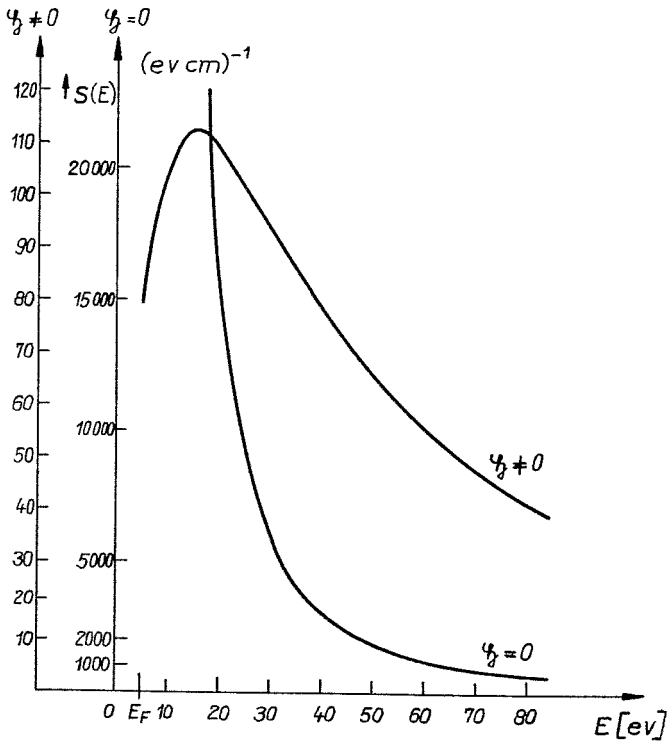

FIG. 26. Energy dependence of excitation functions $S_{\mathbf{H}=0}(E)$ and $S_{\mathbf{H}\neq 0}(E)$. $E_F = 5$ ev, $E_p = 10^3$ ev, $|v_{\mathbf{H}}|^2 = 0.1$ [ev]^2 and $\lambda = 10^8$ cm^{-1}. [H. W. Streitwolf, *Ann. Physik*, [7] **3**, 183 (1959)].

of these valence electrons. The electrons excited in the conduction band shall be regarded as free. Then for $\mathbf{H} = 0$ processes

$$F = \int_{\text{unit cell}} u_0(\mathbf{r}) d^3\mathbf{r}$$

i.e., independent of initial and final states. If we take $\lambda = 0$, we can easily find from (31) regarding the dielectric constant ϵ in the denominator of H_w:

$$S(E') = \frac{\pi e_0^4 n^2 |F|^2 D_0}{\epsilon^2 E_p E'^2} \tag{35}$$

where D_0 is the density of the valence electrons. From Fig. (23) it can be seen that (35) describes the excitation only if $k' \geqslant |\tfrac{1}{2}|\mathbf{C}_0| - R_0|$. Thus, the excitation function of our insulator model has the form

$$S(E') = \begin{cases} 0 & E' < \dfrac{(\Delta E)^2}{4E_p},\ E' > E_p - \Delta E \\ \dfrac{\pi e_0^4 n^2 |F|^2 D_0}{\epsilon^2 E_p E'^2} & E' > \dfrac{(\Delta E)^2}{4E_p} \end{cases} \tag{36}$$

Thus the simplifying supposition "$\mathbf{k} = 0$ for all valence electrons" causes a gap in the excitation function.

3. $\mathbf{H} \neq 0$ *Processes. a. Energy angular dependence.* Contrary to $\mathbf{H} = 0$ processes, only qualitative investigations could be carried out here. At first one can find a condition for $S_{\mathbf{H}\neq 0}(\mathbf{k}') \neq 0$ in analogy to (32) by eliminating $\mathbf{K}'$ from the laws of conservation of energy and momentum:

$$|(\mathbf{k}' - 2\pi\mathbf{H},\mathbf{K} - (\mathbf{k} - 2\pi\mathbf{H})) + 2\pi^2 H^2 - 2\pi(\mathbf{H},\mathbf{k}')| \leqslant k_F|\mathbf{K} - (\mathbf{k}' - 2\pi\mathbf{H})|$$

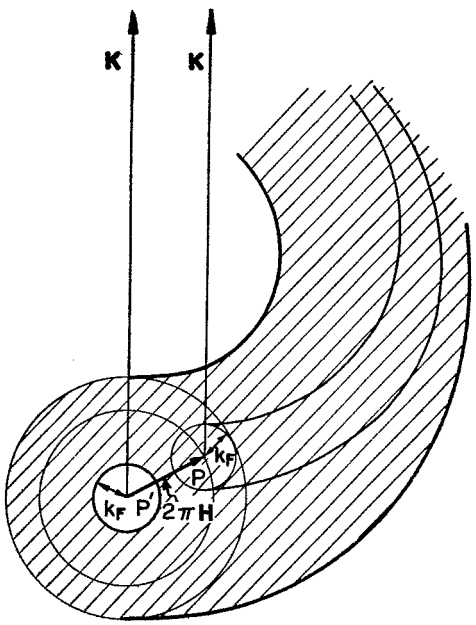

FIG. 27. Shadowed area gives the range for excitation function $S_{\mathbf{H}\neq 0}(\mathbf{k}') \neq 0$ [H. W. Streitwolf, *Ann. Physik* [7] **3**, 183 (1959)].

or for sufficiently large $\mathbf{K}$:

$$|(\mathbf{k}' - 2\pi\mathbf{H},\mathbf{K} - (\mathbf{k}' - 2\pi\mathbf{H}))| \leqslant k_F|\mathbf{K} - (\mathbf{k}' - 2\pi\mathbf{H})|$$

It is obvious that this is the same relation for $\mathbf{k}' - 2\pi\mathbf{H}$ as was found for $\mathbf{k}'$ in $\mathbf{H} = 0$ processes. Thus for each $\mathbf{H}$ the allowed range for $\mathbf{k}'$ results from that of $\mathbf{H} = 0$ processes by a translation by $2\pi\mathbf{H}$ (Fig. 27).

In a cubic space-centered crystal there are 12 minimal vectors $\mathbf{H} \neq 0$ with magnitude $H = \sqrt{2}/a$ (a lattice constant). As in the theory of stopping power, we confine ourselves to these vectors of the reciprocal lattice for $\mathbf{H}$ summation. In the case of a polycrystal whose elementary orientations are distributed at random, one has further to average over

them. This results in an allowed range for $\mathbf{k}'$ — vectors for $\mathbf{H} \neq 0$ processes as shown in Fig. 27.

Because of q^4 in the denominator of (29), it may be supposed that processes with $k' = |\mathbf{k} + 2\pi\mathbf{H}|$ will be particularly frequent. It can further be seen that electrons with energies up to about $(\hbar^2/2m)(2\pi H + k_F)^2 \approx 35$ ev will be excited nearly isotropically, in contrast to $\mathbf{H} = 0$ excitation processes. Here the influence of the rigid lattice in the $\mathbf{H} \neq 0$ processes becomes clearly visible. With increasing excitation energy, however, the S are more and more thrown into the $\mathbf{K}$ direction.

It is remarkable that in $\mathbf{H} \neq 0$ processes there are excitations antiparallel to the direction of $\mathbf{K}$ increasing the probability of escape of these S with respect to those thrown into the solid or parallel to the surface. Of course, quantitative results regarding the relative importance of $\mathbf{H} \neq 0$ processes for SE can only be obtained if the energy-angular dependence of the excitation function is known quantitatively. For various reasons, this is not yet the case.

b. Energy dependence. Proceeding from (29) we obtain at once

$$S(E') = \frac{m^2 e_0^4 n^2}{\pi^3 \hbar^4 K} k' \sum_{\mathbf{H}} \int d^3\mathbf{k} \int d\Omega_{\mathbf{k}'} \frac{|F|^2}{(q^2 + \lambda^2)^2} \delta(E_{\mathbf{kK}} - E_{\mathbf{k}'\mathbf{K}'})$$

This has to be averaged over crystal orientation as required in the case of a polycrystal. Since only the angle between $\mathbf{H}$ and $\mathbf{K}$ is involved, the averaging procedure can be replaced by an averaging over $\mathbf{K}$ which leads to (*68*)

$$S(E') = \frac{m^2 e_0^4 n^2}{\pi^3 \hbar^4 K} \, 12 \frac{1}{4\pi} \int d^3\mathbf{k} \int d\Omega_{\mathbf{k}'} \int d\Omega_{\mathbf{K}} \frac{|F|^2}{(q^2 + \lambda^2)^2} \delta(E_{\mathbf{kK}} - E_{\mathbf{k}'\mathbf{K}'}) \tag{37}$$

In order to carry out the integrations in (37) we have to take the explicit form of F. If we choose the free electron approximation (21) for $\psi_{\mathbf{k}'}(\mathbf{r})$ and further substitute for $u_{\mathbf{k}}(\mathbf{r})$ the nearly free electron approximation, all integrations in (37) can be carried out, the last one over k, however, only numerically. The result of this calculation (*68*) for Na is shown in Fig. 26. It can be seen that in this case the excitation by $\mathbf{H} = 0$ processes is clearly predominant for all energies of S and that the function $S_{\mathbf{H}\neq 0}(E')$ resulting as $\sim 1/E_p$ has a maximum at an energy near $(h^2/2m)(2\pi H)^2$. But it must be pointed out again that the result of the calculation of $\mathbf{H} \neq 0$ processes shown in Fig. 26 has rather an illustrative character, since it is essentially based on approximation (21) for F, the applicability of which is doubtful. Certainly, it will only be possible to obtain reliable results on the function $S_{\mathbf{H}\neq 0}(E')$ for a definite substance after the wave functions of the electrons contained in the substance will have been worked out explicitly

and after the necessary integrations will have been made with the term then obtained for F. Until then we shall have to content ourselves with qualitative and semiquantitative statements.

D. Transport of Secondary Electrons

1. Boltzmann Equation. The transport of S from their origin to the surface of the emitter is, like all transport problems, described by the Boltzmann equation, which has the general form

$$\frac{\partial N(\mathbf{r},E,\Omega,t)}{\partial t} + (\mathbf{r}, \operatorname{grad} N(\mathbf{r},E,\Omega,t)) = S(\mathbf{r},E,\Omega,t) + b - a \qquad (38)$$

a denoting the number per second and cubic centimeter of particles thrown out of the state E,Ω by collisions:

$$a = N(\mathbf{r},E,\Omega,t)\frac{1}{t_0(E,\Omega)} = N(\mathbf{r},E,\Omega,t)\frac{v}{l}$$

where $t_0(E,\Omega)$ means the time between two collisions of the particles in the state E,Ω, and $l = vt_0$ their free path. b denotes the respective number of electrons thrown into the state (E,Ω) by collisions.

In the case of metals, to which we shall confine our attention here, these quantities can be calculated in the following manner: Let us suppose that the motion of an electron excited to a few electron volts is predominantly determined by interaction with the electrons of the Fermi sea. Then the transition probability per sec and for the process in which the S passes from E,Ω into the state $E'_1\Omega'_1$, and the Fermi electron into $E'_2\Omega'_2$ can be written as

$$P_{E\Omega}(E'_1,\Omega'_1;E'_2,\Omega'_2)$$

Then obviously

$$\int P_{E\Omega}(E'_1,\Omega'_1;E'_2,\Omega'_2)dE'_1d\Omega'_1dE'_2d\Omega'_2 = \frac{v}{l}$$

and we can write

$$a = \int N(\mathbf{r},E,\Omega,t)P_{E\Omega}(E'_1,\Omega'_1;E'_2,\Omega'_2)dE'_1d\Omega'_1dE'_2d\Omega'_2$$

When calculating the corresponding expression for b, we have to take into account that both particles from E',Ω' and such from the Fermi sphere can be thrown into the state E,Ω. Therefore, the number of S is doubled with each collision. This fact was first pointed out by Wolff (*71*). By the above definition for $P_{E\Omega}(E'_1,\Omega'_1;E'_2,\Omega'_2)$, b has to be written thus:

$$\begin{aligned} b &= \int N(\mathbf{r},E',\Omega',t)P_{E'\Omega'}(E,\Omega;\tilde{E},\tilde{\Omega})d\tilde{E}d\tilde{\Omega}dE'd\Omega' \\ &\quad + \int N(\mathbf{r},E',\Omega',t)P_{E'\Omega'}(\tilde{E},\tilde{\Omega};E,\Omega)d\tilde{E}d\tilde{\Omega}dE'd\Omega' \\ &= \int N(\mathbf{r},E',\Omega',t)P_{E'\Omega'}dE'd\Omega' \end{aligned}$$

If, in addition, we define a function $p_{E'\Omega'}(E,\Omega)$ by the relation

$$P_{E'\Omega'}(E,\Omega) = p_{E'\Omega'}(E,\Omega)\frac{v'}{l'}$$

we can prove at once that

$$\int p_{E'\Omega'}(E,\Omega)dEd\Omega = 2 \tag{39}$$

It is evident that $p_{E'\Omega'}(E,\Omega)$ means the probability that being given a S in the state E',Ω', after a collision there will be an E,Ω electron, which need not necessarily be the original one.

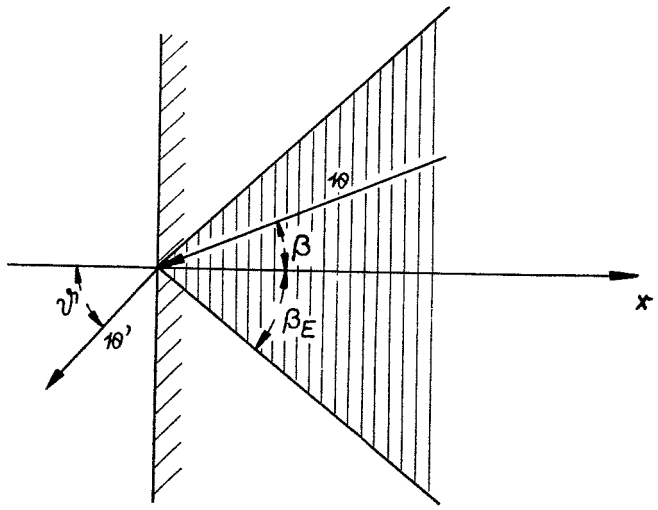

FIG. 28. Escape of a secondary electron. Shadowed area denotes the escape cone of a secondary of energy E.

If the expressions derived for a and b are introduced into (38), taking into account the stationary condition and the special geometry of the emitter (Fig. 28), then the Boltzmann equation will take the form

$$-v\cos\beta\frac{\partial N(x,E,\Omega)}{\partial x} = S(x,E,\Omega) - \frac{v}{l}N(x,E,\Omega) + \int N(x,E',\Omega')\frac{v'}{l'} p_{E'\Omega'}(E,\Omega)dE'd\Omega' \tag{40}$$

Since in our case the scattering potential is spherically symmetric, we have

$$p_{E'\Omega'}(E,\Omega) = p[E,E',\cos(\Omega,\Omega')] = p(E,E',\cos\Theta)$$

Let us further suppose that the primary beam is impinging normally on the

surface. Then the source function $S(x,E,\Omega)$ in (40) will not depend on the azimuth. The same will be true for the distribution function $N(x,E,\Omega)$. Then

$$-v \cos\beta \frac{\partial N(x,E,\beta)}{\partial x} = S(x,E,\beta) - \frac{v}{l} N(x,E,\beta) + \int N(x,E',\beta') \frac{v'}{l'} p(E,E', \cos\Theta)\, dE' d\Omega' \quad (41)$$

with

$$N(x,E,\beta) = \int_0^{2\pi} N(x,E,\Omega) d\varphi = 2\pi N(x,E,\Omega)$$

and so for $S(x,E,\beta)$. In order to solve (41), it is usual to expand the functions $N(x,E,\beta), S(x,E,\beta), p(E,E', \cos\Theta)$ into Legendre polynomials:

$$N(x,E,\beta) = \frac{1}{2} \sum_{l=0}^{\infty} (2l+1) N_l(x,E) P_l(\cos\beta)$$

$$S(x,E,\beta) = \frac{1}{2} \sum_{l=0}^{\infty} (2l+1) S_l(x,E) P_l(\cos\beta) \quad (42)$$

$$p(E,E', \cos\Theta) = \frac{1}{2} \sum_{l=0}^{\infty} (2l+1) p_l(E,E') P_l(\cos\Theta)$$

For the functions

$$\psi_l(x,E) = \frac{v}{l(E)} N_l(x,E)$$

this yields the following system of equations:

$$-l(E) \left[\frac{l}{2l+1} \frac{\partial \psi_{l-1}}{\partial x} + \frac{l+1}{2l+1} \frac{\partial \psi_{l+1}}{\partial x} \right] = -\psi_l + S_l + 2\pi \int_E^{\infty} \psi_l(x,E') p_l(E,E') dE' \quad (43)$$

For a further treatment of (43), it is necessary to define the function $p(E,E', \cos\Theta)$ explicitly. According to Wolff (*71*), this can be done by the following two suppositions: The scattering of the two interacting electrons is spherically symmetric in the center of mass system, and the metal electrons are to be regarded as being at rest before the collision.

While the first supposition could be proved to be true by means of a numerical integration of the Schroedinger equation for this scattering problem in the range $0 < E < 100$ ev (*71*) (the phase δ_0 in the well-known scattering formula

$$\sigma = \frac{4\pi}{k^2} \sum_{l=0}^{\infty} (2l + 1) \sin^2 \delta_l$$

exceeding all other δ_l in this energy range), the second supposition must be made in order not to overcomplicate the calculation. This involves a certain neglection of the Pauli principle for metal electrons; yet it seems that the second supposition can be avoided only with great difficulty. Combined with (39) these suppositions determine the function $p(E,E', \cos \Theta)$ uniquely as

$$p(E,E', \cos \Theta) = \frac{2}{\pi} \cos \Theta \delta(E - E' \cos^2 \Theta)$$

Then it follows from (42) that

$$p_l(E,E') = \frac{1}{\pi E'} P_l\left(\sqrt{\frac{E}{E'}}\right)$$

If introduced into (43)

$$l(E)\left[\frac{l}{2l+1}\frac{\partial \psi_{l-1}}{\partial x} + \frac{l+1}{2l+1}\frac{\partial \psi_{l+1}}{\partial x}\right] = -\psi_l + S_l + 2\int_E^{\infty} \psi_l(x,E') P_l\left(\sqrt{\frac{E}{E'}}\right) dE' \quad (44)$$

This equation can be solved uniquely only under certain boundary conditions. One can assume

$$N(0,E,\beta) = 0 \text{ for } \pi - \beta_E \leqslant \beta \leqslant \pi \quad (45)$$

and reflection in all other cases. Here

$$\cos \beta_E = \sqrt{\frac{W}{E}} \quad (46)$$

where W potential step at the surface, and (45) signifies that the S of energy E falling to the surface from inside the metal in the angular range $0 \leqslant \beta \leqslant \beta_E$ will escape without exception and not be reflected. As a matter of course, $N(x,E,\beta)$ must remain finite for $x \to \infty$.

This problem, which has not yet been solved explicitly in its general form, will now be simplified in the following manner: We shall suppose that the excitation of S is practically independent of space coordinates, and we shall further neglect the influence of the surface and thus also the boundary condition (45). Then the function $N(x,E,\beta)$ will become independent of x, so that (44) will take the form (*71*):

$$\psi_l(E) = S_l(E) + 2\int_E^{\infty} \psi_l(E') \frac{1}{E'} P_l\left(\sqrt{\frac{E}{E'}}\right) dE' \quad (47)$$

Obviously our supposition of an excitation independent of x can only be valid for primary energies $E_p^\circ > E_{pm}^\circ$, so that from a theory based on (47) one cannot, e.g., obtain the yield maximum.

The solution of the equations (47) is obtained by first providing for the appropriate Green's functions. They are defined by

$$G_l(E,E_0) = \delta(E - E_0) + 2\int_E^\infty G_l(E',E_0)\,\frac{1}{E'}\,P_l\left(\sqrt{\frac{E}{E'}}\right)dE' \qquad (48)$$

The required functions $\psi_l(E)$ will then result from

$$\psi_l(E) = \int_{E_F}^{E_m} G_l(E,E_0)S_l(E_0)dE_0 \qquad (49)$$

E_m denoting a maximum energy of the S, such that the suppositions made on deriving (47) will hold just for $E \leqslant E_m$. According to what has been said above $E_m \approx 100$ ev.

2. P_0 Approximation. By (48) we can calculate the function

$$G_0(E,E_0) = \begin{cases} 2E_0/E^2 + \delta(E - E_0) & E_0 \geqslant E \\ 0 & E_0 < E \end{cases}$$

Because of

$$S_0(E) = \int S(E,\beta)\sin\beta d\beta = S(E)$$

we require only the energy dependence of the excitation function $S(E)$ in order to obtain the distribution function in the P_0 approximation by (47).

For $\mathbf{H} = 0$ processes in metals, we can take this function from (34). Then (*72*)

$$N_0(E) = \frac{l(E)}{v}\int_E^{E_m}\left\{2\frac{E_0}{E^2} + \delta(E - E_0)\right\}\frac{e_0^4k_F^3}{3\pi E_p(E_0 - E_F)^2}\,dE_0$$

$$= \frac{(2m)^{1/2}l(E)e_0^4k_F^3}{6\pi E^{1/2}E_p}\left\{\frac{2}{E^2}\left[\ln\frac{E_m - E_F}{E - E_F} + E_F\left(\frac{1}{E - E_F} - \frac{1}{E_m - E_F}\right)\right] + \frac{1}{(E - E_F)^2}\right\} \qquad (50)$$

While the last term in (50) describes those S which did not suffer any collision after their excitation, the preceding terms denote the influence of energy-diminishing collisions on the distribution function. A diagram of the inner distribution (50) (Fig. 29) will differ from Fig. 26 only in so far as there is now a somewhat greater number of slow S generated out of faster S by means of energy-diminishing collisions. The shape of the curves is very similar.

3. P_2 Approximation. In order to calculate higher P_l approximations, the functions $S_l(E)$ for $l = 1, 2, \ldots$ have to be defined by (32). This can approximately be carried out in the following way (*72*): We see from

(32) that for small $k'(\gtrsim k_F)$ and large K the angular dependence of the excitation function can approximately be written as

$$S_{\mathbf{H}=0}(\mathbf{k}')d^3\mathbf{k}' = Q(E') \sin^2\beta dE' d\Omega \tag{51}$$

$Q(E)$ is defined by the requirement that

$$\int Q(E) \sin^2\beta d\Omega = S_{\mathbf{H}=0}(E) \tag{52}$$

$S_{\mathbf{H}=0}(E)$ being given by (34).
By (51) and (52) we obtain an approximate excitation function

$$S_{\mathbf{H}=0}(E,\beta) = \frac{e_0^4 k_F^3}{4\pi E_p (E - E_F)^2} \sin^2\beta \tag{53}$$

From (53) follows

$$S_1(E) = 0, S_2(E) = \frac{-e_0^4 k_F^3}{15\pi E_p (E - E_F)^2}, S_3(E) = S_4(E) = \ldots = 0 \tag{54}$$

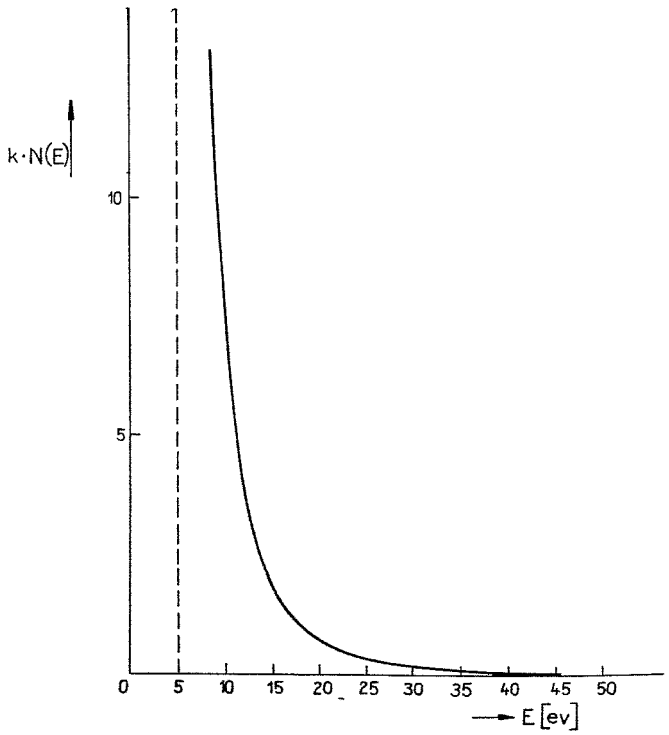

FIG. 29. Energy dependence of distribution function corresponding to $S_{\mathbf{H}=0}(E)$ in Fig. 26 [H. Stolz, *Ann. Physik* [7] **3**, 197 (1959)].

$$\kappa = \frac{6 \times 10^2 \pi^2 E_p \hbar^3}{lm^2 e_0^4 E_F^{3/2}}; \; E_F = 5 \text{ ev}, \; E_m = 10^2 \text{ ev}.$$

and from (48)

$$G_2(E,E_0) = \begin{cases} \dfrac{2}{(EE_0)^{1/4}} \cos\left[\sqrt{3} \ln (E_0/E)^{1/2}\right] + \delta(E - E_0) & E_0 \geqslant E \\ 0 & E_0 < E \end{cases} \quad \text{for} \tag{55}$$

If (54) and (55) are introduced into (49), we obtain a rather complicated expression for $N_2(E)$, which will not be stated explicitly here (*72*).

From the functions $N_0(E)$ and $N_2(E)$, one receives the inner energy-angular distribution $N(E,\beta)/N(E,0)$. The evaluation is shown in Fig. 30.

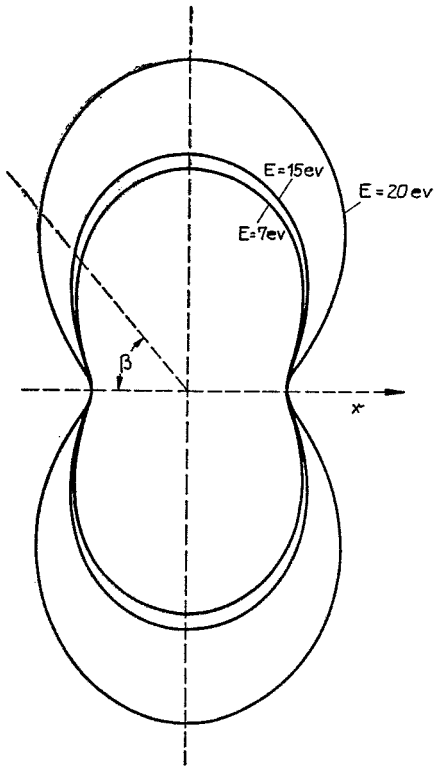

FIG. 30. Angular dependence of the distribution function for different energies in P_2 approximation [H. Stolz, *Ann. Physik* [7] **3**, 197 (1959)].

It can be seen that the marked asymmetry of the excitation function has been lessened, but by not means eliminated, by the collisions of S. It can therefore be stated that collisions of S in metals are not capable of changing an anisotropic excitation function such as (53), approximately corresponding to (32), into such an isotropic distribution as there seems to exist in reality.

E. Escape of Secondary Electrons

1. General Formulas. Let us now turn to the question of how the functions measurable in free space have to be calculated from the solution of the Boltzmann equation at $x = 0$, $N(0,E,\beta)$.

For this purpose we start from the connection between $N(x,E,\mathbf{\Omega})$ and the current density $j_s^{(i)}(x,E,\mathbf{\Omega})$ at an arbitrary point in the emitter (Fig. 28):

$$j_s^{(i)}(x,E,\mathbf{\Omega})dEd\Omega = N(x,E,\mathbf{\Omega})v\cos\beta dEd\Omega \tag{56}$$

In order to derive the relation between $j_s^{(i)}(0,E,\mathbf{\Omega})$ and $j_s(E',\mathbf{\Omega}')$, i.e. the current density measurable outside, we must consider the conservation laws for energy and momentum of S on their escape from the surface (Fig. 28):

$$E = E' + W,\ v\sin\beta = v'\sin\vartheta \tag{57}$$

Then we have at $x = 0$

$$j_s^{(i)}(E,\mathbf{\Omega})dEd\Omega = j_s(E',\mathbf{\Omega}')dE'd\Omega' \tag{58}$$

From (57) and (58) follows

$$j_s(E',\mathbf{\Omega}') = j_s^{(i)}(E,\mathbf{\Omega})\frac{E'}{E}v\cos\vartheta \tag{59}$$

If we introduce (56) into (59), we obtain

$$j_s(E',\mathbf{\Omega}') = N(0,E,\mathbf{\Omega})\frac{E'}{E}v\cos\vartheta$$

If particularly $N(x,E,\mathbf{\Omega})$ is independent of the azimuth φ it follows that

$$j_s(E',\vartheta) = N(0,E,\beta)\frac{E'}{E}v\cos\vartheta \tag{60}$$

Relation (60) connects the boundary value of the solution of the Boltzmann equation with the outer current density. The (E,β) values belonging to $(E'\vartheta)$ can be calculated by (57). Equation (60) gives the relative energy-angular distribution referred to $j_s(E',0)$ as

$$\frac{j_s(E',\vartheta)}{j_s(E',0)} = \frac{N(E,\beta)}{N(E,0)}\cos\vartheta \tag{61}$$

From (61) can be inferred that

$$\frac{j_s(E',\vartheta)}{j_s(E',0)} \underset{E'\to 0}{\longrightarrow} \cos\vartheta$$

is valid independent of the particular shape of the function $N(E,\beta)$.

Very slow S, therefore, must always be distributed in current density according to the cosine law. This statement has not yet been proved because of immense difficulties in experimenting with extremely slow electrons (below 1 ev). The above-mentioned measurements by Jonker for Ni (*20*) down to $E' = 1.5$ ev deviate rather clearly from the cosine law. As, however, with $W = 10$ ev for such S the angle β_E (46) of the escape cone is about 21°, we are still far from the limit $\beta \approx 0$ in the case of such energies.

An exact cosine distribution of S with energy E' is found if and only if $N(E,\beta) = N(E,0)$ for $0 \leqslant \beta \leqslant \beta_E$, i.e., if there is an isotropic distribution of inner S at least within the escape cone. Strictly speaking, no conclusions on the inner S outside the escape cone can be drawn from measurements of outer S.

Hence, it is clear that the supposition of an isotropic distribution of S of all energies in the emitter cannot be correct (*73*, *74*). On the contrary, slow S seem to possess a preferred direction of velocity parallel to the surface.

The absolute energy distribution of outer current density is given by the formula

$$j_s(E') = \int j_s(E',\Omega')d\Omega'$$

that is to say, by means of (60) and (57),

$$j_s(E') = v\int_0^{\beta_E} N(E,\beta)\cos\beta\sin\beta d\beta \tag{62}$$

Since by (57) it is always true that $\beta \to 0$ for $E' \to 0$, it can be seen from (62) that in general $j_s(E') \to 0$ in this limiting case. Thus the outer energy distribution curve will always start from the origin of the $E' - j_s(E')$ coordinate system, a direct consequence of the potential barrier at the surface.

In the special case of isotropic distribution of the inner S, it follows from (62) that

$$j_s(E') = \frac{v}{4}N(E)\left(1 - \frac{W}{E}\right),\ N(E) = \int_0^{\pi} N(E,\beta)\sin\beta d\beta \tag{63}$$

The relative energy distribution occurring in most experimental investigations is defined by

$$j_{s,\mathrm{rel}}(E') = \frac{j_s(E')}{\int j_s(E')dE'}$$

such that

$$\int j_{s,\mathrm{rel}}(E')dE' = 1$$

If the calculation of the excitation function is based on unit primary current density, as we did, then

$$\int j_s(E')dE' = \delta \tag{64}$$

and the relation between absolute and relative energy distribution can be written as

$$j_{s,\mathrm{rel}}(E') = \frac{1}{\delta} j_s(E')$$

The pure angular distribution is obtained as

$$j_s(\vartheta) = v \cos\vartheta \int N(E,\beta) \frac{E'}{E} dE', E = E' + W, \beta = \beta(\vartheta,E')$$

It can be seen again that irrespective of the energy dependence of $N(E,\beta)$ each inner isotropic distribution in free space results in a cosine distribution of current density.

2. P_0 Approximation. According to (42) and (61), the relative energy-angular distribution has the general form

$$\frac{j_s(E',\vartheta)}{j_s(E',0)} = \frac{\Sigma(2l+1)N_l(E)P_l(\cos\beta)}{\Sigma(2l+1)N_l(E)} \cos\vartheta \tag{65}$$

From this follows in the P_0 approximation

$$\frac{j_s^{(0)}(E',\vartheta)}{j_s^{(0)}(E',0)} = \cos\vartheta$$

i.e., the angular distribution curves of S of all energies are circles. Apart from Jonker's weak breathing effect these curves are in accordance with experience. It follows that the pure angular distribution (integrated over energies) is exactly a cosine distribution here, while according to measurements it appears as a slightly flattened circle.

Energy distribution is calculated by (62) and (42):

$$j_s(E') = \frac{v}{2} \sum (2l+1)N_l(E) \int_0^{\beta_E} P_l(\cos\beta) \cos\beta \sin\beta d\beta$$

In the P_0 approximation this becomes

$$j_s(E') = \frac{v}{4} N_0(E) \left(1 - \frac{W}{E}\right) \tag{66}$$

This function is plotted in Fig. 31. The general form is obtained correctly, as was to be expected, but the half-width with 12 ev is too large.

If we finally calculate the yield by (64) and (66), we find that

$$\delta^{(0)} = \frac{(2m)^{3/2} e_0^4 l}{12\pi\hbar^3 E_p} \frac{E_F^{3/2}}{W} \left(\ln \frac{E_m - E_F}{W - E_F} - \frac{E_m - W}{E_m - E_F}\right) \tag{67}$$

In order to obtain numerical values, it is necessary to know the mean free path l. If we use the expression derived by the Goldberger method (*71*),

$$l(E) = \frac{3\pi\hbar}{4(2m)^{1/2}E_F^{1/2}\sin^2\delta_0}\frac{E}{E - 7/5E_F}$$

we obtain for typical energies of S, $l = 5.2 \times 10^{-7}$ cm for Ag and $l = 8.4 \times 10^{-7}$ cm for K.

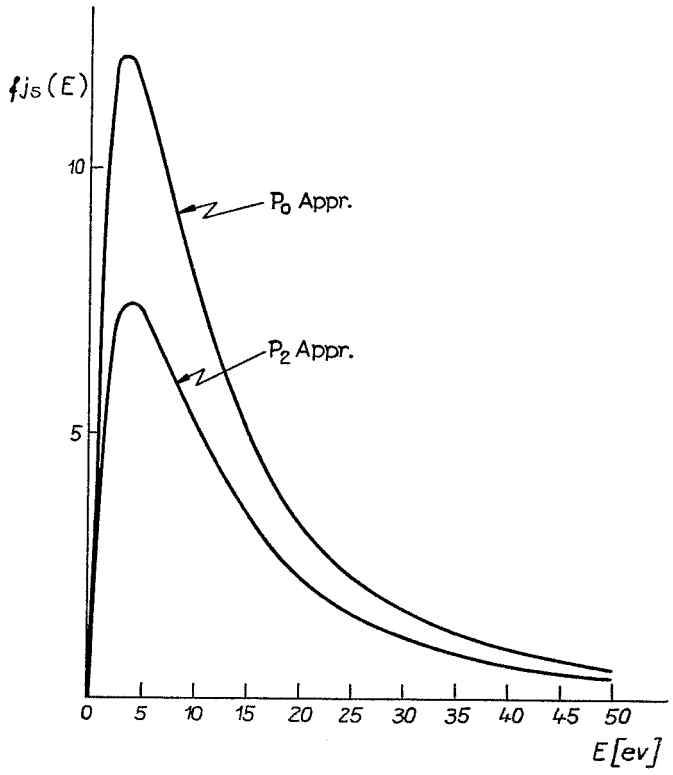

FIG. 31. Energy distribution of outer secondaries in P_0 and P_2 approximation [H. Stolz, *Ann. Physik* [7] **3**, 197 (1959)].

$$f = \frac{12 \cdot 10^3\pi\hbar^3E_p}{(2m)^{3/2}e_0^4lE_F^{3/2}}.$$

For Ag we obtain a theoretical yield $\delta^{(0)} \approx 0.22\delta_{exp}$ for $E_p = 1{,}000$ ev, for K we find $\delta^{(0)} \approx 0.76\ \delta_{exp}$. Because of the uncertainty in calculating mean free paths, the yields obtained do not seem to be very reliable.

Since $\delta^{(0)}$ is obviously a function of the two parameters E_F and $W = E_F + \phi$, which are independent of each other, it seems hardly possible to assume a simple relation between $\delta^{(0)}$ and one of these two parameters when considering various metals.

Baroody (*24*) attempted to show by means of a yield formula derived by himself that the rule $\delta \sim \phi$ found by McKay (*1*) can be understood theoretically. It would be in accordance with his considerations to write (67) in the following manner:

$$\delta^{(0)} = \frac{(2m)^{3/2}e_0^4}{12\pi\hbar^3 E_p} \frac{l}{(W/E_F - 1)^{1/2} W/E_F} \left[\ln \frac{E_m - E_F}{W - E_F} - \frac{E_m - W}{E_m - E_F} \right] \phi^{1/2}$$

and then to suppose that l and W/E_F have little influence on $\delta^{(0)}$ as compared with the influence of $\phi^{1/2}$. Unfortunately, it seems somewhat difficult to confirm this supposition.

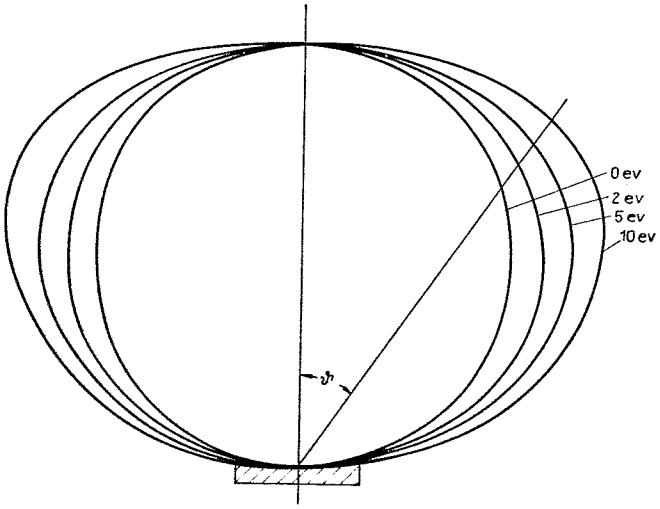

FIG. 32. Energy angular distribution of outer secondaries corresponding to the excitation function (53) [H. Stolz, *Ann. Physik* [7] **3**, 197 (1959)].

3. P_2 Approximation. If we calculate the relative energy angular distribution $j_s(E',\vartheta)/j_s(E'0)$ by (65) using $N_0(E)$ and $N_2(E)$, we obtain a result given in Fig. 32. As was shown in our discussion of the inner-energy angular distribution, the calculated distribution curves, contrarily to those measured by Jonker, turn out to be too flat, and the greater the energy of S the flatter they are. While there is a similar discrepancy also for the pure angular distribution of outer current density, the pure energy distribution, as compared with that following from the P_0 approximation, proves to be practically unchanged (Fig. 31).

As a result of these calculations and after comparing them with measurements, we can state that at least one of the suppositions finally leading to a strongly anisotropic distribution function cannot be correct.

Now it seems implausible to assume that the cause of this discrepancy might be found in the surface being neglected in the transport process. It is hard to see how the surface should be capable of changing the markedly anisotropic initial distribution of inner S into an isotropic one for sufficiently high energies.

It seems more probable to assume that the excitation itself is essentially more isotropic than was supposed in the calculations referred to above. The reason may be found in either excitation processes other than those with $\mathbf{H} = 0$ playing an essential role, or else in the primary beam having no distinguished direction in the solid because of its possible straggling. In the latter case, excitation would already be nearly isotropic in $\mathbf{H} = 0$ processes, and the marked discrepancies between theory and experiments would be largely eliminated.

Of course, also in $\mathbf{H} \neq 0$ processes additional S are excited in forward and backward direction by cooperation of the lattice, but it will not be possible to obtain valid information on the quantitative influence of these processes unless we should succeed in calculating the detailed energy angular distribution of excitation. Even then, the result of such calculations will be likely to depend to a large extent on the respective substance of the solid.

It still seems impossible to obtain with certainty a statement on the detailed excitation function by means of the experiments that have as yet been made. It would be very useful to measure the outer-energy angular distribution in a wide range of primary energy with different angles of incidence, since, if there is a change in primary energy, the behavior of the primary beam within the solid, at least within the layer of thickness d_s, will undergo a qualitative change.

It is possible that also the rediffused P play a certain role, but their influence on the excitation of S could be eliminated by measurements on thin foils or layers with high yield (Ag) evaporated on materials with a low rediffusion coefficient (Be).

F. Yield Dependence

1. Energy Dependence. As in D1, it was necessary to make the assumption $E_p^\circ > E_{pm}^\circ$; hence, we no longer have the possibility to determine the dependence on primary energy of the different distribution functions outside this range. Within it, however, we could conclude from the theory that the relative distribution functions are independent of E_p°.

Since there is no detailed theory for $E_p^\circ < E_{pm}^\circ$, the phenomenon of SE is considered in a rather simplified manner in the so-called semiempirical theory. Nevertheless, this enables us to obtain a fairly satisfactory representation of the dependence of the yield on E_p°. Obviously, the semi-

empirical theory must be regarded as a quasi-heuristic expedient which will eventually have to be replaced by a detailed theory.

Let $S(x,E_p^\circ;E,\Omega)$ denote the number of S per centimeter excited into the state (E,Ω) at the point x by a P with initial energy E_p°. Then

$$\delta(E_p^\circ) = \int_0^\infty dx \int dE d\Omega S(x,E_p^\circ;E,\Omega) p(x,E,\Omega)$$
$$= \int_0^\infty dx \bar{p}(x,E_p^\circ) \int dE d\Omega S(x,E_p^\circ;E,\Omega)$$

Provided that the mean probability of escape $\bar{p}(x,E_p^\circ)$ does not depend considerably on E_p°, which will just be the case if the excitation function contains E_p° only as a factor, this can be written

$$\delta(E_p^\circ) = \int_0^\infty dx \bar{p}(x) S(x,E_p^\circ) \tag{68}$$

$S(x,E_p^\circ)$ representing the total number of S excited per cm at the point x. Beside the assumption on $p(x,E_p^\circ)$ which led to (68), the semiempirical theory is characterized by two further assumptions (*2*):

$$\bar{p}(x) = \bar{p}(0) e^{-\alpha x} \tag{69}$$

and

$$S(x,E_p^\circ) = -K \frac{dE_p}{dx} \tag{70}$$

Relation (69) results from the following simplified treatment of the transport process of S: If we first consider, say, all S in the state (E,Ω) and then separate from these S especially those which in this state had already been at a certain point x_0, we may ask for the spatial distribution of those S in the emitter. We are thereby obviously concerned with those S which, proceeding from x_0 in the state (E,Ω), have not yet suffered any collision. Their spatial distribution is expressed by the reduced Boltzmann equation:

$$v \cos\beta \frac{\partial N(x,E,\beta)}{\partial x} = \frac{v}{l} N(x,E,\beta)$$

with the solution

$$N(x,E,\beta) = N(x_0,E,\beta) e^{\frac{x-x_0}{l\cos\beta}}$$

Because of $\cos\beta \gtrless 0$ for $x - x_0 \lesseqgtr 0$, the density of the S in question will drop exponentially on both sides of x_0. Thus neglect of the collision term b of the Boltzmann equation describing the scattering into (E,Ω) leads to an exponential dependence of electron density as assumed in (69).

In accordance with Lye and Dekker (*75*) whose procedure we shall follow here, we write for $-dE_p/dx$ in a somewhat general form

$$-\frac{dE_p}{dx} = AE_p^n(x) \tag{71}$$

This is likely to represent a simplification of actual conditions, since excitation in the whole range of primary energy would obey the same law. Further, (71) implies the neglect of straggling of the primary beam, since it establishes a correspondence between every x and an energy $E_p(x)$:

$$E_p^{n+1}(x) = E_p^{\circ n+1}(x) - (n+1)Ax \tag{72}$$

Hence (71) implies the range-energy relation

$$R(E_p^\circ) = \frac{E_p^{\circ n+1}}{(n+1)A} \tag{73}$$

By inserting (69) to (73) into (68), we obtain

$$\delta(E_p^\circ) = KA\bar{p}(0)\int_0^R dx e^{-\alpha x}[E_p^{\circ n+1} - (n+1)Ax]^{n/(n+1)} \tag{74}$$

With the substitutions

$$y^{n+1} = \frac{\alpha}{A(n+1)}[E_p^{\circ n+1} - (n+1)Ax]$$

and

$$r = \left[\frac{\alpha}{(n+1)A}\right]^{\frac{1}{n+1}} E_p^\circ, \; K' = K\bar{p}(0)$$

(74) takes the following form:

$$\delta(r) = K'\left[\frac{(n+1)A}{\alpha}\right]^{\frac{1}{n+1}} e^{-r^{n+1}}\int_0^r e^{y^{n+1}}dy \tag{75}$$

$d\delta/dr = 0$ defines that universal r value r_m at which the yield reaches its maximum:

$$\delta_m = K'\left[\frac{(n+1)A}{\alpha}\right]^{\frac{1}{n+1}} e^{-r_m^{n+1}}\int_0^{r_m} e^{y^{n+1}}dy, \; r_m = \left[\frac{\alpha}{(n+1)A}\right]^{\frac{1}{n+1}} \cdot E_{pm}^\circ \tag{76}$$

From (75) and (76) we find that

$$\frac{\delta}{\delta_m} = \left(e^{-r_m^{n+1}}\int_0^{r_m} e^{y^{n+1}}dy\right)^{-1} \exp\left\{-\left[r_m\left(\frac{E_p^\circ}{E_{pm}^\circ}\right)\right]^{n+1}\right\}\int_0^{r_m\left(\frac{E_p^\circ}{E_{pm}^\circ}\right)} e^{y^{n+1}}dy \tag{77}$$

From (77) it can be seen that in this theory the quotient δ/δ_m is a function of E_p°/E_{pm}° independent of the specific substance of the emitter. The reason for this strange property of the theory, which was discovered by

Baroody, is to be found in the fact that the theory includes only two substantial constants, A and α, which are eliminated on reduction to the maximum value of δ and the appropriate $E_{pm}°$. It seems, however, very improbable that there exists a universal curve in a strict sense, since a detailed theory of SE will certainly include more than two material constants. But, as we stated above, the relatively small divergence of measurements obtained for metals shows that the universal yield curve may be taken as a good approximation.

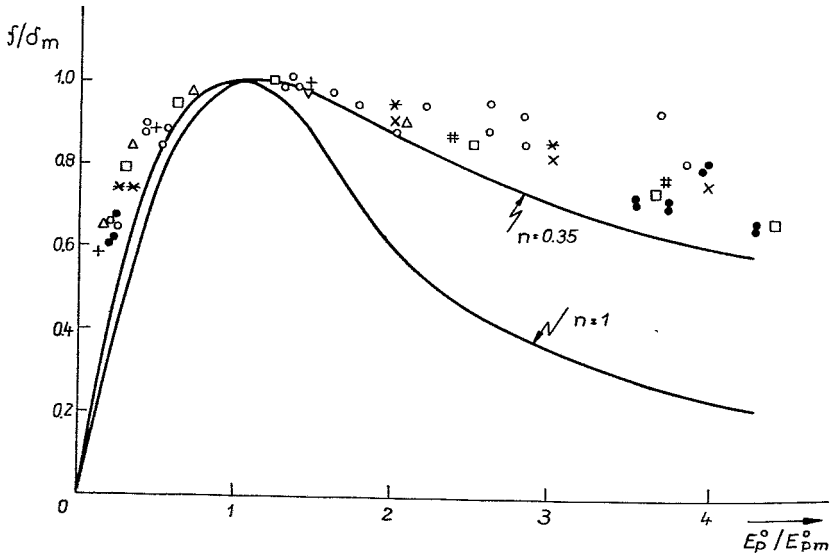

FIG. 33. Universal yield curves for $n = 0.35$ and $n = 1$; for comparison experimental points. [R. G. Lye and A. J. Dekker, *Phys. Rev.* **107**, 977 (1957)].

The shape of the universal curve (77) depends on n, which has still to be chosen. Lye and Dekker take $n = 0.35$, that is, the same value as resulting from Young's experiments on the stopping-power law. Figure 33 shows the result of the evaluation in comparison with the values measured, which will be even closer to the calculated curve if the back scattering of P is taken into account.

Thus, it can be stated that the semiempirical theory of yield renders good service for a first insight into the theory of the SE phenomenon in the case of metals.

Certainly one has to be very careful when concluding from yield curves on excitation functions and escape probabilities, since the yield δ is the result of a series of highly complicated processes. Thus, it is not possible to

conclude from a theoretical universal curve being in good accordance with measurements that the theoretical ideas on which it was based are necessarily correct.

It is therefore no wonder that Sternglass (*76*), proceeding from essentially different ideas, obtained a universal curve

$$\frac{\delta}{\delta_m} = e^2 \frac{E_p^\circ}{E_{pm}^\circ} \exp\left[-2\left(\frac{E_p^0}{E_{pm}^0}\right)^{1/2}\right]$$

which is also a good representation of the values measured for metals. Which of the formulations is the more correct one can therefore only be decided by a detailed theory of SE, which has still to be worked out (*77*).

A few general statements, however, can be made concerning the dependence of yield on energy (*44*). In the case of such small primary energies E_p° that $R(E_p^\circ) \ll 1/\alpha = d_s$, we can write (68) as, using (69) and (70),

$$\delta(E_p^\circ) = \bar{p}(0) \int_0^R dx S(x,E_p^\circ) = K' E_p^\circ$$

that is to say, δ increases linearly with primary energy for small E_p°. In the case of great primary energies, $R(E_p^\circ) \gg d_s$, we obtain by (68)

$$\delta(E_p^\circ) = S(0,E_p^\circ) \int_0^R \bar{p}(x)dx = S(0,E_p^\circ)\bar{p}(0)d_s \tag{78}$$

Equation (78) means that in this range the yield dependence on primary energy is the same as that of the excitation function and that with a given excitation function yield is proportional to the depth of escape d_s of S.

Let us finally remark that above $E_p^\circ \approx 3E_{pm}^\circ$ the experimental values of δ/δ_m may rather be represented by an exponent n near 1, which corresponds to the validity of the Whiddington law.

2. Temperature Dependence. In order to derive the dependence of SE on temperature, one would have to solve a Boltzmann equation whose collision terms are temperature-dependent because of the temperature-dependent Planck distribution of phonons.

In order to avoid the resulting difficulties, Dekker (*43*) suggested a simplified theory of this phenomenon. The starting point is relation (78), which is based on the assumption $E_p^\circ > E_{pm}^\circ$.

Since neither $S(0,E_p^\circ)$ nor $\bar{p}(0)$ seem to depend on temperature T to any noticeable extent, we may suppose that the temperature dependence of δ is given by that of d_s. Thus we have to derive from transport theory a length corresponding to d_s and find out its temperature dependence. This can be done by means of the well-known age equation:

$$\frac{\partial^2 \chi(x,\tau)}{\partial x^2} - \frac{\partial \chi(x,\tau)}{\partial \tau} + g(x)\delta(\tau) = 0 \tag{79}$$

where

$$\tau = \int_E^{E_0} \frac{l^2(E')}{3\eta}\, dE'$$

η = mean energy loss per collision of S, E_0 = initial energy of S immediately after excitation,

$$\chi(x,\tau) = \eta\rho(x,E(\tau)),\ \rho(x,E) = \frac{v}{l}\int_0^{\pi} N(x,E,\beta)\sin\beta d\beta$$

$g(x)$ defining the spatial dependence of the excitation function. The age equation (79) can be derived from the Boltzmann equation (43) by using certain simplifying assumptions which are approximately satisfied for electron-photon interaction. Therefore, the following considerations will hold only on condition that this interaction is the most important for the transport process of S in the emitter under investigation. This is certainly not the case for metals. Here the temperature-independent interaction with conduction electrons will overshadow that with phonons and therefore does not lead to any temperature effect of SE.

The function $\chi(x,\tau)$, the so-called "slowing-down density" states how many S per cubic centimeter and per second reach the age τ at the point x. One can gain insight into this transport process by considering the special case $g(x) = \delta(x)$. Then

$$\chi(x,\tau) = \frac{1}{2\sqrt{\pi\tau}}\, e^{-\frac{x^2}{4\tau}}$$

From this follows for the mean squared displacement of the τ-electrons

$$\langle x^2(\tau)\rangle = \frac{\int_0^{\infty} \chi x^2 dx}{\int_0^{\infty} \chi dx} = 2\tau \tag{80}$$

Now the square root of $\langle x^2(\tau)\rangle$ may be regarded as a measure for that distance by which the τ-electrons have moved from their point of origin.

Therefore Dekker writes

$$\sqrt{\langle x^2(\tau(W))\rangle} \approx d_s,\ \tau(W) = \int_W^{E_0} \frac{l^2}{3\eta}\, dE' \tag{81}$$

where W = electron affinity, $\tau(W)$ denoting the age at which S will just be able to escape.

Using (80) and (81), we can now conclude that the temperature dependence of δ is given by that of

$$\tau^{1/2}(W) = \left[\int_W^{E_0} \frac{l^2}{3\eta}\, dE'\right]^{1/2} \tag{82}$$

As can be seen from (82), we need the energy and temperature dependence of l and η. In the case of ionic crystals, in which the S mainly interact with the longitudinal optical lattice vibrations, one obtains the following approximations by perturbation theory:

$$l = C\frac{E}{2n_\omega + 1},\ \eta = \frac{\hbar\omega}{2n_\omega + 1},\ n_\omega = \frac{1}{e^{\frac{\hbar\omega}{kT}} - 1},\ \hbar\omega = k\theta \tag{83}$$

C is a constant including the coupling constant for interacting electron and phonon fields. ω denotes the angular frequency of longitudinal optical lattice vibrations, and (83) holds only if $E > \hbar\omega$. Thus we obtain by (82)

$$\delta \sim \left(\frac{1}{2n_\omega + 1}\right)^{1/2} \tag{84}$$

As was mentioned above, for polar crystals (84) fits satisfactorily recent experiments.

For high temperatures, $T \gg \theta$, (84) can be replaced approximately by

$$\delta \sim T^{-1/2} \tag{85}$$

Concerning the temperature dependence of energy distribution it follows from (82) and (83) that if T changes, $\tau(E)$ will change by a factor independent of E, so that the relative energy distribution is temperature-independent in this theory. This corresponds to experimental results obtained by Shulman and Dementyev (*15*).

If the same considerations are made for nonpolar crystals a function $\delta(T)$ is obtained which can also be approximated by (85) for high temperatures. Measurements of the temperature dependence for nonpolar crystals with predominating electron-phonon interaction do not yet exist.

G. Miscellaneous Problems

1. Surface Effect. The calculations of the excitation function given in Sec. IV,C are all based on the application of Bloch electron wave functions, the real existence of the emitter surface in the excitation process being entirely neglected. As, however, the surface plays a very important role in the external photoeffect of metals (*78*), since in a wide frequency range the photo yield can be described in a quantitative manner by a potential model referring only to the surface, it seems desirable also in the case of SE to study the influence of the surface on the excitation of S.

Contrary to earlier calculations (*79, 80*), resulting in a considerable contribution of the surface effect of SE to the total yield, more recent calculations (*81, 82*) seem to prove that the surface effect of SE is negligibly small.

The latter investigation quoted is based on Bethe's method of calculating the surface photo effect (*83*), where a metal disk of thickness $2a \gg 10^{-8}$ cm with a surface F is examined, and its potential defined by Fig. 34, using in addition a periodic boundary condition in directions y and z. Then the yield is obtained by $\delta = j_s/j_p$ with $j_p = \hbar K/2\pi m$ and

$$j_s = \frac{d_s}{4\pi^3} \int d^3\mathbf{k} \int\int \sum_{\mathbf{k}'_y\mathbf{k}'_z} \sum_{\mathbf{K}'_y\mathbf{K}'_z} P_{\mathbf{kK}}(\mathbf{k}'\mathbf{K}') d\mathbf{k}'_x d\mathbf{K}'_x \qquad (86)$$

where $\mathbf{k}_x > 0, \mathbf{k}'_x > 0$ also have to be taken into account, the final states $(\mathbf{k}')$ being given by the free states of the metal electrons.

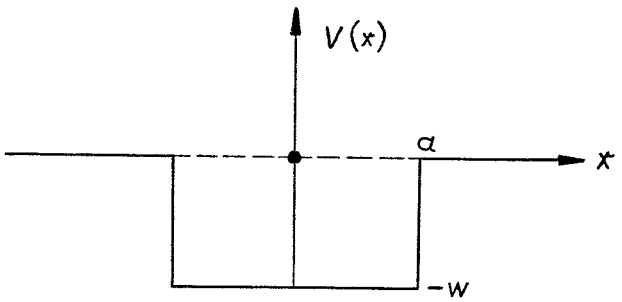

FIG. 34. Potential model for the surface effect [W. Brauer and W. Klose, *Ann. Physik* [6] **19**, 116 (1956)].

After several calculations one first obtains the transition probability

$$P_{\mathbf{kK}}(\mathbf{k}'\mathbf{K}') = \frac{2\pi e_0^4 \delta_{\mathbf{K}'_y,\mathbf{K}_y+\mathbf{k}_y-\mathbf{k}'_y} \cdot \delta_{\mathbf{K}'_z,\mathbf{K}_z+\mathbf{k}_z-\mathbf{k}'_z}}{\hbar F^2 q^4} \sum_{\nu=1,2} \delta(\sigma_\nu)\delta(E_{\mathbf{kK}} - E_{\mathbf{k}'\mathbf{K}'})$$

with

$$\sigma_1 = \mathbf{k}_x - \mathbf{k}'_x + q_x, \qquad \sigma_2 = \mathbf{k}_x - \mathbf{k}'_x - q_x$$

The integrations required by (86) can be carried out in an exact manner, the combined law of conservation of energy and momentum leading to an integration over the part of an energy momentum sphere of the final states that may contribute to the escape of secondaries $\mathbf{k}'_x > [(2m/\hbar^2)W]^{1/2}$.

The numerical evaluation of the highly complicated yield formula for the surface effect is shown in Fig. 35 for two metals. It can be seen that the contribution to yield is practically negligible. It must be pointed out, however, that the theoretical statements for $E_p^\circ < E_{pm}^\circ$ are unreliable inasmuch as there will be two counteracting factors which have been neglected here; on the one hand, the P will not move over the whole distance d_s, thus

generating less S, while, on the other hand, the energy loss of the P will produce more S per unit path length than with fixed $E_p = E_p°$. An additional introduction of these facts would supply the yield maximum lacking in Fig. 35.

Irrespective of these complications, it can be stated that contrary to the photo effect of metals, the influence of the surface on the excitation of S may be neglected in satisfactory approximation.

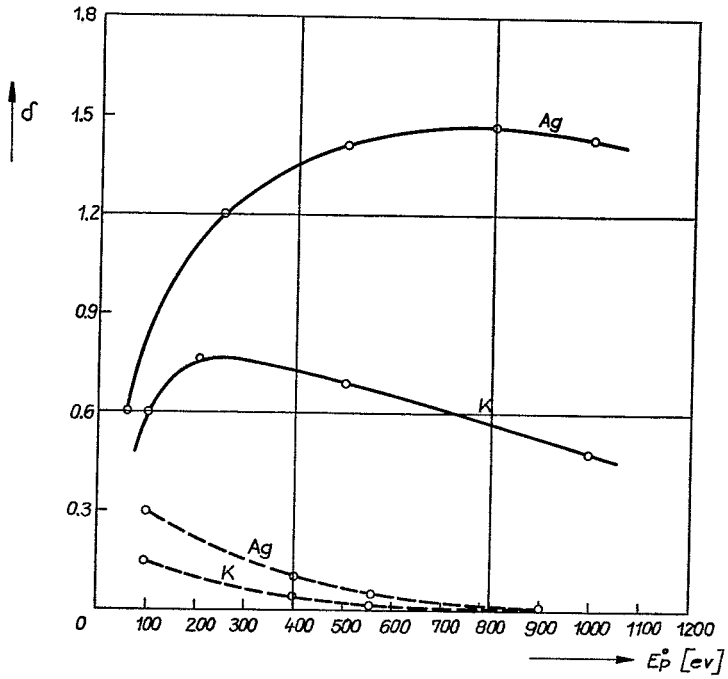

FIG. 35. Comparison of theoretical surface effect (— — — — —) and experimental (————) yield curves · $d_s = 10^{-6}$ cm [W. Brauer and W. Klose, *Ann. Physik* [6] **19**, 116 (1956)].

2. Time Constant of Secondary Emission. So far only the stationary state of the emitter has been considered. As a matter of course, however, when the primary beam is switched on, a finite time τ^* will pass between its incidence on the solid and the formation of a stationary distribution at the inner surface, giving rise to the problem how to calculate the magnitude τ^*, the time constant of SE.

The general solution of this problem would lead to the nonstationary Boltzmann equation (38). By means of a properly chosen excitation function, one would obviously have to calculate the length of time within

which $N(x,E,\beta)$ becomes stationary in the interval $0 \leqslant x \leqslant d_s$. This calculation has not yet been carried out.

On the other hand, van der Ziel (*84*) gave a simple estimation of τ^* based on the following consideration: Up to the time τ^* the emitter receives the energy $j_p E_p^\circ \tau^*$ per cm² from the primary beam. If $\tilde{N}$ denotes the number of excited S per cm² of the surface and $\bar{E}_e$ their mean excitation energy, then

$$j_p E_p^\circ \tau^* = \frac{j_s}{\delta} E_p^\circ \tau^* = \gamma \tilde{N} \bar{E}_e, \; \gamma \leqslant 1 \tag{87}$$

The more completely the energy taken up is directly transformed into excitation energy of S, the more γ will approximate 1. Since the stationary state is required only in the layer $0 \leqslant x \leqslant d_s$, estimation (87) for τ^* refers to primary energies $E_p^\circ \approx E_{pm}^\circ$. With N as the density of S near the surface, we have $\tilde{N} = N d_s$. Hence we obtain

$$\tau^* \geqslant \frac{N \bar{E}_e d_s}{j_s E_p^\circ} \delta \tag{88}$$

In order to make use of this estimation for the time constant, it is necessary to know the inner distribution function $N(x,E,\beta)$. Instead of choosing a formal Maxwell distribution for $N(x,E,\beta)$ as was done by van der Ziel, we shall first recur to the excitation functions stated above and confine ourselves to $\mathbf{H} = 0$ processes (*85*).

For insulators we shall use function (36) and treat the transport process by the age equation for the function $\rho(x,E)$, which reads

$$\frac{l^2}{3} \frac{\partial^2 \rho}{\partial x^2} + \eta \frac{\partial \rho}{\partial E} + S(x,E) = 0 \tag{89}$$

If we neglect the dependence on space coordinates and the interaction of S with electrons of the valence band by taking $N(\Delta E) = 0$, we obtain by (89) and (36)

$$N = \frac{C}{E_p^\circ} (\Delta E)^{1/2} \left[1 - \frac{1}{2} \left(\frac{\Delta E}{E_p^\circ} \right)^{1/2} \right], \; \bar{E}_e = \frac{\Delta E}{5} \left[1 + \frac{1}{2} \left(\frac{\Delta E}{E_p^\circ} \right)^{1/2} \right] + \Delta E \tag{90}$$

If we further suppose that $N(E,\beta)$ be isotropic, we find

$$j_s = \frac{3C\Delta E}{8\sqrt{8mE_p^\circ}} \left[1 - 2 \frac{W}{\Delta E} \ln \frac{\Delta E}{W} - \left(\frac{W}{\Delta E} \right)^2 \right] \tag{91}$$

By introducing (90) and (91) into (88) we obtain for MgO with $W = 0.25$ ev, $\Delta E = 5.77$ ev, $E_{pm}^\circ = 1{,}200$ ev, $\delta_m = 24$, $d_s = 2 \times 10^{-6}$ cm, the time constant $\tau^* \geqslant 3 \times 10^{-14}$ sec.

Because for metals the excitation function (34) diverges for $E = E_F$ and thus also N and $\bar{E}_e$, we have to calculate the excitation function with

$\lambda \neq 0$. As the function $S_\lambda(E)$ will then become very complicated, the following approximation seems convenient (*85*): We define an energy E_1 by the equation

$$S_{\lambda=0}(E_1) = S_\lambda(E_F)$$

and take (Fig. 36)

$$S(E) = \begin{cases} S_\lambda(E_F) & E_F \leqslant E \leqslant E_1 \\ S_{\lambda=0}(E) & E \geqslant E_1 \end{cases}$$

One obtains

$$S_\lambda(E_F) = 0{,}34 \frac{e_0^4 k_F^3}{3\pi E_p} \frac{1}{E_F^2}$$

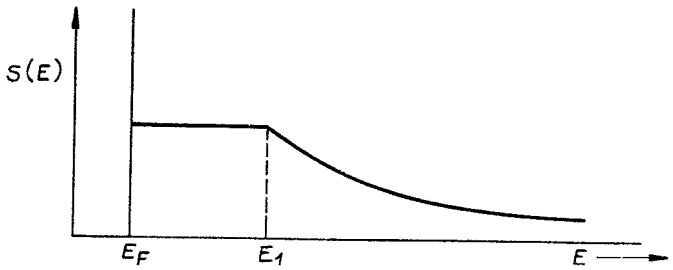

FIG. 36. Energy dependence of the excitation function in order to estimate the time constant for metals [H. W. Streitwolf and W. Brauer, *Z. Naturforsch.* **13a,** 700 (1958)].

Since we earlier recognize the fact that for metals source function and inner distribution function are very similar, Figs. 26 and 29, one can feel justified in taking $N(E)$ in approximation:

$$N(E) = \text{const. } S(E) = \begin{cases} \dfrac{D}{(E_1 - E_F)^2} & E \leqslant E_1 \\ \dfrac{D}{(E - E_F)^2} & E \geqslant E_1 \end{cases}$$

Then it follows that

$$N = \frac{2D}{E_1 - E_F}, \quad \bar{E}_e = \frac{E_1 + 3E_F}{4} + \frac{E_1 - E_F}{2} \ln \frac{E_p - E_F}{E_1 - E_F} - \frac{3}{5} E_F \qquad (92)$$

and with an isotropic distribution of the inner S

$$j_s = \frac{D}{(2m)^{1/2}} \left[\frac{-W^{1/2}}{2E_F} + \frac{W + E_F}{4E_F^{3/2}} \ln \frac{W^{1/2} + E_F^{1/2}}{W^{1/2} - E_F^{1/2}} \right] \qquad (93)$$

With (92) and (93) we obtain by (88) the time constant for Ag ($E_F = 5.5$ ev, $W = 10.2$ ev, $E_{pm}^{\circ} = 800$ ev, $\delta_m = 1.5$) as $\tau^* \geqslant 0.6 \times 10^{-15}$ sec.

Van der Ziel obtained for τ^* the same order of magnitude by using the formal Maxwell distribution. Experimental values of 10^{-11} sec, which were found earlier, represent upper limits for τ^* and still exceed by far the lengths of time obtained by calculation.

3. Relation to Photoeffect. Both the excitation of S and that of photoelectrons is due to the interaction of crystal electrons with external electric fields: in the case of SE, the Coulomb field of the P, in the case of photoeffect, the Maxwell field of an electromagnetic wave. Thus, there seems to exist a certain inner relation between SE and photoeffect, at least from the macroscopic point of view. According to Fröhlich (*86*), this relation can be formulated quantitatively in the special case of thin layers and thus be subjected to experimental examination. We shall describe Fröhlich's consideration in a somewhat modified and simplified manner.

Let the substance be described by a complex dielectric constant $\epsilon = (n + ik)^2$. The intensity of a monochromatic electromagnetic wave in this substance will then be damped according to

$$I(x,\omega) = I(\omega)e^{-2\frac{\omega k(\omega)}{c}x}$$

For

$$x \ll \frac{c}{2\omega k(\omega)}$$

this gives

$$I(x,\omega) = I(\omega)\left(1 - 2\frac{\omega k(\omega)}{c}x\right)$$

In a disk of thickness $d \ll c/2\omega k(\omega)$, the energy

$$2I(\omega)\frac{\omega k(\omega)}{c}d \tag{94}$$

will then be absorbed behind 1 cm²/sec. If we now consider a monochromatic light wave existing of quanta $\hbar\omega$, then for the number of quanta absorbed in the volume under consideration it follows from (94) that

$$\frac{2d}{\hbar c}k(\omega)I(\omega) = \frac{2d}{\hbar c}\left[\frac{n(\omega)k(\omega)}{|\epsilon(\omega)|^2}\right]\frac{|\epsilon(\omega)|^2}{n(\omega)}I(\omega) \tag{95}$$

If we further assume that each quantum absorbed results in the excitation of one inner photoelectron, then (95) will also represent the number of photoelectrons per cm² and sec excited by $I(\omega)$ in the disk. This number we shall denote by $S_L(\omega)$.

Let $j_L(E,\vartheta;\omega)$ define the current density of external photoelectrons in the state (E,ϑ), the incident radiation intensity being $I(\omega)$, then in any case

$$j_L(E,\vartheta;\omega) = h_L(E,\vartheta;\omega)S_L(\omega) = \frac{2d}{\hbar c} f_L(E,\vartheta;\omega)\frac{|\epsilon(\omega)|^2}{n(\omega)} I(\omega),$$

$$f_L(E,\vartheta;\omega) = h_L(E,\vartheta;\omega)\frac{n(\omega)k(\omega)}{|\epsilon(\omega)|^2} \tag{96}$$

will define a function h_L or f_L, which is capable of being determined on principle by measuring the photo effect, provided that the optical constants $n(\omega)$ and $k(\omega)$ are known.

The number of S excited by the electric field of one electron can be found by an analogous consideration, proceeding from the formula given by Fermi in his theory for the energy loss of an electron moving with velocity v_p in the substance under consideration:

$$-\frac{dE_p}{dx} = \frac{4e_0^2}{\pi v_p^2}\int_0^\infty \omega \frac{n(\omega)k(\omega)}{|\epsilon(\omega)|^2} xK_0(x)K_1(x)d\omega, x = \frac{r_{\min}}{v_p}\omega \tag{97}$$

$r_{\min}$ denote a length of the order 10^{-8} cm, $K_0(x)$ and $K_1(x)$ are modified Bessel functions, and (97) holds only under the additional condition that $\beta^2\epsilon \ll 1$. If (97) is interpreted as the sum of the energy losses of the electron caused by emission of monochromatic waves, then again we obtain the number of quanta $\hbar\omega$ absorbed by the substance per cm path length of the electron in the interval $d\omega$:

$$\frac{4e_0^2}{\hbar\pi v_p^2}\frac{n(\omega)k(\omega)}{|\epsilon(\omega)|^2} xK_0(x)K_1(x)d\omega$$

Over a length d one incident electron per cm^2 and sec will then emit

$$\frac{4e_0^2 d}{\hbar\pi v_p^2}\frac{n(\omega)k(\omega)}{|\epsilon(\omega)|^2} xK_0(x)K_1(x)d\omega \tag{98}$$

quanta $\hbar\omega$ per cm^2 and sec.

Expression (98) is in direct analogy with (95). If again we assume that each absorbed quantum results in the excitation of one electron, then (98) is directly the number of excited electrons $S_E(\omega)$. Now the essential assumption in Fröhlich's study seems to consist in the following relation:

$$j_s(E,\vartheta;\omega) = h_L(E,\vartheta;\omega)S_E(\omega) \tag{99}$$

$h_L(E,\vartheta;\omega)$ denotes the function empirically introduced into (96). With (99) and (98) we obtain the total external current density of S as

$$j_s(E,\vartheta) = \frac{4e_0^2 d}{\hbar\pi v_p^2}\int_0^\infty f_L(E,\vartheta;\omega)xK_0(x)K_1(x)d\omega \tag{100}$$

If the function $f_L(E,\vartheta;\omega)$ has thus been determined with sufficient accuracy

by measuring the photo effect, it is possible to find the current density of the external S by (100).

Since formula (97) holds only for a P of fixed velocity v_p, we have to choose at least $d \ll R(E_p^\circ)$; i.e., relation (100) is valid only for thin layers in which the P will practically move at their initial velocity.

An experimental control of (100) by measuring photoeffect, SE, and optical constants for the same thin layer has not been carried out. Yet it would be highly interesting to do so, since in this way it would be possible to obtain information on the correctness of assumption (99), which obviously neglects the influence of the detailed form of the excitation function on the probability of escape of electrons.

4. Influence of Occupied Donor Levels and Indirect Excitation. Though it has not yet been possible to state any distinct relations between the density of donor atoms in a given substance and the SE yield, some preliminary qualitative theoretical considerations have been made on this problem (*43*, *87*). Definite conclusions on the importance of impurities for SE could not be drawn.

Obviously, in such considerations a distinction has again to be made between the influence of occupied donor levels on the excitation process and their influence on the transport process.

According to Dekker, a noticeable influence on the transport process (ionization of donors by S) is not to be expected for concentrations of the donors below $N \approx 10^{20}$ cm^{-3}. Owing to the interaction of S with phonons leading to an energy loss of $\hbar\omega \approx 0.05$ ev per collision, the total path length of a S is $L \approx 10^{-5}$ cm. With an ionization cross section of the donor levels $\sigma \approx 10^{-15}$ cm^2, taking $N = 1/L\sigma$, this leads to the above concentration of impurity atoms.

The excitation process of S can be influenced by the presence of donor levels in two ways. Firstly there is the possibility of direct excitation of electrons from occupied donor levels by their interaction with P. An explicit calculation of this excitation has not yet been carried out. It would have to be based amongst others on the wave functions of such states (*88*), which are already fairly well known. If, on the other hand, one assumes that direct excitation from donor levels could be neglected, then there will remain only indirect excitation of S by excitons which are produced by P (*89*). On collision with an electron from a donor level, these excitons can liberate this electron and make it enter the conduction band. Thus, an additional part of the total excitation function of S will be produced.

For a more quantitative consideration, the transport equation can approximately be replaced by the following diffusion equation:

$$D \frac{d^2 N_{\text{exc}}}{dx^2} + S_{\text{exc}}(x) - \frac{N_{\text{exc}}(x)}{t_d} = 0 \qquad (101)$$

where

$$D = \frac{vl_s}{3}$$

There t_d is the lifetime and $t_s = l_s/v$ the time between two collisions of an exciton. If we further suppose that

$$\frac{1}{t_d} = \frac{1}{t_r} + \frac{1}{t_i}$$

where t_r is the lifetime for recombination and t_i the lifetime of the exciton for ionization of a donor, then, according to Dekker, $t_i \approx t_d$ already at donor concentrations of $\geqslant 10^{18}$ cm^{-3}. If we further suppose the excitation of excitons to be independent of space coordinates, then it is easy to find the following solution of (101) for the stationary distribution of excitons:

$$N_{\text{exc}}(x) = S_{\text{exc}} \frac{t_i}{2} [2 - (1 - \alpha)e^{-x/L}], L = (Dt_i)^{1/2} \tag{102}$$

The parameter α takes the value $+1$ for ideal reflection of excitons at the surface of the emitter, and -1 for total destruction of excitons [$N_{\text{exc}}(0) = 0$]. The indirect part of the electron excitation function follows from (102) as

$$\frac{N_{\text{exc}}(x)}{t_i} = \frac{1}{2} S_{\text{exc}}[2 - (1 - \alpha)e^{-x/L}]$$

and the appropriate part of yield by (68) and (69):

$$\delta_{\text{exc}} = C \int_0^\infty \frac{N_{\text{exc}}(x)}{t_i} e^{-x/d_s} \, dx = \frac{1}{2} CS_{\text{exc}} \left[2d_s - (1 - \alpha) \frac{Ld_s}{L + d_s} \right]$$

If we further take into account (78) for direct yield

$$\delta_{\text{dir}} = CS_{\text{dir}} d_s$$

then we obtain for $\alpha = +1$

$$\frac{\delta_{\text{exc}}}{\delta_{\text{dir}}} = \frac{S_{\text{exc}}}{S_{\text{dir}}}$$

and for $\alpha = -1$

$$\frac{\delta_{\text{exc}}}{\delta_{\text{dir}}} \approx \frac{S_{\text{exc}}}{S_{\text{dir}}} \frac{d_s}{L} \approx \frac{1}{20} \frac{S_{\text{exc}}}{S_{\text{dir}}}$$

In order to decide on the importance of indirect excitation at occupied donor levels, we must therefore have an exact knowledge of the excitation function of excitons and their behavior near the surface. Concerning the latter problem, according to a discussion by Hebb (*90*) on the experiments by Apker and Taft regarding the external photoeffect for alkali halides, we

must suppose that there exists a dead layer for excitons of 100 — 150 A under the surface. Thus, for alkali halides a noticeable contribution δ_{exc} is hardly to be expected.

REFERENCES

1. K. G. McKay, *Advances in Electronics* **1,** 65 (1948).
2. H. Bruining, "Physics and Applications of Secondary Electron Emission." Pergamon Press, London, 1954.
3. O. Hachenberg and W. Brauer, *Fortschr. Phys.* **1,** 439 (1954).
4. D. N. Dobrezow, *Izvest. Acad. Nauk, Ser. Fiz.* **20,** 994 (1956).
5. R. Kollath, *Handbuch d. Physik* **21,** 232 (1956).
5a. A. J. Dekker, *Solid State Phys.* **6,** 251 (1958).
6. C. Ramsauer, *Ann. Physik* [4] **45,** 961 (1914).
7. R. Kollath, *Ann. Physik* [5] **39,** 59 (1941).
8. G. A. Harrower, *Phys. Rev.* **102,** 340 (1956).
9. R. Kollath, *Ann. Physik* [6] **1,** 357 (1947).
10. G. A. Harrower, *Phys. Rev.* **104,** 52 (1956).
11. Yu. M. Kushnir and M. I. Frumin, *J. Tech. Phys.* (*U.S.S.R.*) **11,** 317 (1941).
12. L. J. Haworth, *Phys. Rev.* **48,** 88 (1935); **50,** 216 (1936).
13. J. J. Lander, *Phys. Rev.* **91,** 1382 (1953).
14. G. Appelt and O. Hachenberg, *Ann. Physik*, to be published.
15. A. R. Shulman and B. P. Dementyev, *J. Tech. Phys.* (*U.S.S.R.*) **25,** 2256 (1955).
16. N. R. Whetten and A. B. Laponsky, *Phys. Rev.* **107,** 1521 (1957).
17. K. H. Geyer, *Ann. Physik* [5] **41,** 117 (1942).
18. G. Appelt, Thesis, Dresden (1958).
19. J. L. H. Jonker, *Philips Research Rept.* **6,** 372 (1951).
20. J. L. H. Jonker, *Philips Research Rept.* **12,** 249 (1957).
21. H. Salow, *Z. tech. Physik* **21,** 8 (1940); *Physik. Z.* **41,** 434 (1940).
22. J. B. Johnson, *Phys. Rev.* **73,** 1058 (1948).
23. E. J. Sternglass, *Phys. Rev.* **80,** 925 (1950).
24. E. M. Baroody, *Phys. Rev.* **78,** 780 (1950).
25. A. R. Shulman and J. I. Myakinin, *Doklady Akad. Nauk U.S.S.R.* **91,** 1075 (1953).
26. J. G. Trump and R. J. van de Graaff, *Phys. Rev.* **75,** 44 (1949).
27. P. Palluel, *Compt. rend.* **224,** 1492, 1551 (1947).
28. J. E. Holliday and E. J. Sternglass, *J. Appl. Phys.* **28,** 1189 (1957).
29. H. Hintenberger, *Z. Physik* **114,** 98 (1939).
30. H. Bruining and J. H. de Boer, *Physica* **6,** 834 (1939).
31. M. Knoll, O. Hachenberg, and J. Randmer, *Z. Physik* **122,** 137 (1944).
32. A. R. Shulman, *J. Tech. Phys.* (*U.S.S.R.*) **25,** 2150 (1955).
33. O. Hachenberg, *Ann. Physik* [6] **2,** 403 (1948).
34. P. M. Morotsov, *J. Exptl. Theoret. Phys.* (*U.S.S.R.*) **11,** 402 (1942).
35. D. E. Wooldridge, *Phys. Rev.* **57,** 1080 (1940).
36. D. E. Wooldridge, *Phys. Rev.* **58,** 316 (1940).
37. G. Blankenfeld, *Ann. Physik* [6] **9,** 48 (1950).
38. E. J. Sternglass, *Westinghouse Research Lab., Research Rept.* R 94413-3-J.
39. J. B. Johnson and K. G. McKay, *Phys. Rev.* **93,** 668 (1953).
40. C. W. Mueller, *J. Appl. Phys.* **16,** 453 (1945).
41. A. R. Shulman, W. L. Makedonsky, and J. D. Yaroshetsky, *J. Tech. Phys.* (*U.S.S.R.*) **23,** 1152 (1953).

42. H. Krüger, Thesis, Berlin (1957).
43. A. J. Dekker, *Physica* **21,** 29 (1954).
44. A. J. Dekker, *Phys. Rev.* **94,** 1179 (1954).
45. J. B. Johnson and K. G. McKay, *Phys. Rev.* **91,** 582 (1953).
46. T. L. Matskevich, *J. Tech. Phys.* (*U.S.S.R.*) **26,** 2399 (1956).
47. B. Petzel, Thesis, Dresden (1958).
48. K. Sixtus, *Ann. Physik* [5] **3,** 1017 (1929).
49. L. R. G. Treloar, *Nature* **137,** 579 (1936).
50. M. Knoll and R. Theile, *Z. Physik* **113,** 260 (1939).
51. B. I. Djatlowitskaja, *Doklady Akad. Nauk U.S.S.R.* **63,** 641 (1948).
52. I. G. Nachodkin and W. A. Romanowsky, *Izvest. Akad. Nauk U.S.S.R., Ser. Fiz.* **22,** 454 (1958).
53. M. M. Greenblatt, *RCA Review* **16,** 52 (1955).
54. T. L. Matskevich, *J. Tech. Phys.* (*U.S.S.R.*) **27,** 289 (1957).
55. L. Marton, L. B. Leder, and H. Mendlowitz, *Advances in Electronics and Electron Phys.* **7,** 183 (1955).
56. J. R. Young, *J. Appl. Phys.* **27,** 1 (1956).
57. J. R. Young, *Phys. Rev.* **103,** 292 (1956).
58. R. O. Lane and D. J. Zaffarano, *Phys. Rev.* **94,** 960 (1954).
59. J. R. Young, *J. Appl. Phys.* **28,** 524 (1957).
60. O. Hachenberg, unpublished.
61. A. J. Dekker and A. van der Ziel, *Phys. Rev.* **86,** 755 (1952).
62. E. M. Baroody, *Phys. Rev.* **101,** 1679 (1956).
63. H. Fröhlich, *Ann. Physik.* [5] **13,** 229 (1932).
64. T. F. Marshall, *Phys. Rev.* **88,** 416 (1952).
65. W. Brauer, *Ann. Physik.* [6] **20,** 390 (1957).
66. A. J. Vyatskin, *J. Tech. Phys.* (*U.S.S.R.*) **25,** 1155 (1955).
67. P. N. Butcher, *Proc. Phys. Soc.* (*London*) **A64,** 765 (1951).
68. H. W. Streitwolf, *Ann. Physik,* [7] **3,** 183 (1959).
69. A. van der Ziel, *Phys. Rev.* **92,** 35 (1953).
70. H. A. Bethe, *Ann. Physik* [5] **5,** 325 (1930).
71. P. A. Wolff, *Phys. Rev.* **95,** 56 (1954).
72. H. Stolz, *Ann. Physik,* [7] **3,** 197 (1959).
73. J. L. H. Jonker, *Philips Research Rept.* **7,** 1 (1952).
74. W. Brauer, *Proc. 2nd. Conf. on Solid State Phys., Dresden* p. 159 (1954).
75. R. G. Lye and A. J. Dekker, *Phys. Rev.* **107,** 977 (1957).
76. E. J. Sternglass, *Westinghouse Research Lab. Sci. Paper* No. 1772 (1954).
77. W. Brauer, *Czech. J. Phys.* **7,** 513 (1957).
78. K. Mitchell, *Proc. Roy. Soc.* **A146,** 442 (1934).
79. A. J. Vyatskin, *J. Exptl. Theoret. Phys.* (*U.S.S.R.*) **9,** 826 (1939).
80. A. J. Vyatskin, *J. Exptl. Theoret. Phys.* (*U.S.S.R.*) **20,** 547 (1950).
81. E. M. Baroody, *Phys. Rev.* **92,** 843 (1953).
82. W. Brauer and W. Klose, *Ann. Physik* [6] **19,** 116 (1956).
83. H. A. Bethe, *Handbuch d. Physik* **24/2,** 468 (1933).
84. A. van der Ziel, *J. Appl. Phys.* **28,** 1216 (1957).
85. H. W. Streitwolf and W. Brauer, *Z. Naturforsch.* **13a,** 700 (1958).
86. H. Fröhlich, *Proc. Phys. Soc.* (*London*) **B68,** 657 (1955).
87. A. J. Dekker, *Physica* **22,** 361 (1956).
88. W. Kohn, *Solid State Phys.* **5,** 257 (1957).
89. M. Trlifaj, *Czech. J. Phys.* **7,** 667 (1957).
90. M. H. Hebb, *Phys. Rev.* **81,** 702 (1951).